Ministry of Higher Education & Scientific Research

University of Babylon

College of Science/Chemistry Department

spectrofluorometric quantification of some drugs in its dosage form and spiked human plasma with clinical study

A Thesis Submitted to the Council of College of Science University of Babylon in Partial Fulfillment of the Requirements for the Degree of Doctor Philosophy in Chemistry

By

Ali Fahim Mohammed Al-Khefagy

B. Sc. 2013

M. Sc. 2016

Supervised By

Prof. Dr. Abbas Noor Mohammed Al-Shirify

Prof. Dr. Kasim Hassan Kadhim (God bless on his soul)

2022 A.D **1444 A.H**

بسم الله الرحمن الرحيم

(قالوا سبحانك لا علم لنا إلا ما
علمتنا إنك أنت العليم الحكيم)

صدق الله العلي العظيم

سورة البقرة

الآية (٣٢)

Declaration

I certify that this thesis **"spectrofluorometric quantification of some drugs in its dosage form and spiked human plasma with clinical study"** has been prepared under my supervision at Chemistry Department – College of Science/Babylon University, as a partial requirement for the degree of philosophy doctor in analytical chemistry.

Signature:

Supervisor: Prof. Dr. Abbas Noor Mohammed Al-Shirify

Date: / /2022

Signature:

Supervisor: Prof. Dr. Kasim Hassan Kadhim

Date: / /2022

Forwarding for debate

In view of the available recommendations, I forward this thesis for debate by the examining committee.

Signature:

Name: Prof. Dr. Abbas Jasim Atiyah

Title: Head of Chemistry Department - College of Science/Babylon University

Date: / /2022

Acknowledgements

First, I would like to thank Allah for his merciful and his continuous help over all the period of my life.

I would like to express my great appreciation to the soul of my first supervisors Dr. Kasim Hassan Kadhum (God bless his soul) and to the second supervisors Dr. Abbas Noor Alshirify for their supervision, encouragement, helpful advice and their suggestion subject of the thesis.

I would like to express my gratitude to Dr. Ahmed Sadoon for their generous help, assistance and support during my study.

I thank the University of Babylon for giving me this great opportunity to achieve my goal in completing my PhD degree.

Finally, and most importantly, I must thank my dearest family for giving me the support and encouragement that only a family can give, especially my mother, father and my beloved wife (Dr. Marowa Hashim Abbas).

Ali

Dedication

-To my parents, the most sacrifices

- To my wife

- To my soul (my sons: Ameer & Fatima)

- To my brother and sisters

-To all the honest

To all of them, I dedicate this work.

List of Contents

List of Tables

List of Figures

List of Abbreviations

Abbreviation	Meaning
POPOP	2,2′-(1,4-Phenylene)bis(5-phenyl-1,3-oxazole)
HPLC	High Performance Liquid Chromatography
GC	Gas Chromatography
LC	Liquid Chromatography
FIA	Flow injection analysis
TLC	Thin-layer chromatography
S_1	Singlet state
T_1	Triplet state
CE	Capillary electrophoresis
EDTA	Ethylenediaminetetraacetic acid
NBD	7-nitro-1,2,3-benzoxadiazole
MSDS	Material Safety Data Sheet
MRP	Meropenem
MET	Metformin
AMB	Amlodipine
STA	Sitagliptin
CLZ	Clozapine
rpm	Round per minutes
COVID-19	Coronavirus disease
DMF	Dimethyl formamide
DMSO	Dimethyl sulfoxide
BMI	Body mass index
ANOVA	Analysis Of Variance
TG	Triglyceride
GPT	Glutamate- pyruvic transaminase
SD	Standard Deviation
RSD	Relative Standard Deviation
Re	Recovery
IL-6	Interleukin 6
ICH	International Council for Harmonisation
FI	Fluorescence intensity
SDI	The state Company For Drugs Industry and Medical Appliances Samarra Iraq

Summery

Herein, new click-like protocols for quantification of some drugs in their dosage form and fresh human plasma were developed. The study includes four parts, the first one involves determination of meropenem and clozapine in their pharmaceutical formulation and spiked human plasma using NBD-Cl as fluorescent labeling reagent. The developed method is mainly depending on a nucleophilic substitution reaction of MRP or CLZ with 4-Nitro-7-chlorobenzofurazan (NBD-Cl) in alkaline borate buffer (pH 9.0), which results in a strongly fluorescent yellow fluorophore measured at λ_{em}= 536 nm and 540 when excited at λ_{ex}= 471 nm and 469 for MRP and CLZ respectively. The variables that influence the stability and development of reaction product were thoroughly investigated and optimized. Calibration curve is rectilinear within the concentration range of 25-650 and 80-900 ng mL^{-1} with a linear correlation coefficient (r =0.9981) and (r =0.9984) related to MRP and CLZ respectively. Detection limits were found to be 3.15 and 14 ng mL^{-1} with LOQ 9.55 and 42 ng mL^{-1} related to MRP and CLZ respectively.

The second represent determination of amlodipine besylate and sitagliptin in their pharmaceutical formulation and human plasma using O-phthalaldehyde as analytical fluorogenic reagent in the presence of 2-mercaptoethanol as fluorophore stabilizer agent. The proposed method was based on click-like three-component labeling of primary amine compound (AMB or STA drug) with O-phthalaldehyde and 2-mercaptoethanol (as fluorophore stabilizer agent) in alkaline borate buffer pH=10 and 10.5 for AMB and STA respectively. The resulting N-fused aromatic isoindole moiety provides a high fluorescence intensity measured at λ_{em}= 475 and 458 nm after excitation λ_{ex}= 378 and 335 nm for AMB and STA respectively. Experimental factors that affect on the FI of the formed fluorophore were carefully studied and optimized. The linear drug concentration ranged from 125-1400 and 275-1650 ng mL^{-1} with a linear correlation coefficient (r =0.9986) and (r =0.9985) related to AMB and STA respectively. Detection limits were found to be 31.29 and 58.94 ng mL^{-1} with

quantification limits were 94.84 and 178.62 ng mL^{-1} for AMB and STA respectively.

The third part represent determination of metformin hydrochloride in a fresh human plasma using 3,6-Dibromo-phenanthrenequinone as analytical fluorogenic reagent. The method based on the reaction between MET and PQ-2Br in basic media of 0.2 M NaOH to produce fluorescent product measured at λ_{em}= 420 after excitation λ_{ex}= 253nm. The parameters that affect on the FI of the formed product was studied and optimized. The linear drug concentration ranged from 70-1300 ng mL^{-1} with a linear correlation coefficient (r =0.9989). LOD was 19.5 ng mL^{-1} with LOQ value 59.11 ng mL^{-1}.

The developed approach were validated according to ICH guidelines to prove that the presented methods' results agree with the requirements of the proposed analytical performance.

The fourth part involves assay the level of biomarkers such as (D-dimer, LDH, GPT, TG, and plasma metformin) in Diabetic and non-Diabetic COVID-19 patients administered remdesivir medication.

Chapter Four: Conclusion and Future prospects

The prescribed spectrofluorometric methods provide a simple, rapid and precise methods for the estimation of drugs in their pharmaceutical dosage form and spiked fresh human plasma without interferences from plasma matrix or common excipients. Moreover, the developed methods showed promising selectivity, sensitivity, a good linear range, excellent quantitative recoveries, and low detection limit with (R.S.D%) were less than 2 % for reproducibility and repeatability analysis.

Finally, all the developed methods were successfully utilized for the quantification of drugs in their pharmaceutical dosage form and spiked fresh human plasma. The obtained data were compared statistically to those obtained from the reported or official methods according to t-student test and F- test at the 95% confidence level. The results related to f-test and t-test values are lesser than the corresponding critical (tabulated) values, indicating no significant difference

statistically between the official method as well as reported method with the proposed methods.

The Clinical results show that non-Diabetic COVID-19 patients showed faster recovery than Diabetic-COVID-19 patients because remdesivir medication improve the level of D-dimer and LDH. The results indicate that the D-dimer and LDH biomarkers can helps to diagnosis COVID-19 infection.

Chapter one

Introduction

1. Introduction

1.1 Molecular fluorescence & fluorescence spectroscopy

Molecular fluorescence regards a one kinds of luminescence that occur when a fluorescent substance reemits immediately (within about 10^{-8} seconds) the absorbed light or electromagnetic radiation at different wavelength from the source light. Most of the time, the emitted light has a less energy and thus longer wavelength than the absorbed radiation. When the light is absorbed, fluorescence occurs, and it disappears when the light is turned off. Fluorescence involves two stage, the first one called excitation process in which the molecules that are in the lowest vibrational level of the singlet ground electronic state (usually at room temperature) absorb electromagnetic radiation at a suitable wavelength resulting in promotes the electrons to a singlet-excited state (S_1 or S_2…. etc.). The second state called emission process in which the excited atom or molecules in the first singlet-excited state (S_1) relaxes to a singlet-ground state (usually lower energy state) by release photons as fluorescent radiation (emission) without a change in electron spin (the same multiplicity)[1-5], as shown in *Figure 1-1*.

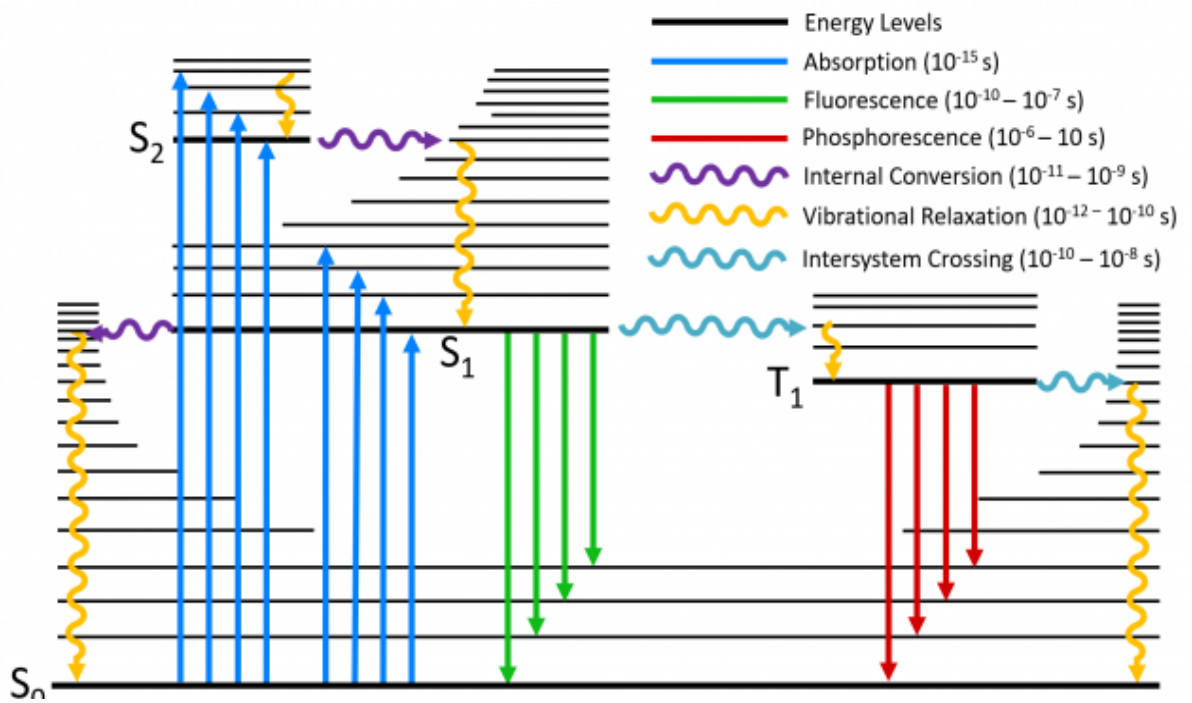

Figure 1-1. Jablonski diagram showing the transitions between different energy levels.

The fluorescence of the most popular fluorescent compounds occurs when the incident source light lies in the ultraviolet region of the spectrum, and thus invisible to the human eye, while the emitted light lies in the visible region, which results in fluorescent compounds with a unique color seen only when exposed to ultraviolet radiation. Of these compounds we can mentions[6]: acridine orange, Fluorescein, rhodamine B, POPOP, Quinine and Pyridine 1 as shown in *Figure 1-2*.

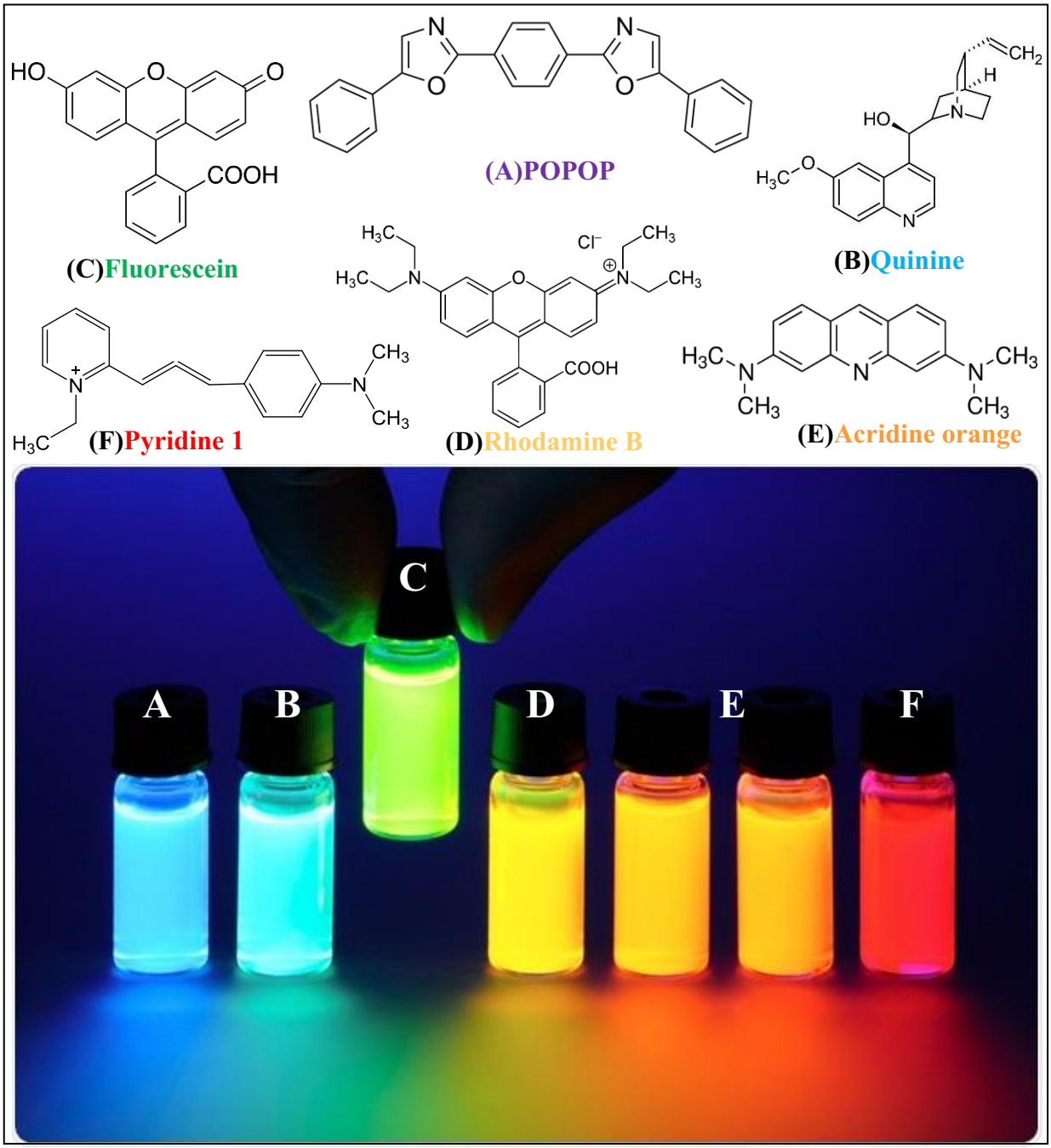

Figure 1-2. visible colored fluorescence of most popular fluorescent compounds with their chemical structure.

The energy of the excited electrons may lose by a mechanism other than fluorescence, known as non-radiative processes which include inter-crossing system to the triplet (T_2) state, internal conversion and transfer of energy to another molecule. It competes with fluorescence emission, lowering its efficiency[7-9]. Fluorescence has numerous practical applications in a variety of fields include medicine, gemology, mineralogy, chemical sensors, fluorescent labeling dyes, vacuum fluorescent displays, cosmic-ray detection biological detectors, and cathode-ray tubes[10-16].

There are many factors affect on the relative fluorescence intensity of the fluorescent compounds[17,18]. Of these,

1. Concentration: Fluorescence intensity is proportional to both the fluorescent substance concentration (ranging from (10^{-4}-10^{-7}M) and intensity of exciting radiation.
2. Substituents: electron donating group like $–NH_2$, $-OCH_3$, –OH, $N(CH_3)_2$ and $-NHCH_3$, usually improve fluorescence intensity because they delocalize electrons which in turn increase the probability of transition between the lowest sub-level of excited singlet state and the singlet ground state. On the other hand, electron withdrawing group such as $-NO_2$, $-NHCOCH_3$, –Cl, -Br, -I, and -COOH reduce fluorescence intensity.
3. Molecular rigidity: compounds with a rigid structure are more prone to be fluorescent because the rigidity decreases the molecular vibration which leads to decrease non-radiative transitions which in turn reduces inter-crossing system to the triplet (T_2) state. Eosin and fluorescein, for example, emit strong fluorescence radiation, whereas phenolphthalein, which has a disturbed conjugate system and non-rigid structure, is not.
4. Changes in pH: Fluorescence of compounds is also strongly influenced by a pH of solution. Aniline, for example, emits blue fluorescence radiation when excited at wavelength 290 nm in the pH range from (5.0-13.0). Aniline exists

as the aniline cation in the solution at low pH and as the anion at high pH. Anion and cation are not fluorescent. Due to the fact that π−π∗ states possess shorter average lifetime than n−π∗.

5. Temperature/Viscosity: increase temperature causes increase in the possibility of collisional deactivation and decrease the viscosity which in turn decrease the fluorescence intensity.
6. Presence of dissolved oxygen: Oxygen oxidizes fluorescent materials, causing loss of their fluorescence.
7. Solvent: The solvent may have a significant effect on the fluorescence spectrum. This property is usually observed in a large dipole moments fluorophore, as a result, fluorescence spectra shifts to longer wavelengths in polar solvent.

Fluorescence spectroscopy (also known as spectrofluorometry or fluorimetry) is an electromagnetic spectroscopy technique for analyzing fluorescence radiation emitted from fluorescent molecules. It considers a simple, popular, fast, versatile, inexpensive and highly-efficient technique for quantifying of an analyte in a real sample[19]. In spectrofluorometry, a beam of light produced from xenon lamp with a wavelength (excitation wavelength) within the range of (180 to 800 nm) passes through the cuvette that contained a sample solution. The sample then emit fluorescence radiation (**emission wavelength**) measured at right angle with the respect to the incident light. The analyte concentration is directly proportional to the fluorescence intensity of the emitted light. The device used to measure the fluorescence radiation emitted from excited analyte called spectrofluorometer[20] as shown in *Figure 1-3*.

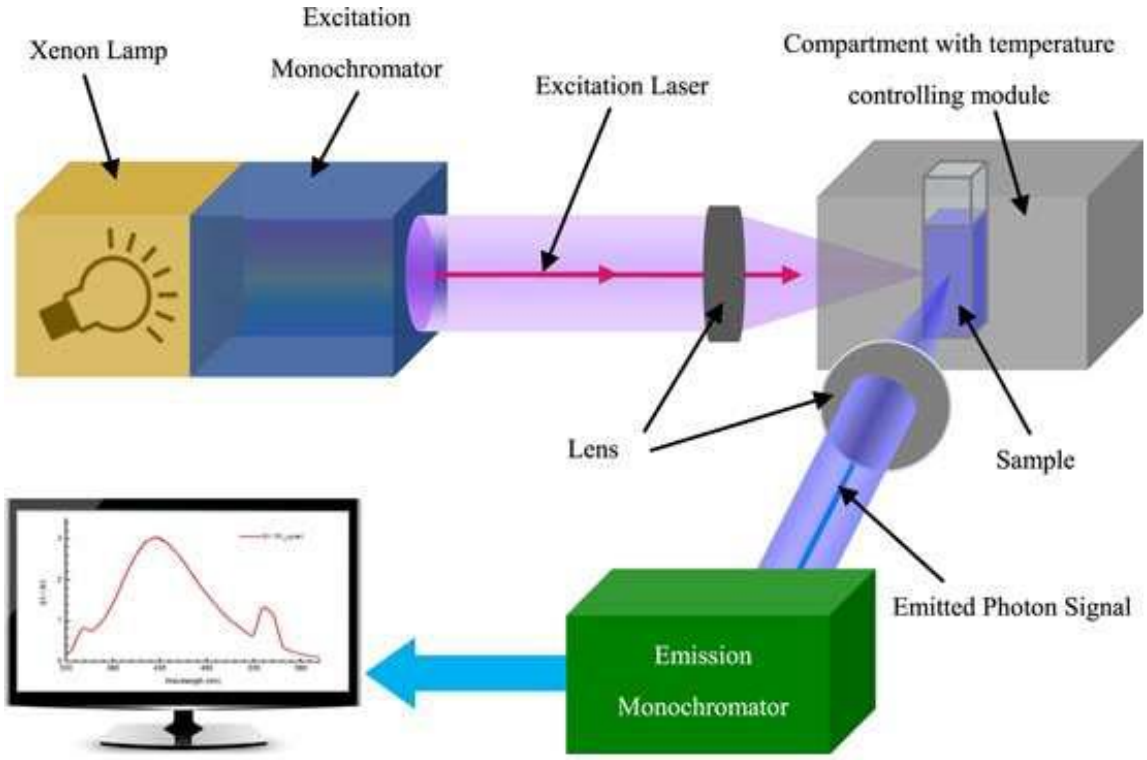

Figure 1-3. The main apparatus in spectrofluorometer.

Fluorescence spectroscopy offers a great sensitivity and specificity. In the case of specificity, the analysis depends on two spectra (excitation and emission spectrum) rather than one. High sensitivity produced from a difference in wavelength between the emitted and excited radiation. These results in a signal contrasted with essentially zero background [(21)].

As a result of its great sensitivity and specificity, The current survey of chemical literature exhibit that the application of fluorescence spectroscopy has been increased to cover most routine analysis, scientific researches, and chemical processes monitoring because of their facilities in the analyzing of enormous sample in the variety of applicative fields such as foodstuff[(22-24)], industrial[(25)], medical[(26,27)], pharmaceuticals[(28-31)], contaminants trace[(32-34)], criminal[(35,36)], agricultural[(37-41)] and environmental[(42,43)].

1.2 Fluorescent labelling

1.2.1 Fluorescent labeling technique

Derivatization methods have recently gained a widespread because they have solved many problems with regard to analytical quantification in several analytical technique such as spectrometric, HPLC, GC, LC, and electrophoresis. Thus, analytical chemists during last decade period have adapted well-known reaction from the organic and organometallic fields to carry out derivatization reactions in order to improve some necessary parameters such as spectral properties, thermal stability, sensitivity, volatility, selectivity, peak shape, and/or separation behavior detection of interested analytes[44].

Only a few compounds have the ability to exhibit fluorescence radiation. Also, the detection limits for fluorometric analytical methods are typically one to four orders of magnitude lower than those for comparable absorption-based methods. For these reasons, Fluorescent labelling technique are carried out in which a non-fluorescent or weakly fluorescent substance is react with fluorogenic ligand forming a highly fluorescent product *Figure 1-4*. The fluorogenic ligand may not itself fluorescent unless it reacts with a targeted analyte to give a fluorescent adduct. To be worthwhile, the technique must be rapid (usually less than 15 minutes), easy to perform, selective, and the derivatizing reagent must react quantitatively with the analyte, yielding only one final product[45,46].

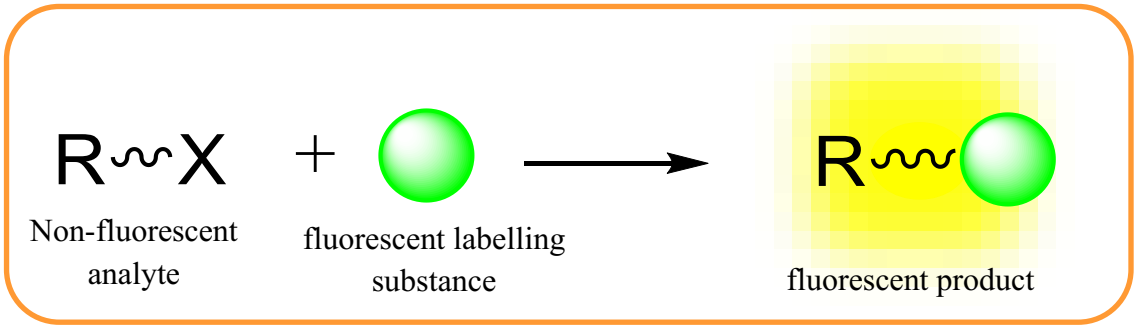

Figure 1-4. fluorescence derivatization method to produce fluorescent product

Fluorescence derivatization procedures improve detection limits as well as increasing selectivity.

Fluorescent labeling techniques are also important for quantifying compounds that do not in general reveal the desired characteristics required for the analytical technique and those that are more prone to decomposition throughout the analysis. As a result, derivatization technique involves all methods that include reaction of fluorogenic compound with targeted substance to produce fluorophore (fluorescent compound). A typical derivatizing reaction should meet a set of analytical requirements that vary depending on the application. Generally, the desirable characteristics of derivatizing reactions involve the following[47-51]:

1. Rapid in moderate conditions, highly specific, quantitative, easy to carry out.
2. produce stable product, difficult to decompose, and free from side reaction. These properties are very important, especially in chromatographic methods because the side-products may cause interfering peaks in the chromatogram.
3. Measurable differences in spectroscopic properties (like wavelength) between the fluorogenic agent and its reaction product.
4. The formed product should have maximum fluorescence efficiency to ensure higher sensitivity.
5. To analyze biological samples. The derivatization reagent should be soluble in aqueous solvent.
6. In the chromatographic techniques, the formed product is easy to separate from the fluorogenic agent.

Fluorescent labeling techniques has been employed in a broad range in biochemistry for detecting biomolecules in which fluorescent dyes binds to functional group of biomolecules such as (peptides, proteins, nucleic acids, antibodies, bacteria or yeast) to produce visualizable biomolecules under fluorescence imaging[52-56]. For example, Immunofluorescence micrograph of a fibroblast monolayer *Figure 1-5*.

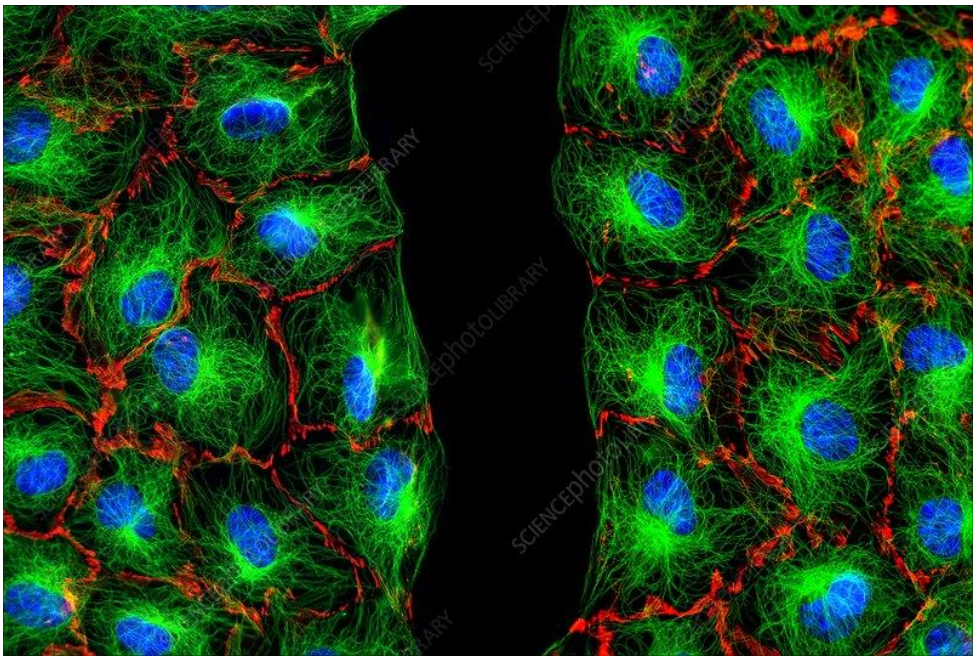

Figure 1-5. Immunofluorescence micrograph of a fibroblast monolayer. The blue color represents cell nuclei. Whereas, Protein filaments, microtubules, that make up part of the cytoskeleton, are green.

Fluorescent labels reveal many advantages in biochemistry such as[57-60]:

i. very sensitive for the targeted substance even at low concentrations.
ii. Stable during long time interval.
iii. Free from chemical interferences.
iv. The targeted imaging of labeled cells enables tracking them in *vitro* and in *vivo*.

Fluorogenic reagent are synthesized to contain binding reaction group and fluorescent moiety. Fluorescein, for example, have isocyanates or N-hydroxysuccinimide group at which the amino or thiol group of proteins bind through amide bond formation to produce fluorescent derivative of protein. Moreover, coumarin derivatives were utilized to measure fatty acid amide hydrolase activity. Further, 4-methyl coumarin amide and Arachidonyl 7-amino have no native fluorescence unless react with enzyme to produce fluorescent hydrolyzed product 7-amino-4-methylcoumarin measured at $\lambda_{emi} = 460$ nm (after excitation 355 nm) and can be used to detect hydrolysis activity of this enzyme[61].

1.2.2 Fluorescent labeling reactions

Fluorescent labeling reactions can be divided into six distinct categories:

1. Reactions that produce an extended aromatic π-Electron System.

As mentioned previously, the planarity and rigidity of the structure have a significant effect on the fluorescence intensity of compounds as they increase the effective delocalization of π-electrons[62,63].

There are three ways reported which increase the aromatic π-electron system which in turn triggered the molecule to exhibit fluorescence radiation.

a. Reaction of non-aromatic analyte with two adjacent substituents on aromatic ring of reagent to produce a new fluorescent ring *Figure 1-6*[64,65].
b. Coupling the analyte to a substituent and non-substituted position on an aromatic ring to form fluorescent product *Figure 1-7*[66-68].
c. Coupling the substituted aromatic analyte with non-aromatic reagent to give fluorescent product *Figure 1-8*[69-73].

Reagent	Analytes	Reaction conditions	Fluorescent product
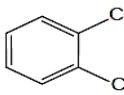 O-Phthalaldehyde	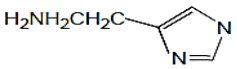 Histamine, indoles, peptides, proteins	Basic	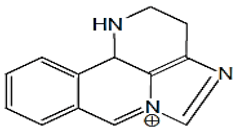 λ_{exc}= 360 nm λ_{em}= 490 nm
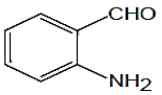 O-Amino-benzaldehyde	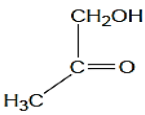 Carbohydrates	KOH/boiled	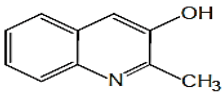 Blue emission
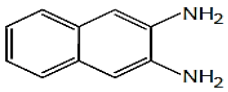 2, 3-Diamino-naphthalene	NO_2^- Nitrite, nitrate	HCl/extraction	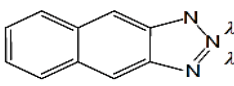 λ_{exc}= 355 nm λ_{em}= 410 nm

Figure 1-6. Reaction of non-aromatic analyte with aromatic ring of reagent to produce a fluorescent ring

Reagent	Analytes	Reaction conditions	Fluorescent product
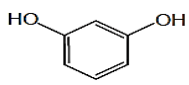 Resorcinol	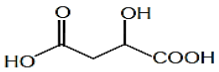 Ketohexoses, ketoacids, dicarboxylic acid	H_2SO_4 50% 20 min 60°C	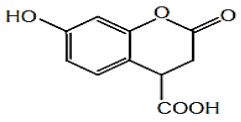 λ_{exc}= 430 nm λ_{em}= 480 nm
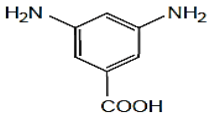 3, 5-Diamdiamino-benzoic acid	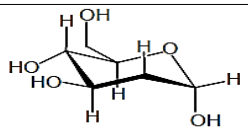 2-Deoxy-D-glucose Acetaldehyde DNA	H_3PO_4 15 min 100°C	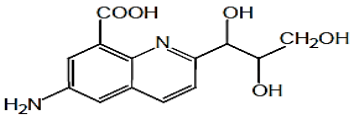 λ_{exc}= 410 nm λ_{em}= 500 nm

Figure 1-7. Coupling the analyte to a substituent and non-substituted position on an aromatic ring to form fluorescent product

Reagent	Analytes	Reaction conditions	Fluorescent product
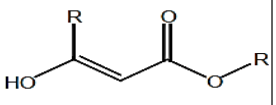 Ethyl acetoacetate	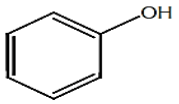 Phenols	H_2SO_4	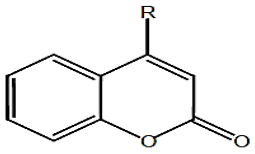 λ_{exc}= 366 nm λ_{em}= 460 nm
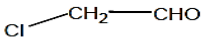 Chloro-acetaldehyde	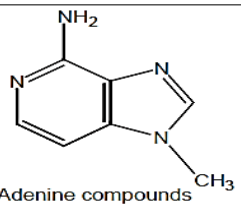 Adenine compounds	pH 6 30 min 100°C	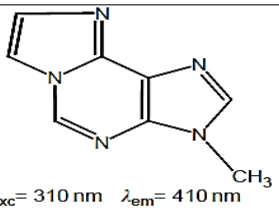 λ_{exc}= 310 nm λ_{em}= 410 nm

Figure 1-8. Coupling the substituted aromatic analyte with non-aromatic reagent to give fluorescent product

2. Redox reactions

Fluorescence labeling reactions involving redox steps have been used for analysis several sample, especially environmental and biological compounds. The most popular oxidizing agents involve potassium permanganate, hydrogen peroxide, strong mineral acids, and cyanogen bromide.

Thiamine (vitamin B1) for example, can easy oxidized to fluorescent product using UV light or oxidizing agents such as (mercuric oxide, cyanogen bromide, and

ferricyanide). The formed thiochrome fluorophore measured at 430 nm when excited at 366 nm. *Figure 1-9*[74-76].

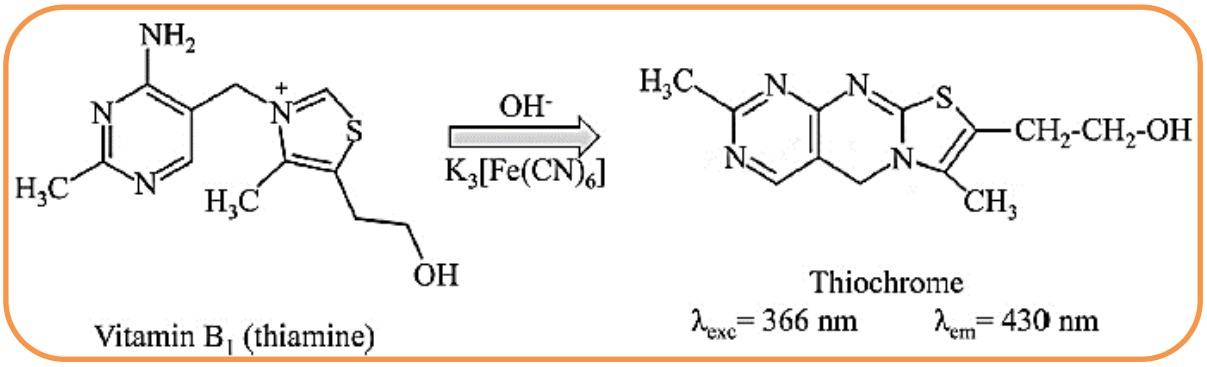

Figure 1-9. Oxidation of thiamine using Potassium hexacyanoferrate (III) in basic media to produce fluorescent product.

Catecholamines, on the other hand, emit fluorescence radiation at 318 nm when excited at 275 nm. However, the direct quantification methods based on their native fluorescence suffer from poor sensitivity and are more prone to chemical interference in the analysis of biological samples owing to matrixes effect (plasma, serum, and urine). Therefore, the selectivity and sensitivity of catecholamines (e.g. Adrenaline) can be enhanced by oxidation of adrenaline with iodine or ferricyanide to produce adrenochrome which then treated with antioxidant such as (ascorbic acid) in alkaline media to produce 3,5,6-trihydroxyindole fluorophore, (*Figure 1-10*). Derivatizing catecholamines with this approach is one of the most sensitive and commonly utilized techniques[77].

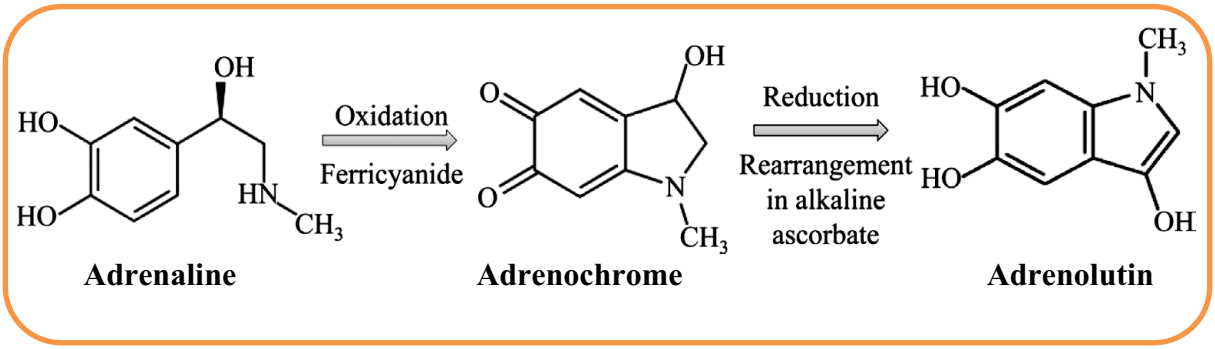

Figure 1-10. Fluorescence derivatization of catecholamines by redox reaction.

3. Hydrolysis Reactions

Non-fluorescent analyte can be converted into a fluorescent product by hydrolysis, which is one of the simplest ways available. In general, the hydrolysis is usually performed in a highly basic medium together with heating if required to form a fluorescent anion.

Since aspirin (acetylsalicylic acid) exhibits weak native fluorescence, whereas the salicylate ion formed by base-hydrolysis of aspirin fluoresces brightly at 400 nm after excitation at 310 nm *Figure 1-11*. As a result, this property were utilized to measure aspirin and salicylates levels in biological fluids[78,79].

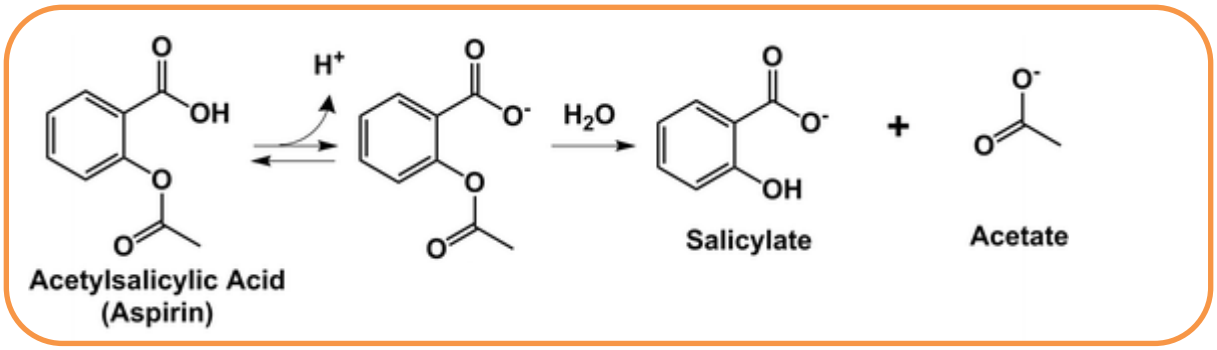

Figure 1-11. Basic hydrolysis of aspirin to produce fluorescence product (salicylates)

4. Photoconversions[80-82]

Many substances can be transformed into fluorescent product when exposed to UV radiation. A typical example that give a rise of this method are the fluorimetric quantification of pesticides and anabolic agent diethylstilbesterol. Even though photochemical derivatization is less used but it offers several advantages over chemical derivatization. Of These:

a. Less chemicals consumption, thus dilution is not necessary.
b. Higher reaction rates because the majority of photochemical reactions are carried out via free radicals.
c. simple to carry out and needing cheap equipment.

d. The method is appropriate for a wide range of technique (e.g. HPLC, flow injection analysis (FIA), thin-layer chromatography (TLC), dynamic systems, and stationary liquid solutions). because it proceeds at room temperature.

Pesticides like deltamethrin, diflubenzuron, and fenvalerate, for example, are easily converted into fluorescent products in protic solvents, whereas polar aprotic solvents are used for fenitrothion and chlorpyriphos *Figure 1-12*.

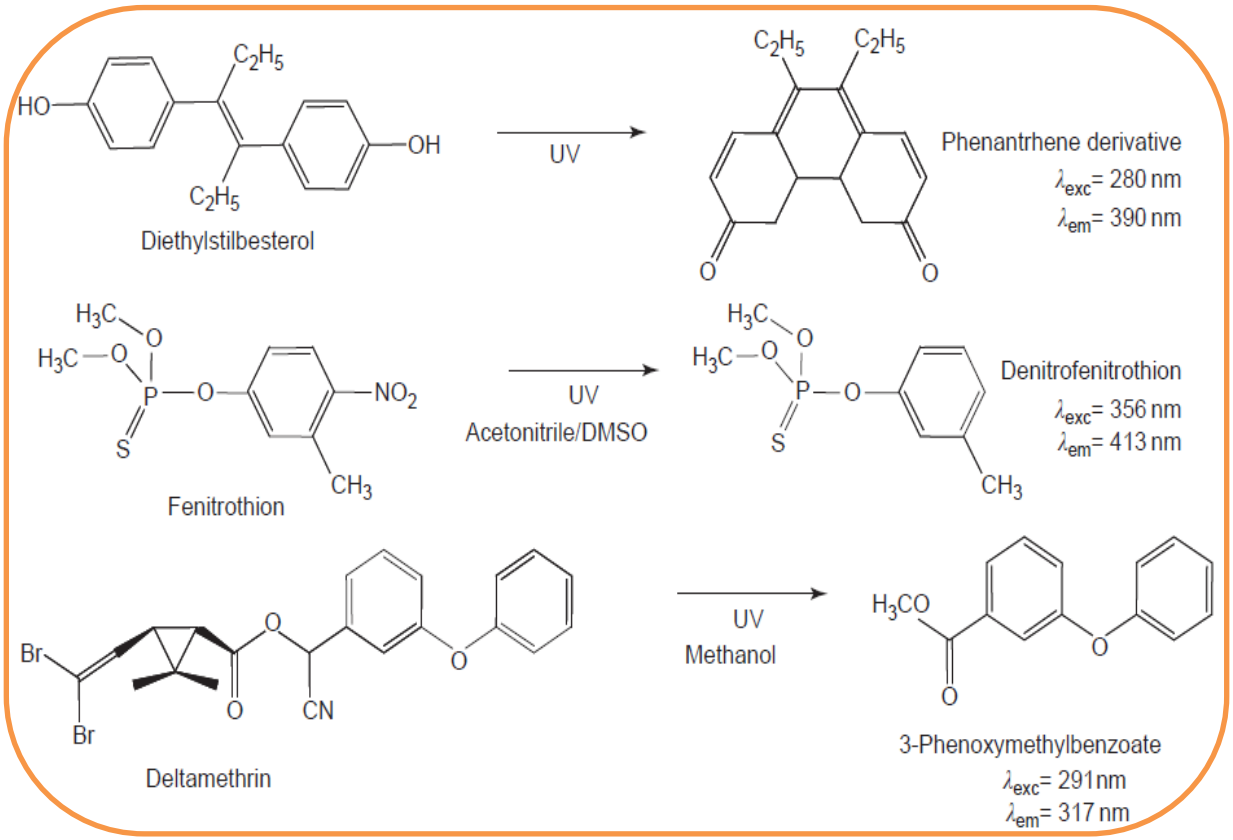

Figure 1-12. Photoconversions of some pesticides to produce fluorescence product

5. Complexation

The basic requirement of any organic chelating reagent is the ability to form a six- or five-member chelating ring via at least two functional groups by covalent and/or coordinate bond with the metal ion to form a rigid structure.

Complexation involves the reaction of a weakly or non-fluorescent organic chelating reagent to form a chelating ring, which in most cases triggers the

compound to emit highly fluorescence radiation because the formation of a chelating ring increases the rigidity of molecules as well as π-π* transition rather than the n-π* transition. This effect was utilized to determine either organic substances (ligand) or metal ions.[83-85].

It was reported that metal complexation has interesting features[86-98]. Of these:

a. Intersystem crossing ($S_1 \rightarrow T_1$) of the aromatic ligand increase when reacted with paramagnetic metal (e.g., Co^{2+}, Fe^{3+}, Cu^{2+}, Ni^{2+}), resulting in a decline in fluorescence intensity.
b. The heavy atom effect is another phenomenon that increases the rate of intersystem crossing. Complexation of heavy diamagnetic metal like TI^{3+}, Pb^{2+}, Hg^{2+}, and Ag^{1+} lead to prevent fluorescence because it increases spin-orbit coupling.
c. Transition metal ions of group VIII d^6 (e.g., Osmium (II), Iridium (III), Rhodium (III), and Ruthenium (II)) form fluorescent chelating complexes with strong-field ligands such as 2,2-bipyridine, 2,2,2,-terpyridine, 1,10-phenanthroline. These complexes reveal $\pi^* \rightarrow d$ emission bands and low-energy-charge-transfer $d \rightarrow \pi^*$ absorption. The complexes of Ruthenium (II)-polypyridine have been frequently utilized as oxygen sensors because they are highly stable, exhibit large quantum yields, and are easily quenched by oxygen.

Metal ions of group IIIA (Indium(III), Gallium(III), Thallium(III), and Aluminum(III)) react with several organic ligands to form a fluorescent chelating complex *Figure* 13.

Flavonol derivatives which are a class of naturally phenolic compounds in the plants react with several ion such as (Al, Zn, Ga, Be, Ba, B, Sn) to form fluorescent chelating complex *Figure* 13[99-102]. Further, the ligand like 8-hydroxy quinoline, fluorescein derivatives, 2,2\-hydroxy azobenzene derivatives form a fluorescent chelating complexes with several metal ions *Figure 1-13*[103-113].

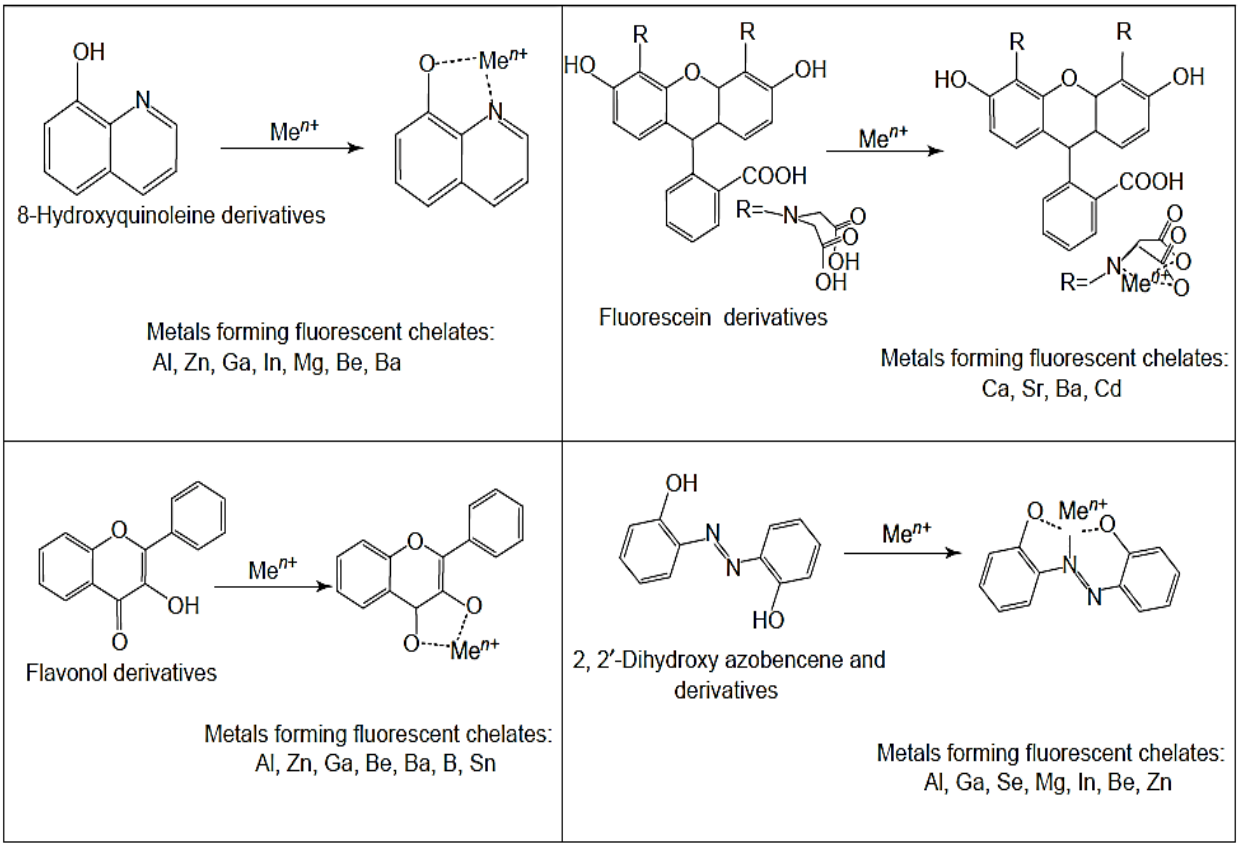

Figure 1-13. Reaction of some organic ligand with several metal ions to produce fluorescence product

In some case, the addition of excess amount of metal ion to a non-fluorescent organic ligand leads to form fluorescent chelating complex. This method was utilized to spectrofluorimetric quantification of tetracyclines and anthracyclines as ligands with Ca^{2+}, Eu^{3+} and Mg^{2+}, in alkaline or neutral solutions, and with Zr^{4+}or Al^{3+} in acidic solutions[114-118].

Metal complexation reaction is the most applicable and convenient fluorescence labeling method because they are rapid and can be driven to completion by adding excess amount of reagent. Hence, it is appropriate for derivatization in post column of chromatographic techniques like capillary electrophoresis and HPLC. For example, quantification of catecholamines derivatives by CE post column method. The method depends on the reaction between catecholic compound with Tb^{3+} ions to form a ternary complex in the presence of EDTA[119].

6. Click reaction

For a long period, the analysis of biomolecules suffered from side reactions owing to the broad range of functionality present resulting in non-specific derivatization. Recently, a set of highly efficient and stereospecific chemical reactions that can performed under a variety of condition were appeared to cover most of biochemical analysis. These reactions known as click reaction.

"Click" can refer to a chemical reaction that fulfills the following requirements [120-123]:

a. Reactions are carried out rapidly at simple conditions in high yields, resulting in the production of a single and stable desired product.
b. The ability to withstand several reaction conditions under various interphases, such as liquid/liquid, solid/liquid, and even solid/solid.
c. Reagents and starting materials are readily available.
d. Use of low toxic or non-harmful solvents. Highly water and oxygen tolerant.
e. If purification is necessary, it must be done in a non-chromatographic technique (e.g. distillation, crystallization).

The most common reactions utilized in click chemistry are Staudinger ligation (involved phosphine as reagent), azide-alkyne cycloadditions *Figure 1-14*. copper free azide-alkyne cycloadditions (strained cyclooctynes was used) *Figure 1-15*, A maleimide with thiol functional group (thiol-Michael addition) *Figure 1-16*, and Diels–Alder cycloaddition[124-129].

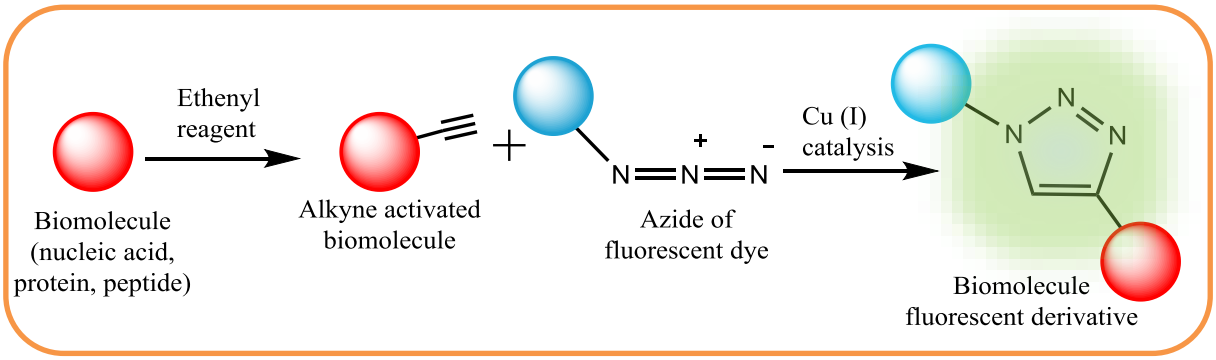

Figure 1-14. Azide-alkyne cycloadditions

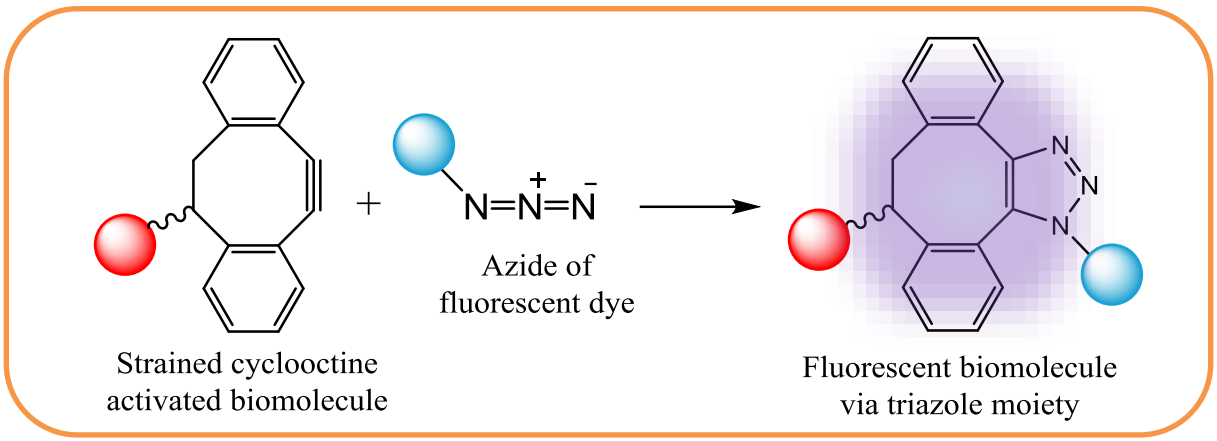

Figure 1-15. Copper free azide-alkyne cycloadditions

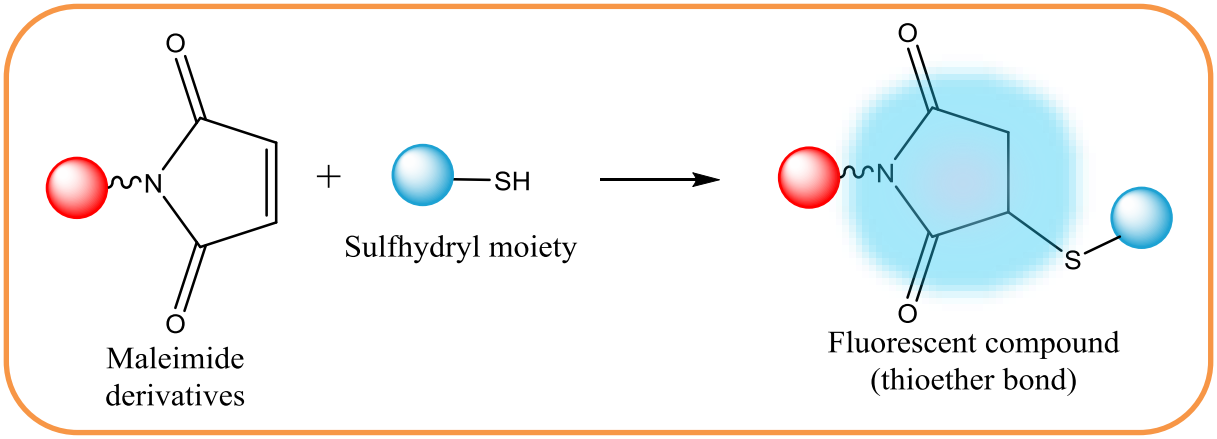

Figure 1-16. Thiol-Michael addition (Click reaction)

1.2.3 Fluorescent labeling dyes

Fluorescent dyes, also known as fluorogenic agent or reactive dyes, have been used by analysts and biologists for decades. An efficient fluorogenic agent is that react rapidly with the desired analyte to produce a highly stable fluorescent product. We can summarize some of the most popular fluorescent labeling dyes as follow[130]:

1. Coumarins[131-135]:

Figure 1-17 exhibit that A and B compounds can be labeled to amino groups in acidic media pH=4.0 to produce blue fluorescence (Fluorescent spectra depend on pH).

Excitation wavelength λ_{ex} max = 342 nm

Emission wavelength λ_{em} max = 447 nm

C and D compounds can be labeled to amino groups in neutral media pH=7.0 to produce a blue fluorescence product (Fluorescent spectra do not depend on pH).

Excitation wavelength λ_{ex} max = 360 nm

Emission wavelength λ_{em} max = 410 nm

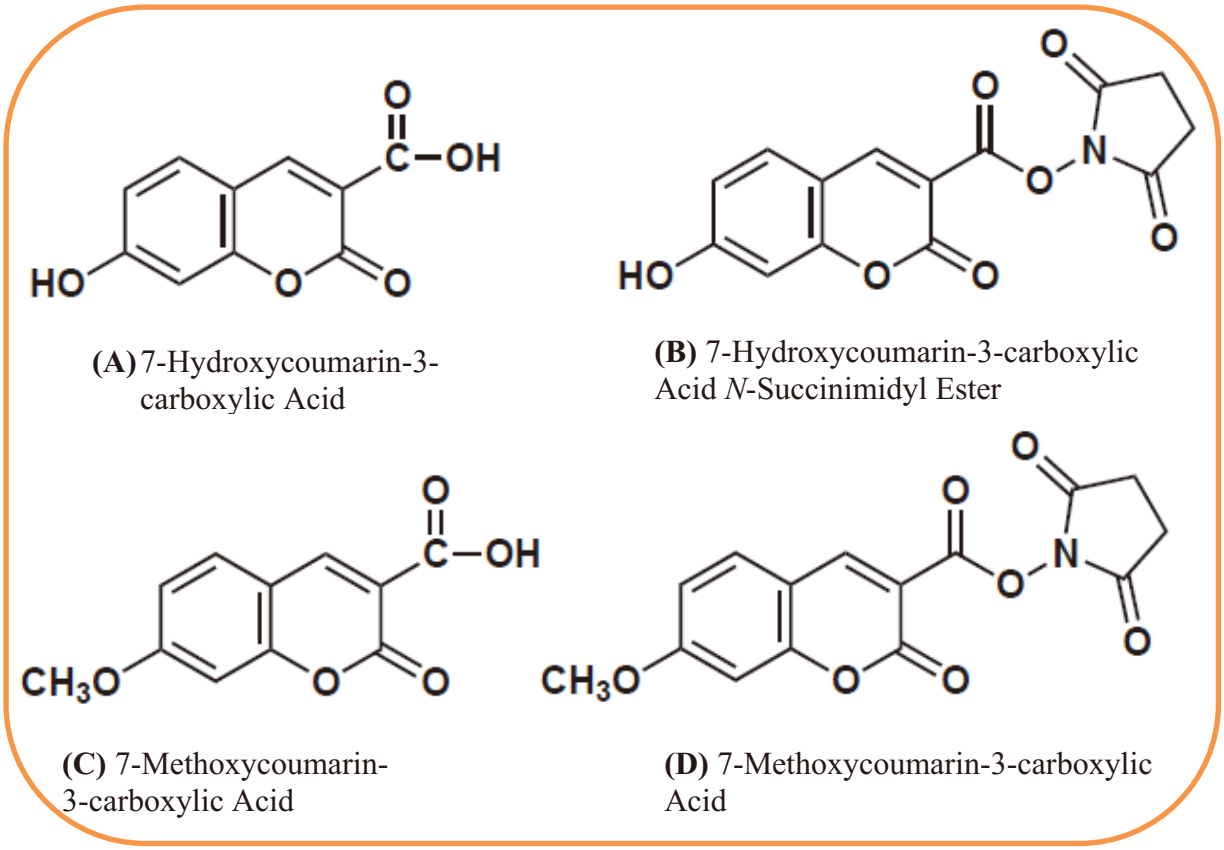

Figure 1-17. Some coumarin derivative compounds.

2. Benzofurazans[136-141]:

As shown in *Figure 1-18*, NBD-F, NBD-Cl, and NBD-PZ emit green-yellow fluorescence owing to NBD core.

Excitation wavelength λ_{ex} max = 468- 490 nm.

Emission wavelength λ_{em} max = 525 - 555 nm

While DBD-F, DBD-ED, DBD-PZ, and DBD-SAH emit yellow fluorescence owing to dimethyl amino sulfonyl benzoxadiazole (DBD) core.

Excitation wavelength λ_{ex} max = 380 nm

Emission wavelength λ_{em} max = 510 nm

NBD-F, NBD-Cl and DBD-F can be labeled to either thiol or amino groups.

NBD-PZ, DBD-ED and DBD-PZ can be labeled to carboxyl groups via amide bond using a coupling agent.

DBD-SAH can be labeled to amino groups due to the active *N*-hydroxysuccinimide group.

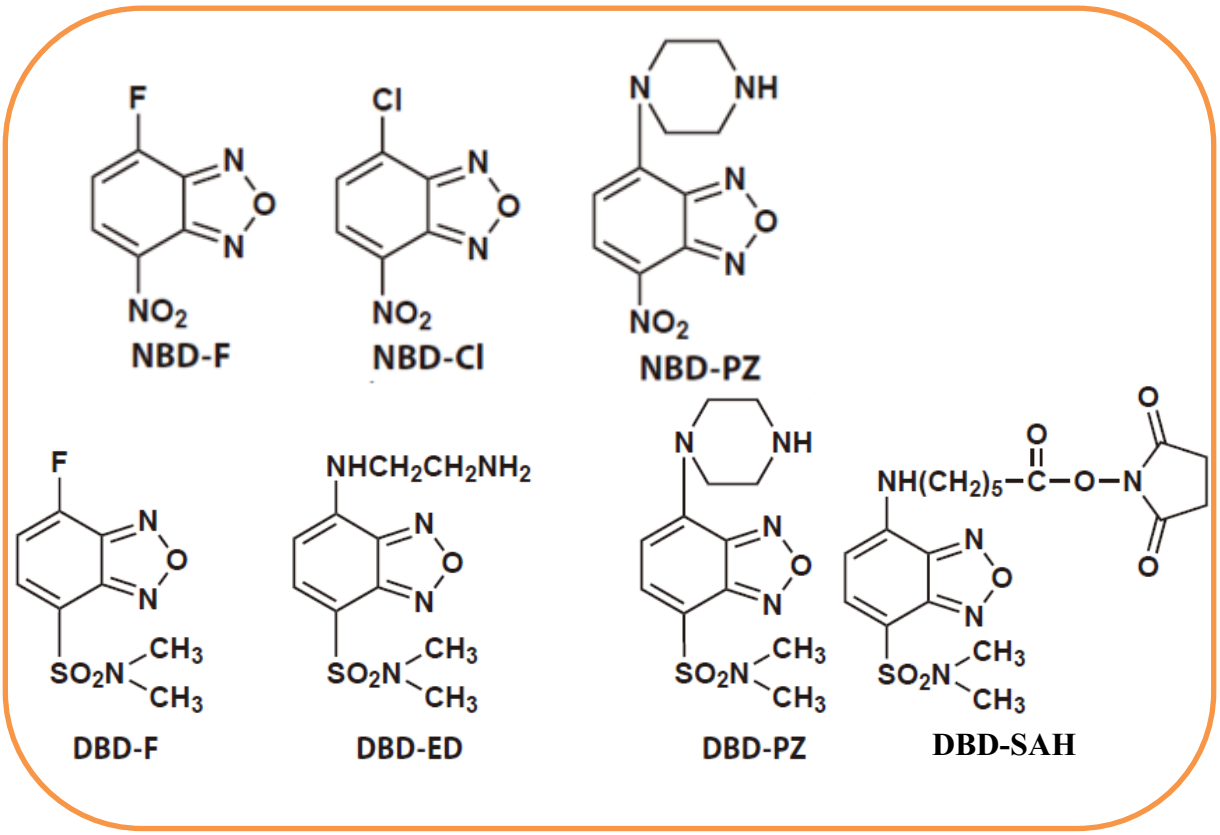

Figure 1-18. Some Benzofurazans derivative compounds.

3. Dansyls[142-145]

Dansyls derivatives emit green-yellow fluorescence owing to dimethyl amino naphthalene sulfonyl (Dansyl) core, as shown in *Figure 1-19*.

Excitation and emission wavelengths depend on the environment.

DNS-Cl can be labeled to amino groups via sulfonamide bond.

DNS-$NHNH_2$ can be labeled to carbonyl groups via hydrazone bond.

DNS-NH-PITC can be labeled to amino groups via thiourea bond.

Excitation wavelength λ_{ex} max = 335 nm

Emission wavelength λ_{ex} max = 460 nm

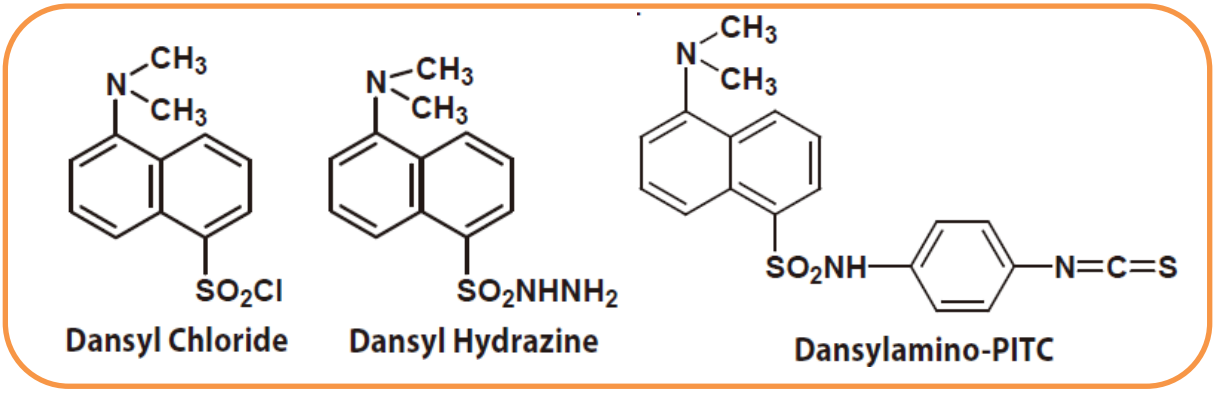

Figure 1-19. Some Dansyl derivative compounds.

4. Fluoresceins[146-159]

Fluoresceins emit green fluorescence. *Figure 1-20* represent the most common Fluoresceins derivative.

Excitation wavelength λ_{ex} max = 494 nm

Emission wavelength λ_{ex} max = 521 nm

5 = -NCS (Fluorescein 5-Isothiocyanate (isomer I) (=5-FITC))

6 = -NCS (Fluorescein 6-Isothiocyanate (isomer II) (=6-FITC))

5 = -COOH (5-Carboxyfluorescein Hydrate (=5-FAM))

6 = -COOH (6-Carboxyfluorescein Hydrate (=6-FAM))

5 = -CO-NHS (5-Carboxyfluorescein *N*-Succinimidyl Ester (=5-CFSE))

5 = -maleimide (Fluorescein-5-maleimide)

5 = -NH_2 (5-Aminofluorescein (isomer I))

6 = -NH_2 (6-Aminofluorescein (isomer II))

5 = -CONH-Alkyne (5-FAM-Alkyne)

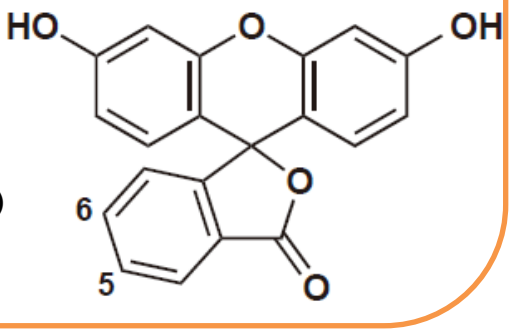

Figure 1-20. Some Fluoresceins derivative compounds.

5-FITC and 5-FITC can be labeled to amino groups or thiol groups.

5-FAM and 6-FAM can be labeled to amino groups by amide bond formation using a coupling agent.

5-CFSE can be labeled to amino groups without a coupling agent due to the active *N*-hydroxysuccinimide group.

Fluorescein-5-maleimide can be labeled to thiol groups due to the maleimide group.

5 or 6-Aminofluorescein can be labeled to carboxyl groups by amide bond formation using a coupling agent.

5-FAM-Alkyne can be labeled to azido groups via click reaction.

5. Europium Chelate Complex[160]

ATBTA-Eu^{3+} (*Figure 1-21*) emit red fluorescence derived from Europium (Eu^{3+}). It exhibits stable fluorescence in various aqueous buffers and is suitable for time-resolved fluorometry due to its long fluorescent life time.

ATBTA-Eu^{3+} easily labeled to an amino group after conversion to DTBTA-Eu^{3+} by cyanuric chloride.

Excitation wavelength λ_{ex} max = 335 nm

Emission wavelength λ_{ex} max = 616 nm

6. Boron Di-pyromethenes[161]

BDP FL and BDP FL NHS Ester (*Figure 1-22*) emit green fluorescence.

They can be labeled to amino groups.

Excitation wavelength λ_{ex} max = 490-505 nm

Emission wavelength λ_{ex} max = 513 nm

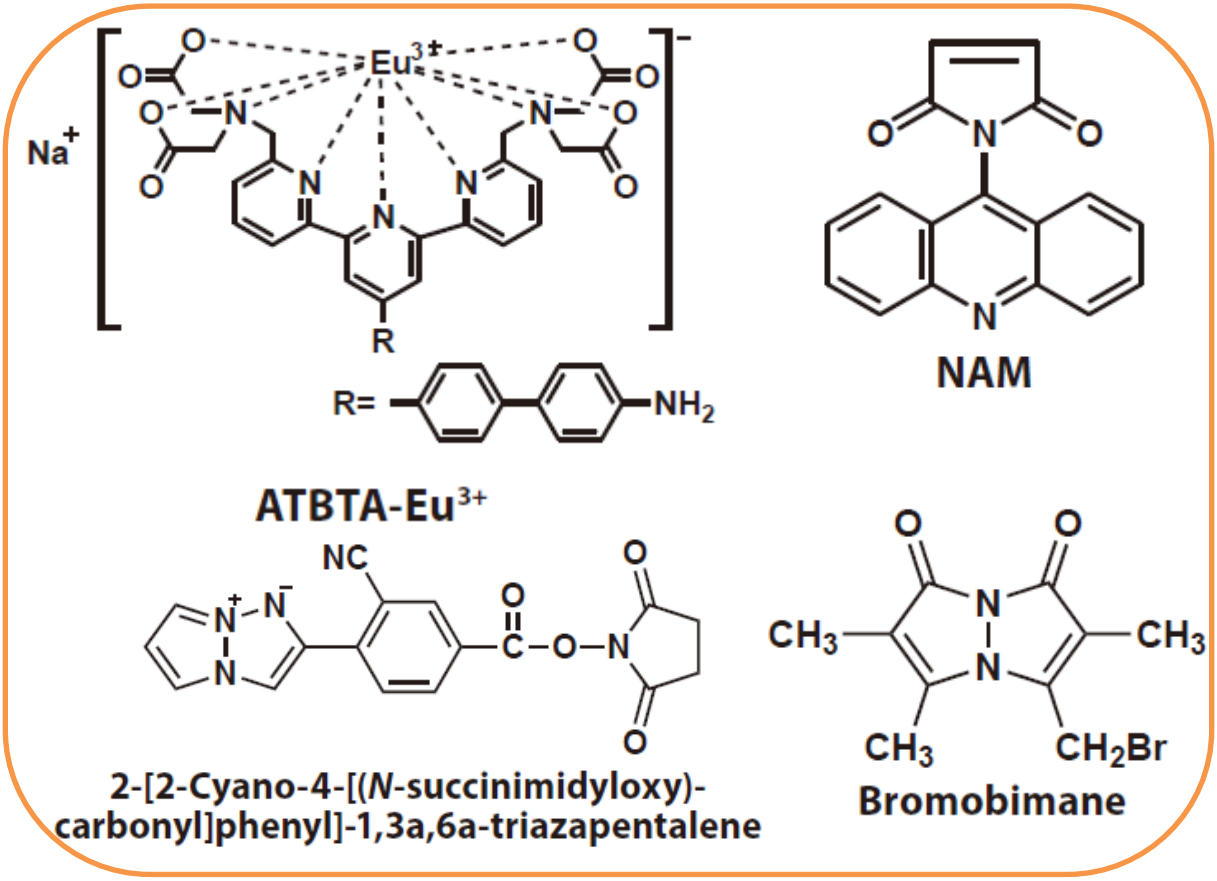

Figure 1-21. Chemical structure of some fluorogenic compounds.

Pyrenes[162-166]

Pyrenes (*Figure 1-22*) emit blue fluorescence.

Excitation wavelength λ_{ex} max = 342 nm

Emission wavelength λ_{ex} max = 386 nm

N-(1-Pyrenyl)-maleimide can be labeled to thiol groups.

1-Pyrenebutyric Acid can be labeled to amino groups by amide bond formation using a coupling agent.

1-Aminopyrene can be labeled to carboxyl groups by amide bond formation using a coupling agent.

1-Ethynylpyrene and 1-[(2-Propynyloxy)methyl]pyrene can be labeled to azido groups via click reaction.

1-(Azidomethyl)pyrene can be labeled to terminal alkynes or cyclooctynes via click reaction.

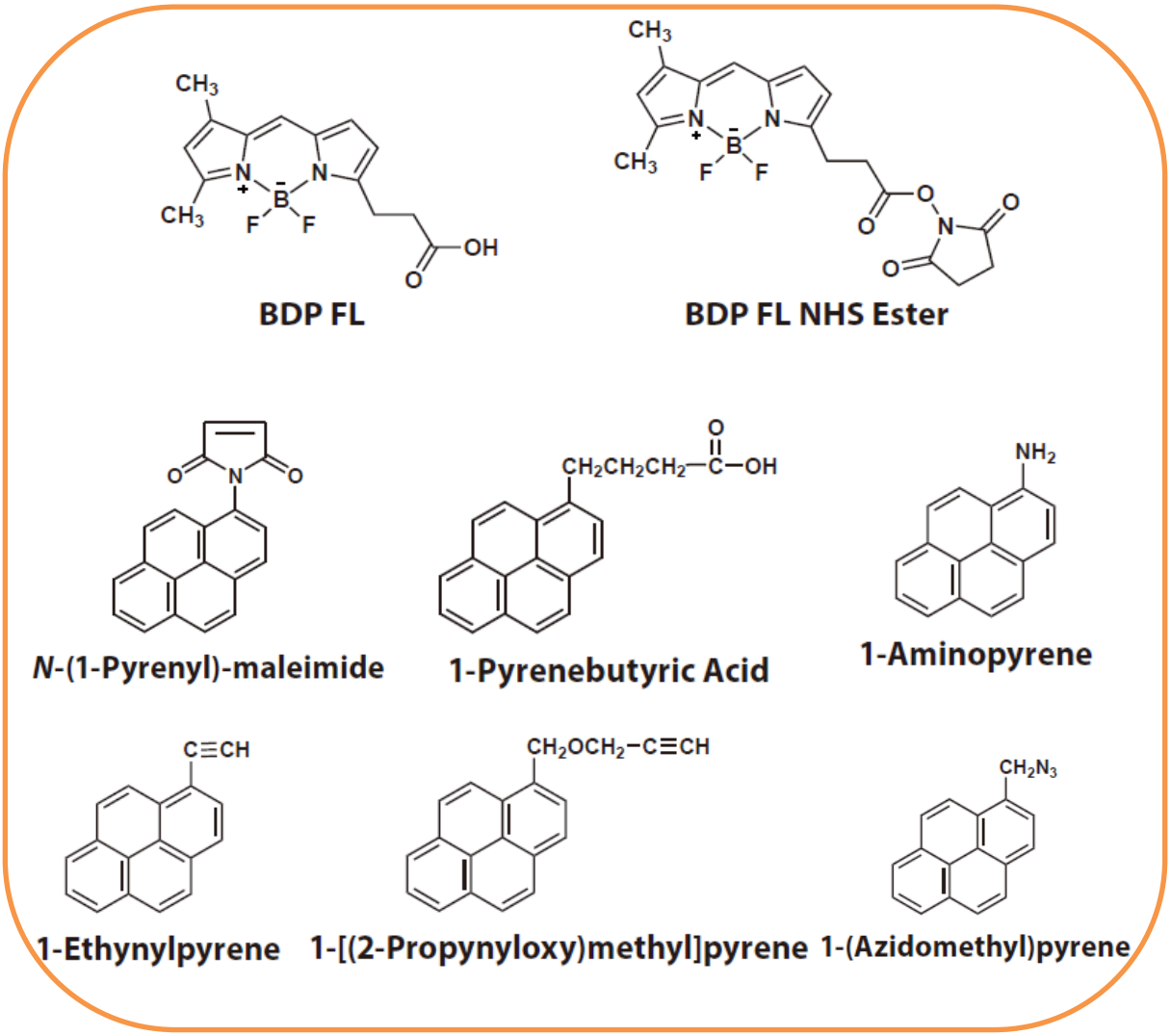

Figure 1-22. Derivatives of pyrene and boron Di-pyromethenes compounds.

7. Acridine[167,168]

Acridine (*Figure 1-21*) emits blue fluorescence.

NAM can be labeled to thiol groups through click reaction.

Excitation wavelength λ_{ex} max = 365 nm

Emission wavelength λ_{ex} max = 440 nm

8. Bimane[169,170]

Bromobimane (*Figure 1-21*) emits blue fluorescence only when bonding to a thiol group. Bromobimane can be specifically labeled to thiol groups.

Excitation wavelength λ_{ex} max = 390 nm

Emission wavelength λ_{ex} max = 480 nm

10. Triazapentalene[171]

Triazapentalene (*Figure 1-21*) emit yellow fluorescence in dichloromethane such as [2-[2-Cyano-4-[(*N*-succinimidyloxy)-carbonyl]phenyl]-1,3a,6a-triazapentalene] which exhibits fluorescence solvatochromism. It can be labeled to amino groups due to the active *N*-hydroxysuccinimide group.

Excitation wavelength λ_{ex} max = 420 nm

Emission wavelength λ_{ex} max = 572 nm

1.3 Meropenem

Meropenem (*Figure 1-23a*) is an intravenous beta-lactam antibacterial with an ultra-broad spectrum of activity against both gram-positive and gram-negative bacteria[172-175]. Meropenem reveals good stability toward β-lactamases and is used as a last-resort antibiotic, particularly in intensive care units, to treat intra-abdominal infection, peritonitis, bacterial meningitis, febrile neutropenia, gynaecological, pneumonia, anthrax, and sepsis. Meropenem is a new antibiotic from the carbapenem family of antibacterial that has a truly extended spectrum when used alone[176-179]. Meropenem can be used to treat various infections that are caused by multiple drug-resistant organisms, as well as infections due to mixed aerobic and anaerobic organisms[180]. Meropenem, like other beta-lactam antibiotics, penetrates the cell wall of bacteria and inhibits the enzymes known as penicillin-binding proteins (PBPs), which catalyze the cross-linking of glycopeptides that form the bacterial cell wall. Consequently, preventing cell wall synthesis[181]. Despite having a similar structure to imipenem, meropenem has some advantages over it, including a lower seizure proclivity and being stable against human renal damage caused by dehydropeptidase I (DHP-I), So it does not require to be combined with cilastatin[182-184].

1.4 Clozapine

Clozapine (*Figure 1-23b*) [3-chloro-6-(4-methylpiperazin-1-yl)-11H benzo[b][1,4]benzodiazepine], a member of the dibenzodiazepine derivatives, is considered a second-generation anti-psychotic commonly used in the treatment of both negative and positive symptoms of schizophrenic patients[185-187]. CLZ is regarded as an effective choice for patients who suffer from resistance or are unresponsive to conventional neuroleptic medications like haloperidol[188,189]. Clozapine is metabolized by liver through microsomal oxidative cytochrome to the relatively inactive metabolites clozapine-Noxide and N-Desmethylclozapine[190]. Despite its excellent effectiveness, clozapine's usage is severely limited due to the incidence of drug-induced agranulocytosis in 1-2 % of patients[191-194]. This effect is attributed to the toxicity of one of the clozapine's metabolites, Ndesmethylclozapine, that appears to be more harmful to the bone marrow than CLZ itself, leading to decreased white blood cells. Thus, Regular monitoring of the white blood cell count is recommended to reduce this risk[195-198]. It was reported that clozapine metabolism is inhibited by fluvoxamine medication, resulting in considerably higher clozapine levels in the blood[199].

1.5 Amlodipine

Amlodipine (*Figure 1-23c*) chemically is a third generation and most effective antihypertensive medication that belongs to the calcium channel blockers family that works by obstructing calcium ions (Ca^{+2}) movement through calcium channels, which leads to a reduction in blood pressure in hypertension patients[200-202]. Moreover, amlodipine has vasodilation activity makes it suitable to be used to treat ischemic heart disease in patients with either vasospastic angina or stable angina and without cardiac failure [203,204]. Like other calcium channel blockers, amlodipine offers better protection against stroke and is an excellent choice to treat Raynaud's phenomenon[205].

1.6 Sitagliptin

Sitagliptin (*Figure 1-23d*) is a new anti-diabetic drug belongs to dipeptidyl peptidase-4 inhibitors that work by increasing insulin production while lowering glucagon production by the pancreas. It less favored than a sulfonylurea or metformin drugs in the United Kingdom. Sitagliptin can be used alone or in combination with other antihyperglycemic drugs such, metformin, simvastatin or thiazolidinediones[206-209].

1.7 Metformin hydrochloride

Metformin (*Figure 1-23e*), N, N-dimethylimidodicarbonimidic diamide mono-hydrochloride, is the most effective and widely used medication for the treatment of type 2 diabetes, particularly in overweight people. It acts by inhibiting the gluconeogenesis pathway in the liver. It is also used to treat polycystic ovarian syndrome and improve weight loss in certain cases. It lowers LDL cholesterol levels and increases insulin sensitivity by boosting peripheral glucose absorption[210-214]. Metformin not only reduced glucose levels in severely burnt patients, but it also increased muscle protein synthesis[215]. Common adverse effects involve lactic acidosis, nausea, diarrhea, and abdominal pain[216-218].

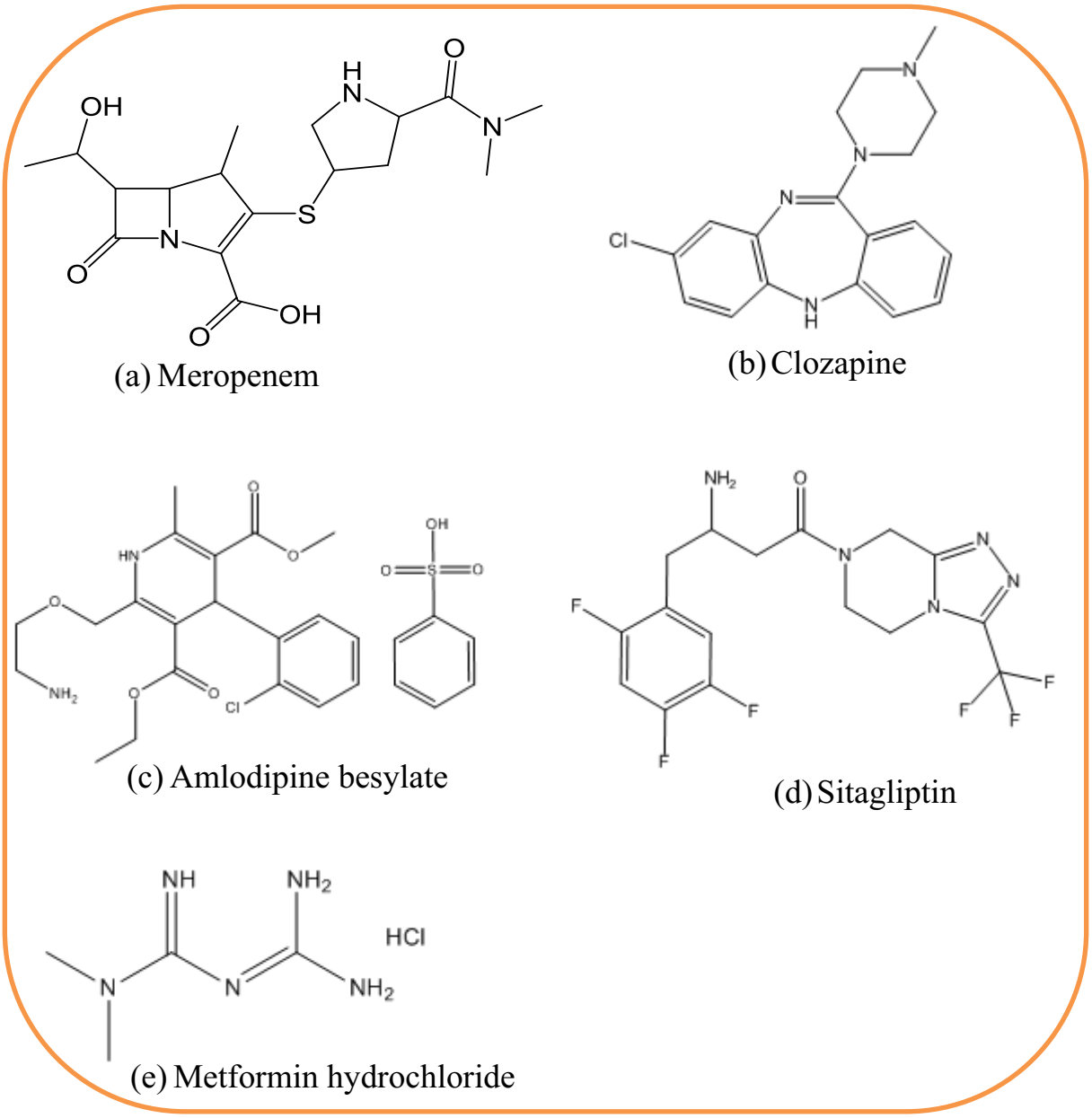

Figure 1-23. Chemical structure of the studied drugs.

Aims of the study:

1- Develop new fluorometric methods for analysis of MRP, CLZ, AMB, STA, and MET in real samples.
2- Optimize the experimental conditions to increase sensitivity.
3- Construction of calibration curves with ANOVA for their regression lines.
4- Validate the proposed methods according to ICH recommendations.
5- Applying the methods for determination of the studied drugs in their dosage form and spiked human plasma.
6- Compare the proposed methods with official or reported one using student's t and f tests.
7- Determination of biomarkers levels such as (D-dimer, LDH, GPT, TG, and plasma MET) in the diabetic and non-diabetic COVID-19 patients before and after remdesivir administration to show the effect of this drug on these biomarkers.

Chapter Two

Experimental part

2. Experimental Part

2.1. Apparatus

1. Spectrofluorometric measurements were done using shimadzu (RF-5301 PC, Kyoto, japan) equipped with xenon lamp (150 watt) together with 1 cm quartz cuvette. Scanning wavelength range was 220-900 nm (± 0.3 accuracy and ± 0.1 repeatability). Scanning and measurements adjustments were:

   i. Slit width set at 5 nm for both excitation and emission monochromator.

   ii. sensitivity: High

   iii. response time: Auto

   ix. scanning speed: Super
2. Thermostatically controlled water bath (LCB-22D, daihan Labtech CO., Korea) was utilized for heating purpose.
3. pH meter wtw (inolab pH 720, Germany) for pH adjustment.
4. Sensitive digital balance (BP 3015, Sartorius Germany).
5. Centrifuge PLC model (03 USA).
6. Oven BS size two, Gallenkamp (England).
7. Hot plate stirrer, J Lab, model (LMS-100).
8. D-dimer level was measured using VIDAS (BIOMERIEUX SA, MARCY L'ETOILE-France).
9. LDH, GPT and TG levels were measured using ARCHITECT c4000 Clinical Chemistry Analyzer (Abbott, Japanese).

2.2. Chemical materials

The chemical material involved in this study are showed in the *Table* 2.1. The physical and chemical characteristic of these chemical materials were supplied by MSDS.

Table 2.1. Chemical material used in this study

Seq.	Name	Molecular Formula	Purity%	Supplier
1	1,4-dioxan	$C_4H_8O_2$	99.8	Merck
2	2-Mercaptoethanol	C_2H_6OS	99	Sigma-Aldrich
3	NBD-Cl	$C_6H_2ClN_3O_3$	98	GK biotechnology.china
4	Amlodipine Besylate	$C_{20}H_{25}ClN_2O_5$	≥ 99	SDI-Iraq
5	Acetone	C_3H_6O	≥ 99.5	Merck
6	Acetonitrile	CH_3CN	≥ 99.9	Merck
7	Aluminum chloride	$AlCl_3$	99.9	BDH
8	Boric acid	BH_3O_3	99.8	Sigma-Aldrich
9	Butanol	$C_4H_{10}O$	≥ 99.5	Merck
10	Clozapine	$C_{18}H_{19}ClN_4$	99.1	GK biotechnology.china
11	DMF	C_3H_7NO	≥ 99.5	Merck
12	DMSO	$(CH_3)_2SO$	≥ 99.0	Merck
13	Ethanol for HPLC	C_2H_5OH	Absolute	Sigma-Aldrich
14	Ethyl acetate	$C_4H_8O_2$	99.8	Merck
15	Hydrochloric acid	HCl	Con.37%	J T Baker
16	PQ-2Br	$C_{14}H_6Br_2O_2$	98	GK biotechnology.china
17	Meropenem.3H_2O	$C_{17}H_{25}N_3O_5S\cdot 3H_2O$	98.9	SDI-Iraq
18	Metformin.HCl	$C_4H_{11}N_5$.HCl	99.6	SDI-Iraq
19	Methanol	CH_3OH	99.8	J T Baker
20	Sitagliptin phosphate	$C_{16}H_{18}F_6N_5O_5P$	99.5	GK biotechnology.china
21	O-phthalaldehyde	$C_8H_6O_2$	≥ 97	GK biotechnology.china
22	Potassium chloride	KCl	99.8	Reachim
23	Sodium hydroxide	NaOH	≥ 97	BDH

2.3 Preparation of standard solutions

2.3.1 NBD-Cl reagent 1 mg mL^{-1}

The reagent solution was freshly prepared by dissolving 50 mg of reagent with small amount of methanol in 50 mL volumetric flask and diluted to the mark with the same solvent. Aluminum foil was used to protect the solution from light.

2.3.2 O-Phthalaldehyde reagent 0.1 w/v %

A stock reagent solution was freshly prepared by dissolving 100 mg of reagent with small amount of methanol in 100 mL volumetric flask and diluted to the mark with the same solvent.

2.3.3 2-Mercaptoethanol 1 v/v %

A stock 2-ME solution was freshly prepared by pipetting 1 mL of 2-ME into 100 mL volumetric flask and diluted to the mark using methanol.

2.3.4 3,6-Dibromo-9,10-phenanthrenequinone 15 µg mL^{-1}

A reagent solution was freshly prepared by dissolving 0.01 g of PQ-2Br in a small amount of DMF in 100 mL calibrated flask and completed to the mark with the same solvent. A further dilution was performed to prepare a working solution with 15 µg mL^{-1}.

2.3.5 Borate buffer 0.2 M

A solution of 0.2 M borate buffer of pH (7.0 – 12.0) was prepared by dissolving 1.237 g of boric acid (H_3BO_3) and 1.5 g of potassium chloride (KCl) in 100 mL of distilled water. The solution of required pH value was attained by adjust the pH of solution using 0.2 M sodium hydroxide.

2.3.6 Sodium hydroxide 0.2 M

A stock solution of 0.2 M NaOH was prepared by dissolving 0.8 g in small amount of distilled water (in methanol in the case of MET determination) in 100 mL calibrated flask and diluted to the mark with the same solvent.

2.3.7 Hydrochloric acid 0.2 M

A working solution of 0.2 M HCl was prepared by pipetting 1.67 mL of 37% HCl in 100 mL calibrated flask and diluted to the mark using methanol.

2.3.8 Drugs 100 μg mL^{-1}

A stock solution of 100 μg mL^{-1} of each studied drug was prepared by dissolving 10 mg of the required drug in a suitable solvent (acetone for clozapine; methanol for metformin hydrochloride; distilled water for the other drugs) in a 100 mL volumetric flask. The solution was then diluted to the mark with the same solvent. The working standard solutions containing 10 μg mL^{-1} were prepared from stock solutions by dilution. There is a six-day shelf-life of the stock solution when stored at 4 °C.

2.4. Procedure for pharmaceutical formulation

2.4.1. Procedure for meropenem vials[219]

An amount of meropenem®(1g) vial powder equivalent to 10 mg meropenem trihydrate was accurately weighed and dissolved in 25 mL distilled water in 100 mL volumetric flask. The solution was diluted to the mark to prepare a stock solution labeled to contain 100 μg mL^{-1} of MRP. This solution was further diluted to obtain a solution with final MRP concentrations of 100 ng mL^{-1} in the calibration curve procedure detailed in chapter 3. MRP concentrations were calculated using the linear regression equation.

2.4.2. Procedure for clozapine, Amlodipine Besylate, and Sitagliptin phosphate tablets[220]

Five (Clozapex® 100 mg, or Amlodipine Besylate tablets 5 mg, or Januvia® tablets 128.5 mg) tablets have been carefully weighed and crashed into a fine powder using a stoneware grinder. An accurate quantity of the obtained powder equivalent to 10 mg pure drug was weighed and then dissolved using distilled water (acetone and methanol in the case of clozapine and Amlodipine respectively). The resultant solution was filtered and diluted to the mark with the same solvent into 100 mL volumetric flask to make a drug stock solution with 100 μg mL^{-1}. After further dilution, a solution with concentrations of 10 μg mL^{-1} was produced. This solution has been further diluted to make a solution with a final concentration within calibration curve range of each drug. The linear regression equation of each calibration graph was used to calculate the corresponding drug concentration.

2.5. Procedure for spiked human plasma

A fresh healthy human whole blood plasma was obtained by collect 4 mL of drug -free blood from four healthy human volunteers into a vacutainer sodium heparin tube, which has been subsequently centrifuged at 4000 rpm for 30 minutes. Thereafter, in centrifugal tubes, 1 mL of drug stock standard solution was spiked with 1 mL of fresh plasma and 3 mL of acetonitrile solvent (proteins denaturation agent). The resulting solution was diluted to 10.0 mL using distilled water (acetone and methanol in the case of clozapine and Amlodipine respectively) and centrifuged again at 4000 rpm for 20 minutes[221]. The produced supernatant was diluted with the same solvent to obtain a final drug concentration within a range of calibration curve for each drug.

2.6 Clinical subject

2.6.1 Study design

The clinical study flow chart was illustrated in scheme 2-1.

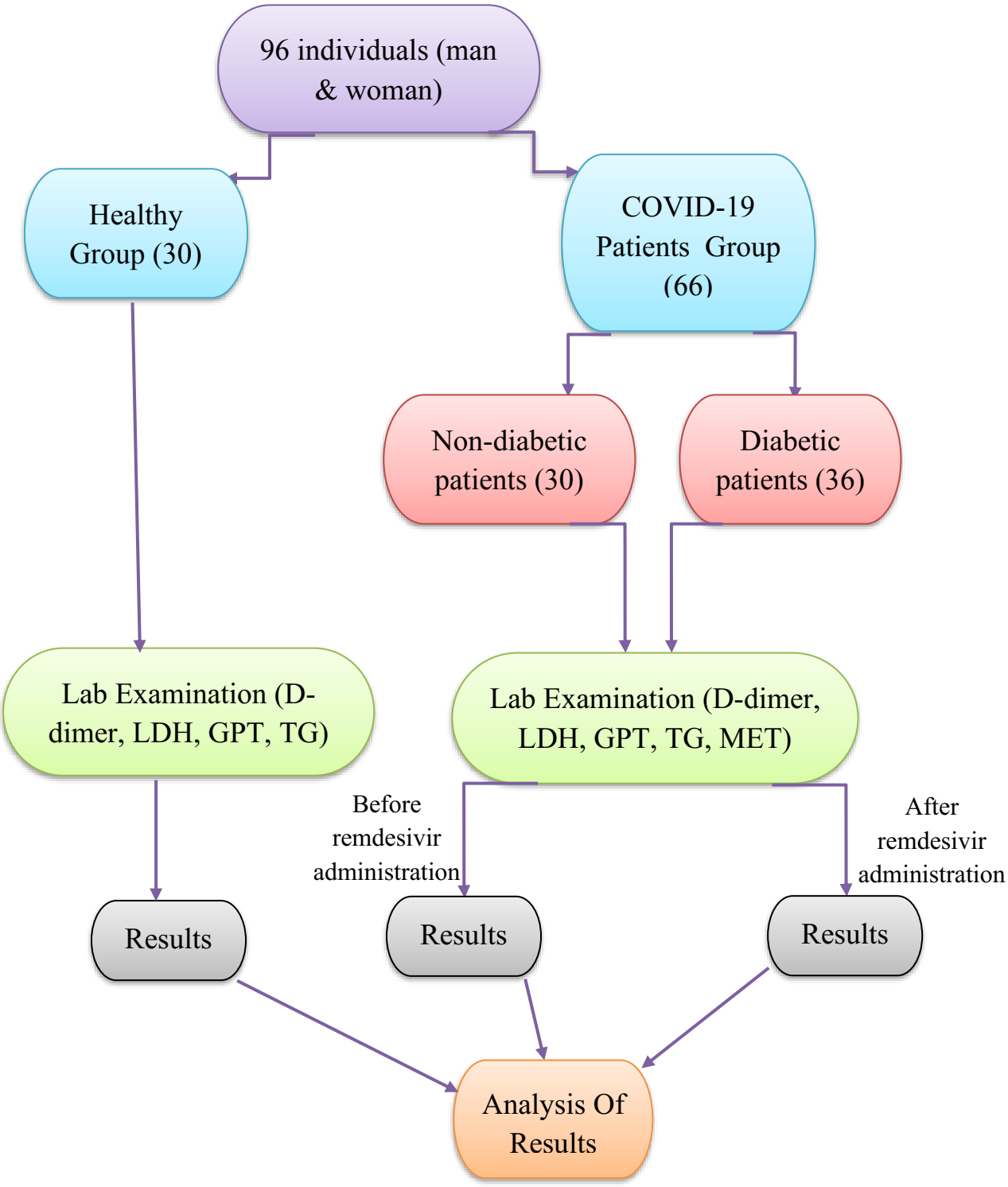

Scheme 2-1. Schematic diagram represents the flow chart for the clinical study

2.6.2 Study duration

This study was conducted from January 2021 to April 2021 in al-Hayat Care Center (seven Lobby Building) in Merjan Medical City for Internal Medicine and Cardiology.

2.6.3 Collection of Samples

Blood sample was collected using disposable syringes together with needles. Five mL of blood samples were gained from each control and patients groups. These samples were centrifuged at 4500xg for 10 minutes in EDTA tube or gel tube. Serum or plasma are separated and divided into two fractions. One of these fractions going to central clinical biochemistry lab of Merjan hospital and undergoes the required routinely examination. The second was collected using Epperdrof tubes and then frozen until use.

2.6.4 Body Mass Index (BMI)

Body mass index was calculated in all subjects according to ratio depend on weight and height obtained by applying a mathematical equation, in which the weight in kilogram is divided by the square height in meter, and the results were considered as follows[222]:

BMI (kg/m^2) = weight (kg) / height (m^2)

Underweight ≤ 18.5(kg/m^2)

Normal weight between 18.5 - 24.9(kg/m^2)

Overweight between 25-29.9(kg/m^2)

Obese ≥30(kg/m^2).

2.6.5 Administration of Remdesivir

The COVID-19 patients were administered with 200 mg I/V dose of remdesivir as a first dose followed by a dose of 100 mg I/V for five days. The infectious diseases physician made a personalized decision for remdesivir dosage, followed by treatment extension up to 10 days depending on the patient's clinical condition or based on patient's comfort with the medication or bacterial co-infection and ventilation duration. The remdesivir is accessible in two dosage forms including a fluid and a powder. The powder should be blended in liquid and imbued (gradually infused) into a vein over by a specialist or medical caretaker in a clinic. It is commonly given once in a day for a duration of five to ten days. The duration of treatment is dependent on patient's body reaction to medication[223,224].

Chapter Three

Results & Discussion

3. Result and discussion

3.1 Introduction

The recent literature survey of the analytical papers in the world exhibits that the analytical chemists during the last decade adopted several efficient rapid organic reactions and are continually looking for highly sensitive analytical methods in pharmaceutical, biochemical, and clinical fields using micro samples. Fluorescence spectroscopy is one of the most popular and efficient technique that meets the requirement of high sensitivity without loss of precision or specificity.

In order to estimate the concentration of non-fluorescent pharmaceutical products spectrofluorometrically, a variety of fluorescent labeling reagent is used. Some of which were illustrated in chapter one.

Herein, we present new click-like validated methods for quantification of some drugs in their dosage form and fresh human plasma. The study includes three parts, the first one involves determination of meropenem and clozapine in their pharmaceutical formulation and human plasma using NBD-Cl as analytical fluorogenic reagent. The second represent determination of amlodipine besylate and sitagliptin in their pharmaceutical formulation and human plasma using O-phthalaldehyde as analytical fluorogenic reagent in the presence of 2-mercaptoethanol as fluorophore stabilizer agent. The third part represent determination of metformin hydrochloride in a fresh human plasma using 3,6-Dibromo-phenanthrenequinone as analytical fluorogenic reagent.

Both the studied drugs and fluorescence derivatizing reagents do not exhibit fluorescence intensity unless a reaction occurs between the analytical derivatizing reagent and the drug of interest to form a fluorescent product which can be measured spectrofluorometrically.

3.2. Determination of meropenem and clozapine using NBD-Cl as fluorogenic derivatization reagent.

3.2.1 Assigning the fluorescence spectrum of NBD-Drug fluorophore

NBD-Cl is one of the most fluorescence derivatizing reagents that has been utilized for quantifying a wide range of compounds with a secondary or primary amine moiety. The mentioned drug acts as a source of the secondary amino group. Under heated alkaline conditions, a nucleophilic aromatic substitution reaction occurred in which these drugs acted as a nucleophile which attacked an electron-poor aromatic molecule (NBD-Cl), resulting in the substitution of a leaving group (Cl) by one of the mentioned drug *Figure* 3-1. The reaction produces a highly fluorescent colored adduct whose excitation and emission wavelengths were detailed in *Table* 3-1. This variation in wavelength depends on the molecular structure of reacted molecule and environment. *Figure* 3-2 & 3-3 represent the fluorescence spectra for NBD-MRP and NBD-CLZ fluorophores respectively against blank solution prepared under the same condition without drug.

Table 3-1 Excitation and emission wavelengths of the NBD-Drug product

No.	NBD-Drugs	Wavelengths (nm)	
		Excitation	Emission
1	NBD-Meropenem	471	536
2	NBD-Clozapine	469	540

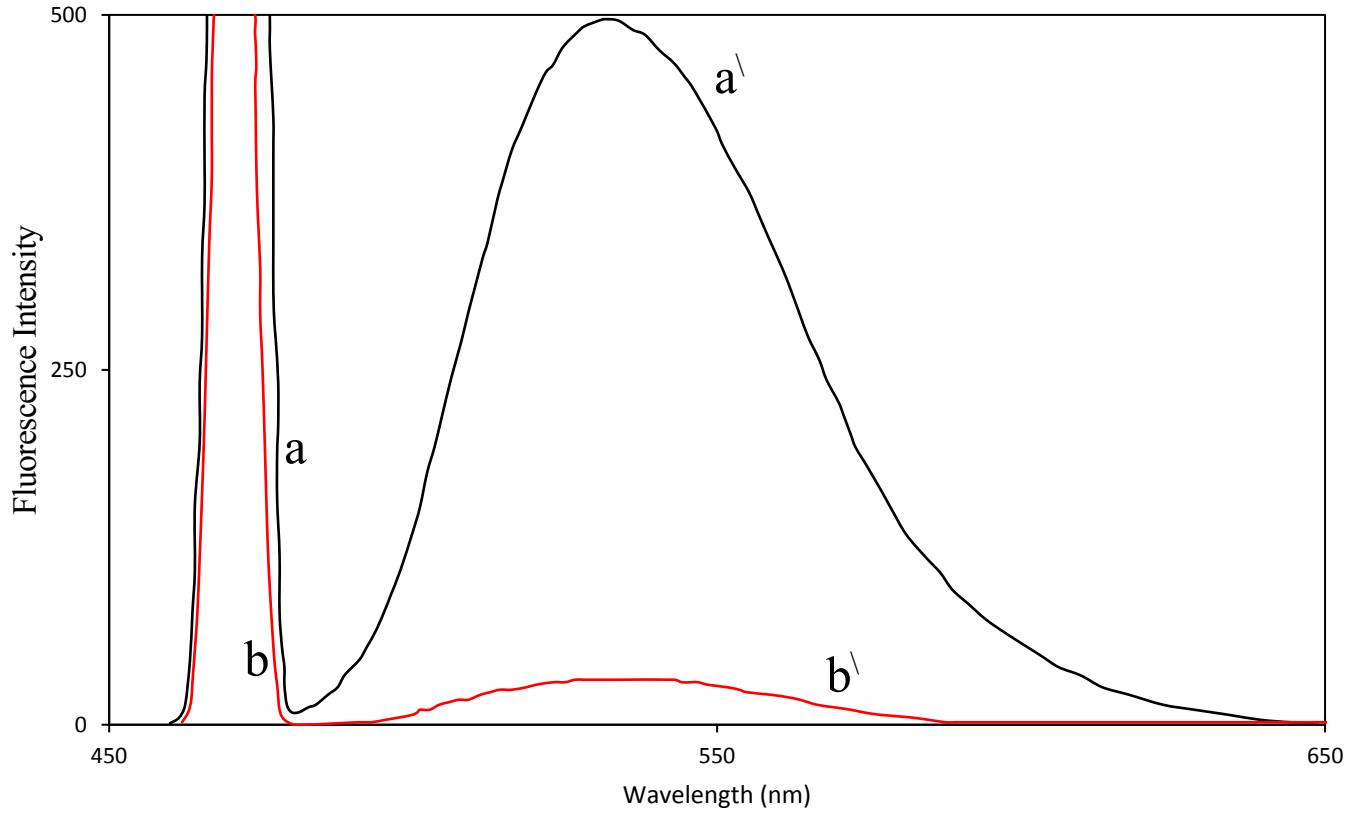

Figure 3-2. Excitation and emission spectra of MRP-NBD product (a,a\) with blank solution (b,b\) using optimal experimental condition.

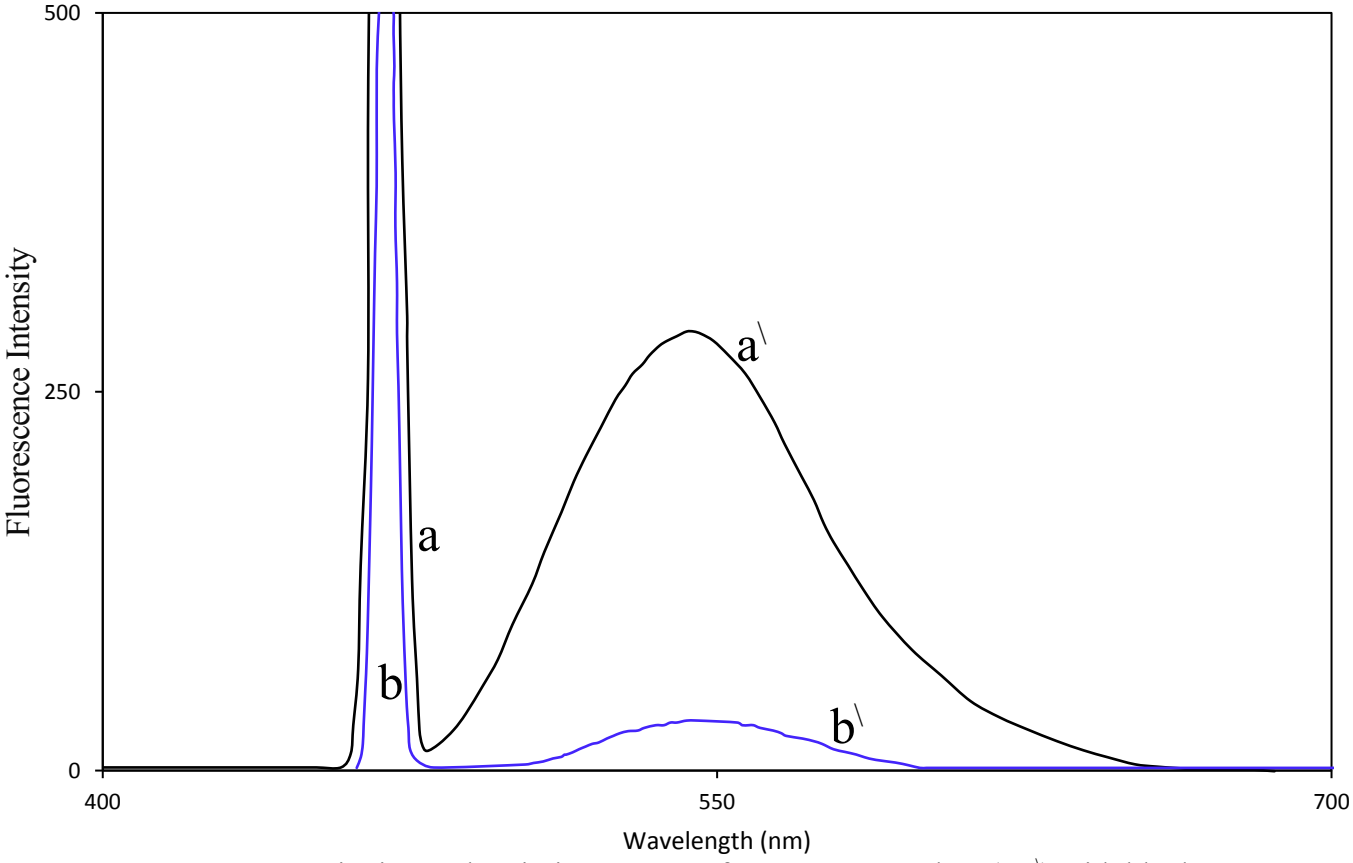

Figure 3-3. Excitation and emission spectra of CLZ-NBD product (a,a\) with blank solution (b,b\) using optimal experimental condition.

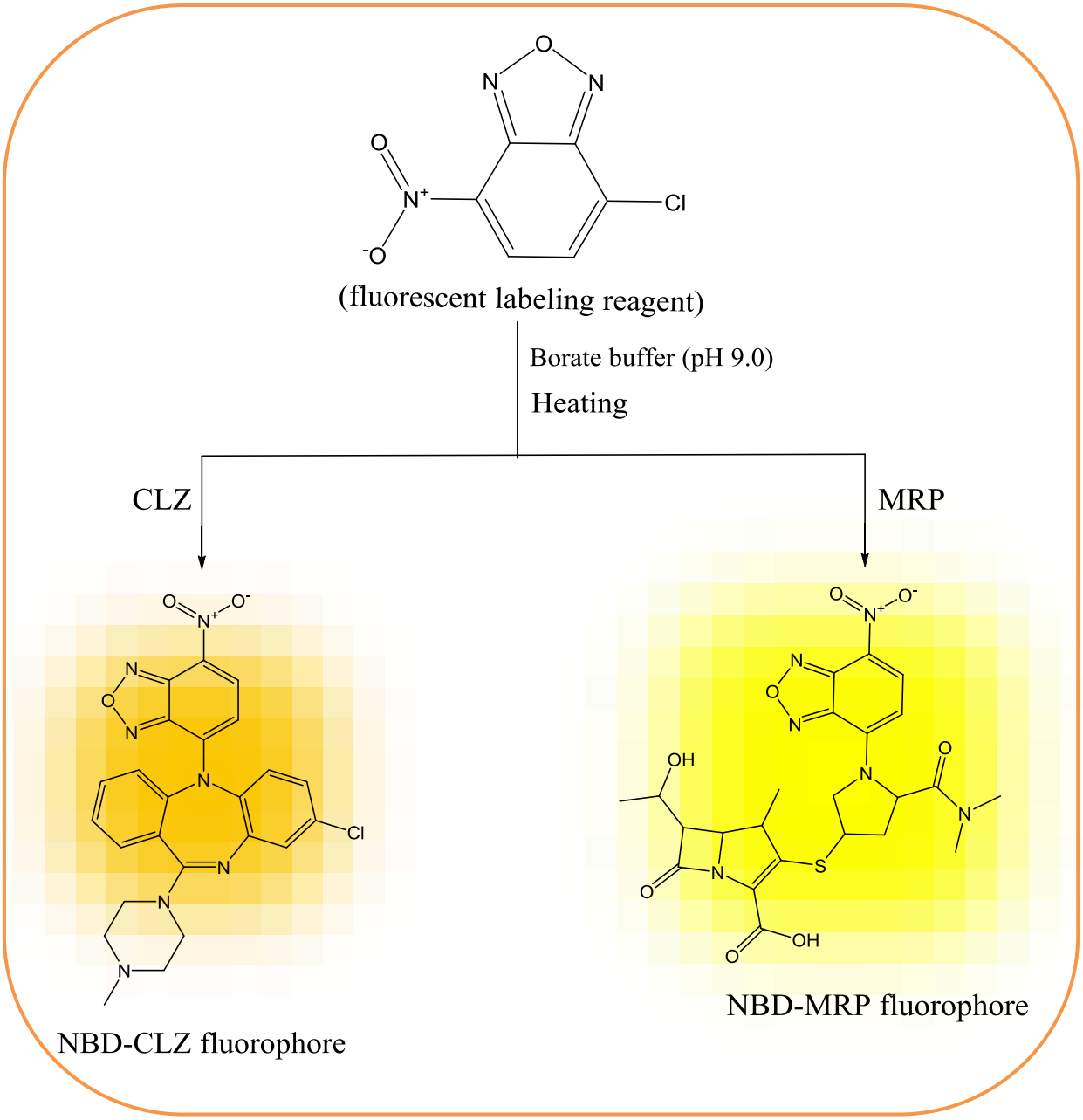

Figure 3-1. The suggested reaction pathway of NBD-Cl reagent with meropenem and clozapine.

3.2.2 Optimization of experimental conditions of NBD-MRP fluorophore

The experimental parameters of the suggested method that affect the stability and intensity of the NBD-MRP product were carefully estimated and optimized. Each parameter was investigated individually while the other parameters remained constant.

3.2.2.1 Effect of reagent volume

Different volumes of 1 mg/mL NBD-Cl (0.1-2.5 mL) were used and, as observed in *Figure 3-4*, the fluorescence intensity increased with respect to the reagent volume increment until reaching a steady state point (0.5 mL) and there was no further increase in fluorescence intensity. As a result, 0.5 mL of reagent was chosen for subsequent experiments.

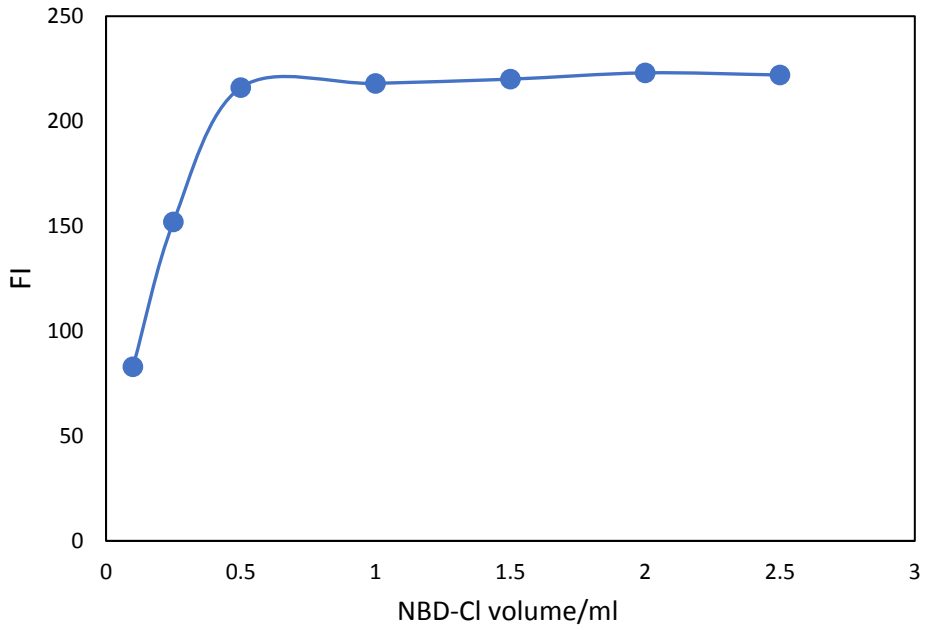

Figure 3-4. Effect of reagent volume on the fluorescence intensity of reaction product between MRP and NBD-Cl.

3.2.2.2 Effect of pH and buffer's volume

Different borate buffer solutions in the pH range (7.0-12.0) were used to check the influence of pH value upon the formation of the fluorescent product. As shown in *Figure 3-5*, the intensity of the fluorescent product increased gradually with pH increase until reaching an optimal point at pH value 9.0, after which it decreased significantly owing to an increase in hydroxide ion concentration, which increased background signal through NBD-OH formation and hold-back the nucleophilic reaction between NBD-Cl and MRP[225]. Different borate buffer volumes of pH 9.0 covering the range (0.25-2.25 mL) were used to find out the volume that gives

the highest fluorescence intensity of reaction product. It was obvious from *Figure 3-5*, that 0.75 mL of borate buffer volume exhibited a maximum fluorescence intensity. Decrease or increase the buffer's volume leads to decrease in the intensity of fluorescence, thus, 0.75 mL of buffer was considered as the optimum volume.

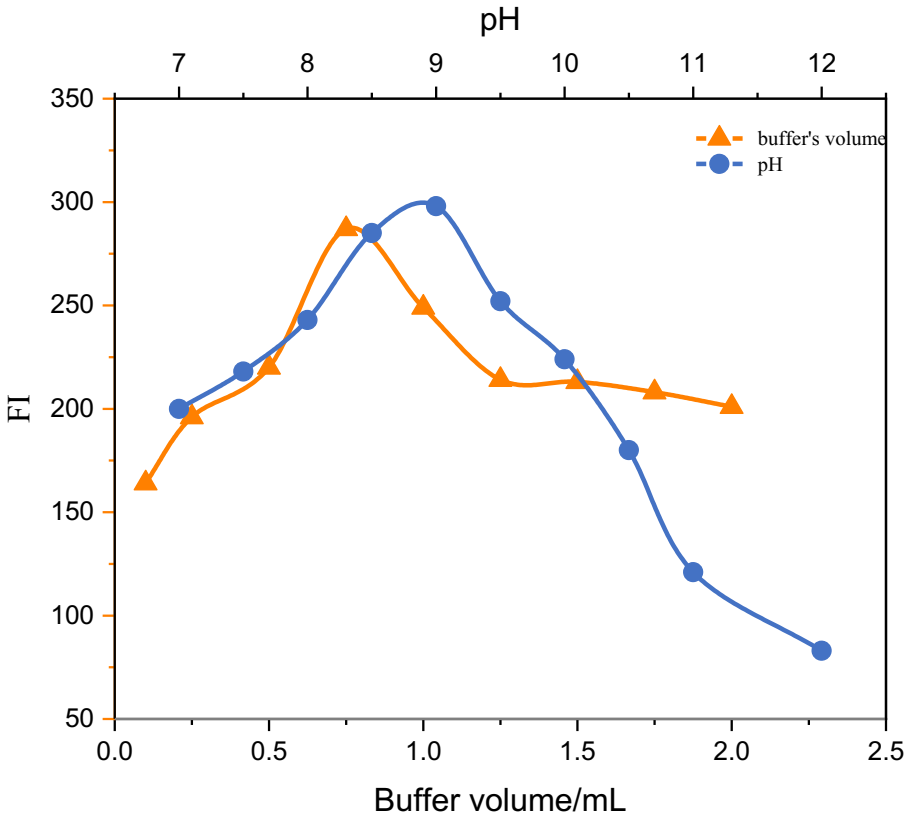

Figure 3-5. Effect of pH and buffer's volume on the fluorescence intensity of reaction product between MRP and NBD-Cl

3.2.2.3 Effect of the warming time and temperature

The Temperature effect on the intensity of fluorescent product was studied at various temperature ranging from (30-100 ºC) over period of time. *Figure 3-6* shows that the maximum fluorescence intensity was observed at 80 ± 2 ºC followed by a steady state until 90 ºC, above which there was a slight decline in fluorescence intensity. At 80 ºC, various time intervals ranging from (2 to 30 min) were used to determine the optimal time required to complete the reaction. As

shown in *Figure 3-6*, the optimal intensity of the fluorescent product was achieved after 15 minutes at 80±2 °C.

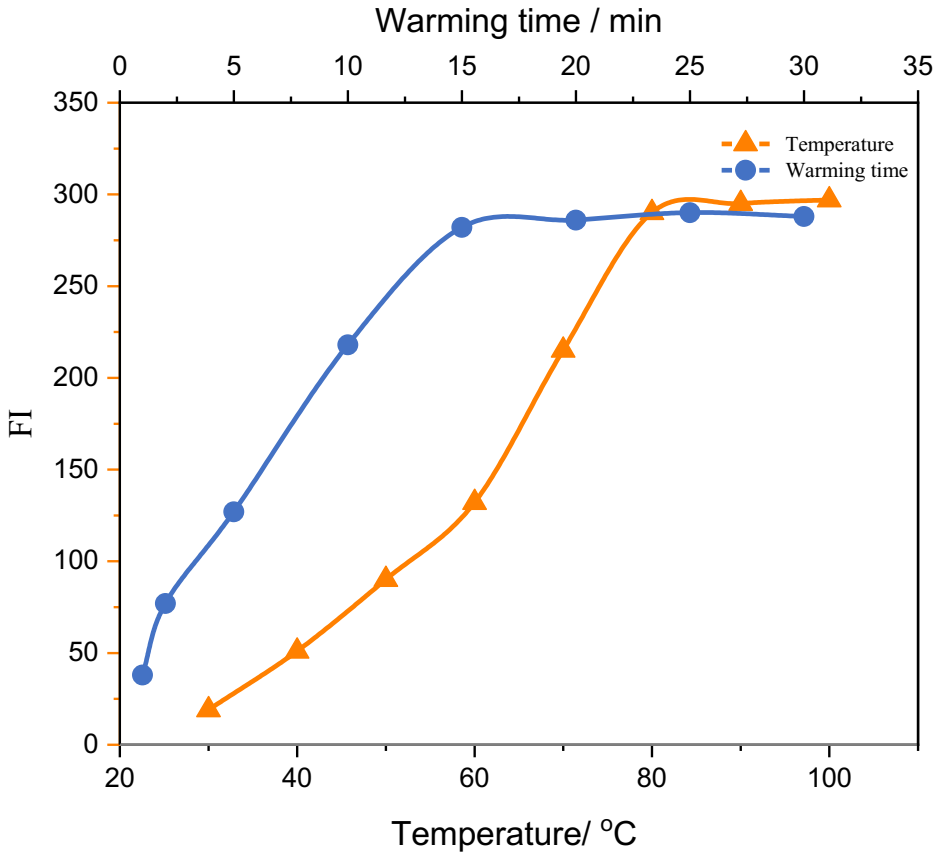

Figure 3-6 Effect of Temperature and warming time on the fluorescence intensity of reaction product between MRP and NBD-Cl.

3.2.2.4 Effect of concentrated HCl volume

It has been reported that NBD-Cl hydrolyzes under alkaline heated conditions to yield a side product known as 4-hydroxy-7-nitro-2,1,3-benzoxadiazole (NBD-OH)[(226)], that has high fluorescence intensity at λ_{emi} 500-550 nm. Therefore, acidification of the reaction mixture before dilution was required to reduce the fluorescence intensity of the interfering background without affecting the NBD-Drug product and, as a result, improve sensitivity. Different volumes of concentrated HCl were used. The results reveal that the ideal HCl volume is 0.5 mL.

3.2.2.5 Effect of diluting solvents

Several diluting solvents were tested, including methanol, acetone, ethanol, butanol, 1,4-dioxan, acetonitrile, ethyl acetate, DMF, and DMSO, to find the solvent that reveals the highest intensity of the fluorescent product. The results show that the maximum intensity value was obtained after diluting with acetone, as shown in *Figure 3-7*.

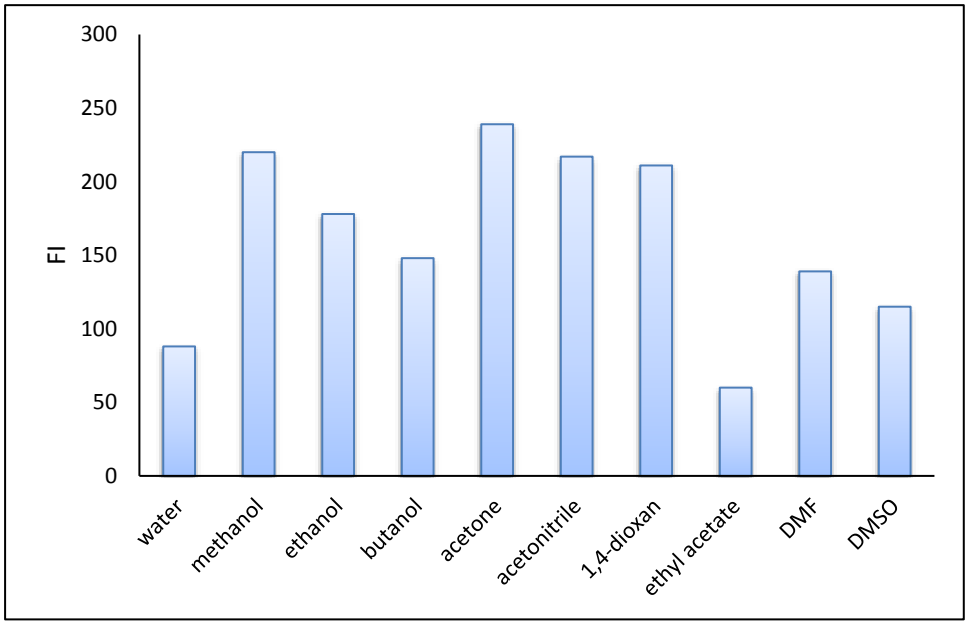

Figure 3-7 Effect of diluting solvents on the fluorescence intensity of reaction product between MRP and NBD-Cl

3.2.3 Validation of method

The developed method has been validated according to International Conference on Harmonization (ICH) guidelines[227].

3.2.3.1 Calibration curve (Recommended procedure)

To a set of 10 mL volumetric flasks, appropriate aliquots of the working standard solution (10 µg mL^{-1}) were accurately transferred using a micropipette to prepare solutions with drug concentration ranging from (25-650 ng mL^{-1}), Then, 0.75 mL of borate buffer pH 9.0 and 0.5 mL of NBD-Cl were added. The flask contents

were gently mixed before being heated at 80 °C for 15 min in a thermostatically controlled water bath, then allowed to cool in an ice bath. After that, the cooled mixture was acidified by adding 0.5 mL of concentrated hydrochloric acid then diluted to mark using acetone. The intensity of the resulted fluorescent product was measured at 536 nm when excited at 471 nm against blank solution prepared under similar conditions. Calibration curve was constructed by plotting the fluorescence intensity at 536 nm (after excitation 471 nm) as a function of meropenem concentration *Figure 3-8* (a) and (b), and the corresponding regression equations were derived.

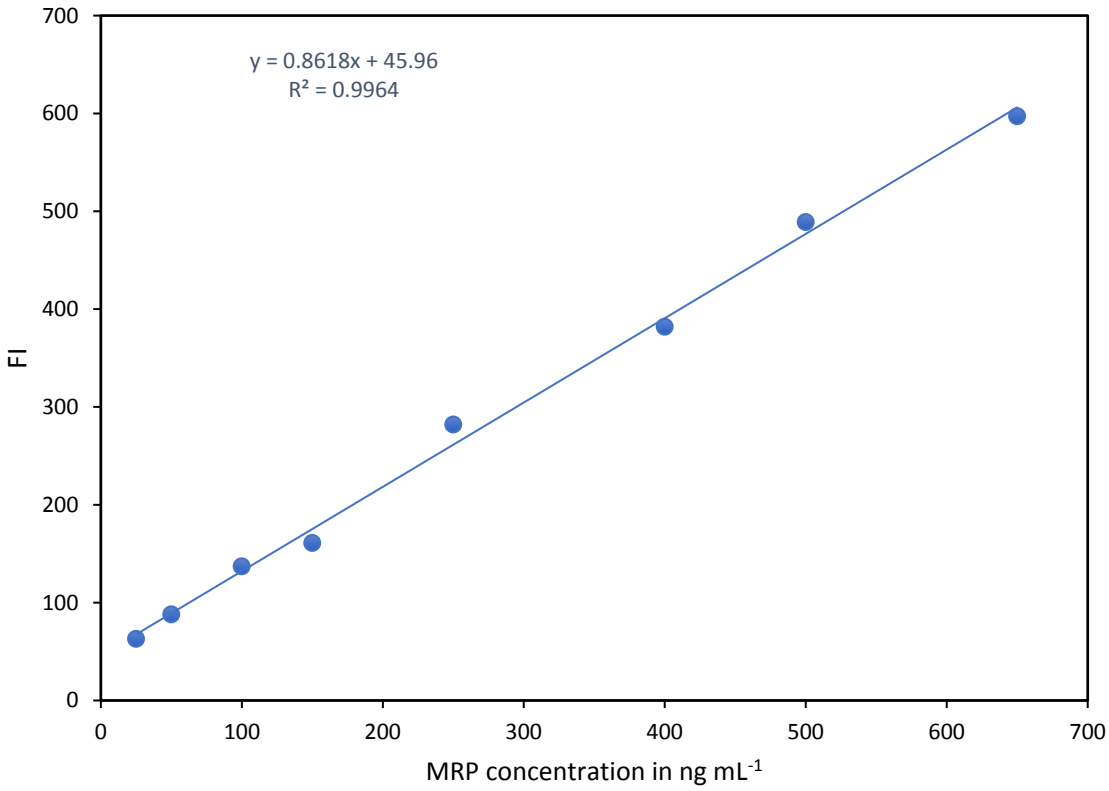

Figure 3-8 (a) Calibration curve of meropenem drug

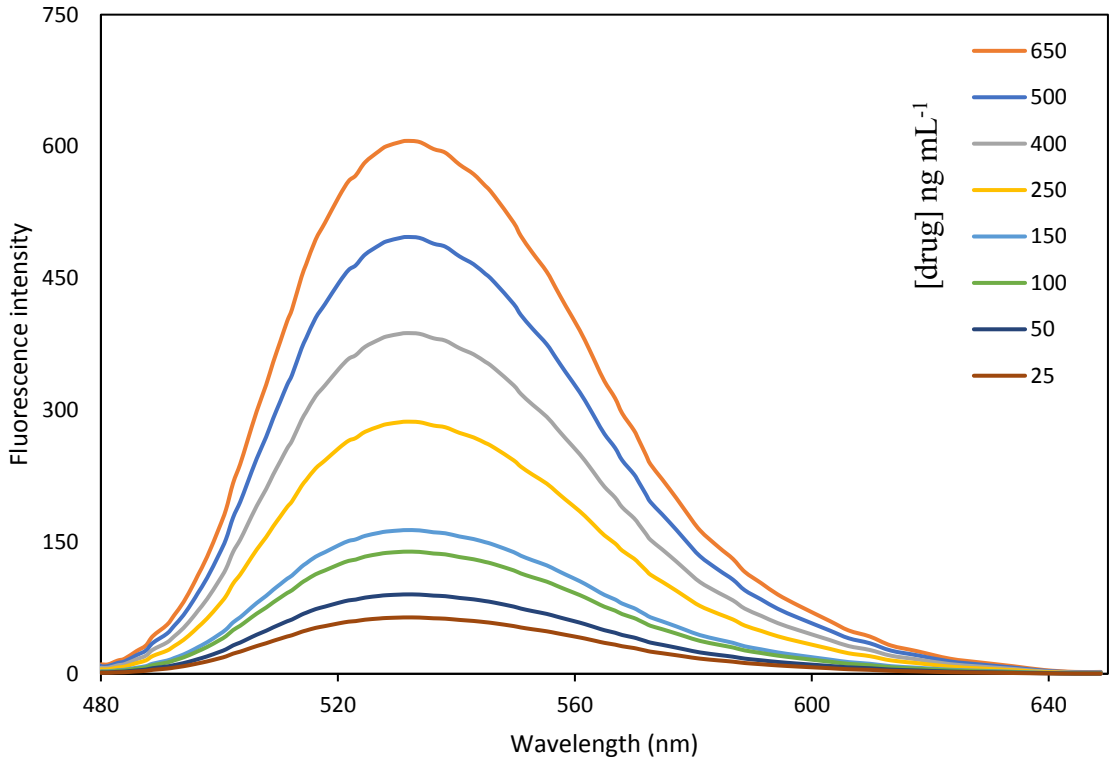

Figure 3-8 (b) Calibration curve of meropenem in dependence to scan spectra

Analysis of variance (ANOVA) was calculated for calibration curve, in which the value of $F_{statistic}$ (F=1669.21) is larger than $F_{significance}$ ($F^{1}_{6} = 5.987$), indicating there is a non-significance difference at confidence level 95% due to the regression and error around regression (residual), So these results are approaching to the ideal state (linearity)[228] as illustrated in *Table 3-2*.

Table 3-2 Results of ANOVA analysis for linear regression equation

Source	*DF	*SS	***MS	F statistic	F significance	
Regression	1	271953.3	271953.3	1669.21	5.987	
Residual	6	977.5370	162.9228			
Total	7	272930.8				
	Coefficients	Standard Error	t Stat	P-value	Lower CL:95%	Upper CL:95%
Intercept	45.9603	7.194	6.388	0.0007	28.356	63.564
Slope	0.8618	0.0211	40.8560	5.987	0.8102	0.9134

*Df=Degree of freedom, **SS=Sum of Square, ***MS=Mean of Square, CL = confidence level

3.2.3.2 Linearity and range

The linear regression equation of the analyzed data was given in the following formula:

$F = 0.8618\ C + 45.9603$

Where F represent fluorescence intensity, C represent MRP concentration in ng mL^{-1}.

The calibration curve is linear in the concentration range of 25 - 650 ng mL^{-1} with an excellent correlation coefficient (r = 0.9981). Furthermore, the obtained results were statistically analyzed and the regression parameters were summarized in *Table 3-3*.

Table 3-3 Analytical parameters of the suggested spectrofluorimetric method.

Parameter	suggested method
λ_{exc} (nm)	471
λ_{emi}(nm)	536
Concentration range (ng mL^{-1})	25-650
Slope	0.8618
SD of slope	0.0145
Determination coefficient (r^2)	0.9964
Correlation coefficient (r)	0.9981
Intercept	45.96
SD of intercept	8.74
LOD[a] (ng mL^{-1})	3.15
LOQ[b] (ng mL^{-1})	9.55

[b]**LOQ:** Limit of quantitation. [a]**LOD:** Limit of detection

3.2.3.3 limit of quantitation (LOQ) and Limit of detection (LOD)

LOQ and LOD of the proposed spectrofluorometric method were calculated using the formula provided by the ICH Q2 (R1) recommendation. The low value of LOQ and LOD indicates that the developed method has high sensitivity, as observed in *Table 3-3*.

3.2.3.4 Accuracy

Accuracy of the analytical method represent the closeness of the measurement to the true or accepted value. Three concentrations (75, 150, 250 ng mL^{-1}) have been used to verify the accuracy of the proposed method using five replications for each concentration. The data was expressed as percent recovery (R%) as illustrated in *Table 3-4*. The obtained results exhibit a high degree of agreement between calculated and true values. As a result, the suggested method is highly accurate.

Table 3-4 Accuracy data of the suggested spectrofluorimetric method

Sample	Concentrations ng mL^{-1}	Recovery%[a]± SD
1	75	99.69 ± 1.81
2	150	99.20 ± 1.92
3	250	99.34 ± 1.87

[a]Mean of five determinations

3.2.3.5 Precision

The analytical method precision was expressed as intermediate precision (inter-day precision) and repeatability (intra-day precision). The precision of the proposed method was checked by analyzing three distinct concentrations of MRP (100, 200,300 ng mL^{-1}) at successive time intervals on the same day and different day for intra-day precision and inter-day precision respectively, followed by measuring the fluorescence intensity of the solution whose concentration was calculated using the previously computed regression equation. The value of the

calculated relative standard deviation (R.S.D%) was found to be less than 2 %, indicating acceptable precision as detailed in *Table 3-5*.

Table 3-5 Intra- and inter-day precisions of the suggested spectrofluorimetric method

Concentration ng mL^{-1}	Intra-day precision		Inter-day precision	
	Recovery%[a]	R.S.D	Recovery%[a]	R.S.D
100	98.90	0.99	99.83	1.19
200	99.00	0.52	100.16	0.52
300	99.80	0.77	100.27	0.42

[a]Mean of five determinations

3.2.3.6 Robustness

The proposed method's robustness was checked by measuring the fluorescence intensity after making a little variation in some experimental parameters such as pH, borate buffer volume, and reagent volume. The data was presented as relative standard deviation (R.S.D) and percent recovery (R%) and as illustrated in *Table 3-6*, and the results reveal that the low value of R.S.D (less than 2%) indicates that the little variation in experimental parameters has no significant effect on the determination of MRP.

Table 3-6 Robustness evaluation for the suggested spectrofluorimetric method.

Experimental parameters	Recovery%[a] ± R.S.D
Volume of NBD-Cl (mL)	
0.4	97.98 ± 0.87
0.5	98.44 ± 0.63
0.6	98.90 ± 0.99
Buffer pH	
8.8	99.83 ± 0.75
9	99.60 ± 0.63
9.2	99.14 ± 1.02
Warming time (min)	
12	97.51 ± 0.76
15	99.60 ± 0.98
18	100.30 ± 0.86

[a]Mean of five determinations.

3.2.3.6 Applications

3.2.3.6.1 Application in the pharmaceutical vial

The proposed method was successfully applied for the determination of MRP concentration in commercial vials (Meropenem trihydrate® 1 g vial) *scheme 3-1*. The obtained data were compared statistically to those obtained from the reported and official method according to t and F- tests at 95% confidence level[229]. *Table 3-7* shows that the values of t and f-test were lower than the corresponding critical (tabulated) values, denoting there was no statistically significant difference between the official or reported method and the suggested methods.

Table 3-7 Statistical comparison of data obtained by suggested spectrofluorometric method with the reported and official methods for quantification of meropenem in pharmaceutical vials.

Parameter	Proposed method	Reported method	Official method
Recovery%	99.48	100.55	100.18
S.D	1.67	1.56	1.32
Variance	2.81	2.44	1.75
Observation (n)	5	5	5
t test	$t_{critical}$ = 2.3 (p= 0.05)	1.05	1.60
f test	$f_{critical}$ = 6.38 (p= 0.05)	1.15	0.73

3.2.3.6.2 Application in the spiked human plasma

In order to prove the ultra-sensitivity of the proposed spectrofluorimetric method, different MRP concentrations (50, 75, 100, 150, and 200 ng mL^{-1}) were assayed in spiked human plasma *scheme 3-1*. The data was presented as a percentage of recovery (R%), as shown in *Table 3-8*.

Table 3-8 Application of the suggested spectrofluorimetric method for quantification of MRP in human plasma.

Added conc. (ng mL^{-1})	Found conc. (ng mL^{-1})	Recovery% [a] ± SD
50	48.78	98.02 ± 1.30
75	73.46	97.84 ± 1.64
100	98.90	98.90 ± 2.16
150	147.18	98.12 ± 1.30
200	196.84	98.42 ± 1.14

[a]Mean of five determinations.

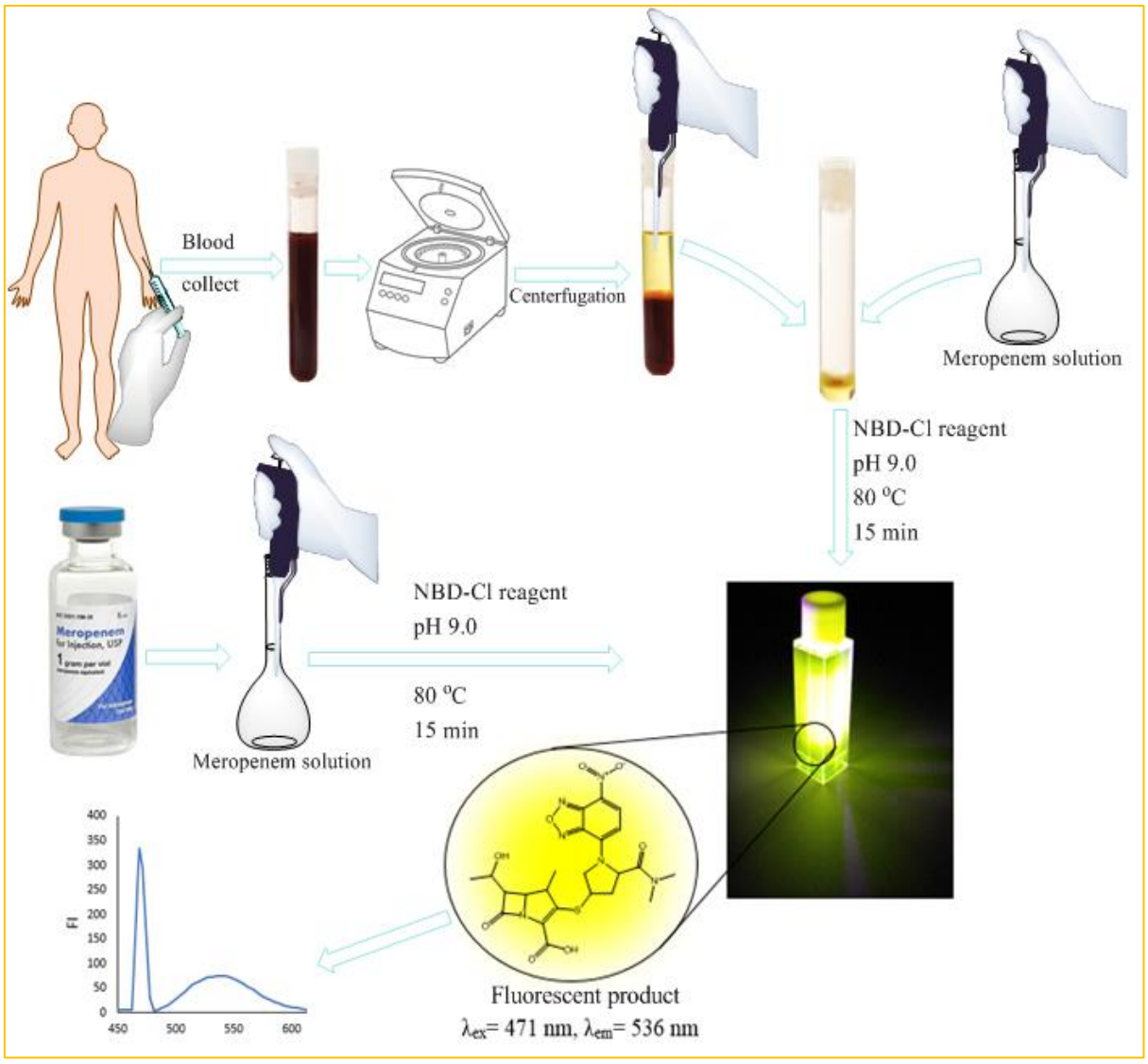

Scheme 3-1. Graphical abstract for quantification of MRP in pharmaceutical formulation and spiked human plasma

3.2.4 Optimization of experimental conditions of NBD-CLZ fluorophore

The experimental factors of the subjected approach that enhance the stability and fluorescence intensity of NBD-CLZ product were thoroughly determined and optimized. Each factor has been studied independently while the other factors kept constant.

3.2.4.1 Effect of reagent volume

The effect of reagent volume on the fluorescence intensity of reaction product has been studied in the range (0.25-3.0 mL). the fluorescence intensity improved as the reagent volume increased until reach a point (1.5 mL) and the intensity did not increase further. As a consequence, 1.5 mL of NBD-Cl has been chosen for subsequent experiments as detailed in *Figure 3-9*.

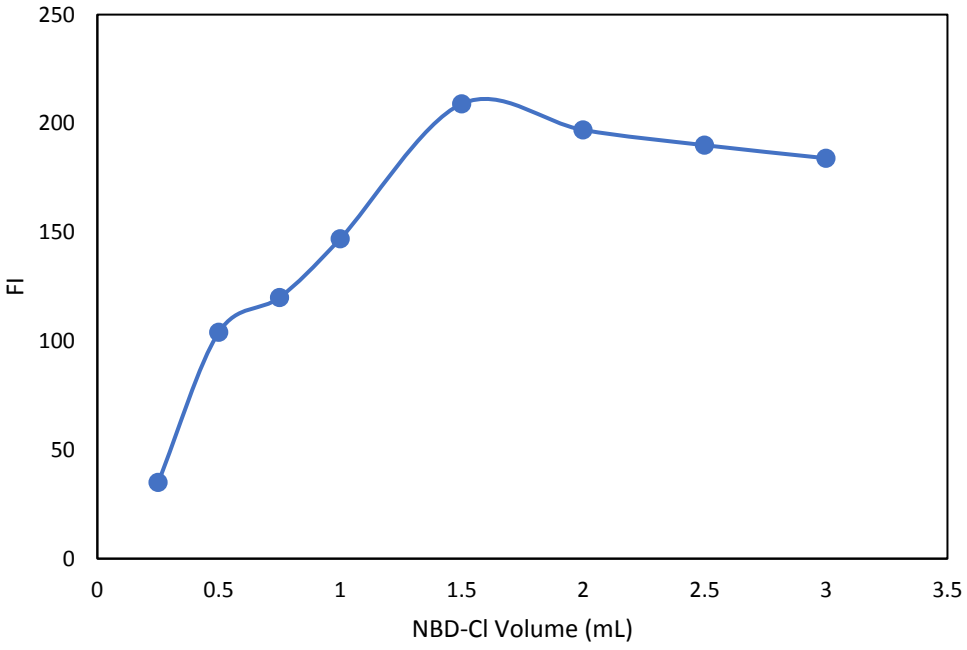

Figure 3-9 Reagent volume effect on the FI of CLZ-NBD product

3.2.4.2 Effect of pH and borate buffer's volume

In order to study the effect of the acidity and basicity of the reaction media on the formation of the NBD-CLZ product, several borate buffer solutions with pH

ranging from 7.0-12.0 have been employed. *Figure 3-10* illustrates the gradual increase in fluorescence intensity with the respect to pH value until it attained a maximum value (pH 9.0), above which there was no further increase. Instead, it diminished considerably as a result of the formation of NBD-OH compound, which increased the background signal. Thus, pH 9.0 was selected as the optimal value.

To select the volume that produces the greatest fluorescence intensity of NBD-CLZ product, several volumes of borate buffer (pH 9.0) within the range (0.1-2 mL) were used. As shown in *Figure 3-10*, the FI increases as a function of buffer volume until reach a steady state region from (1.0-1.5 mL). followed by marked decrease. Therefore, 1 mL is optimal buffer's volume.

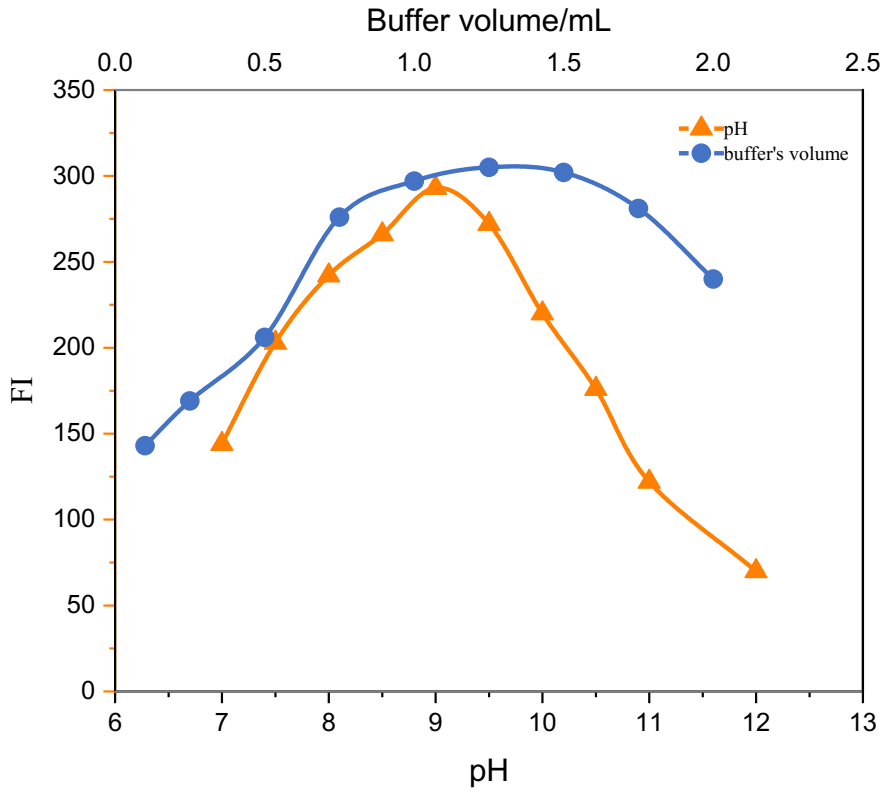

Figure 3-10 Effect of pH and borate buffer's volume on the FI of NBD-CLZ product

3.2.4.3 Effect of the heating temperature and heating time

The influence of heating temperature on the FI of NBD-CLZ product has been checked at different temperature within the range (30 - 100 °C) through a certain time interval. *Figure 3-11,* illustrate that the highest FI has been achieved at 80 ± 2 °C. At this temperature, the sufficient time required to complete the reaction has been determined using different heating time (1-30 min). As detailed in *Figure 3-11*, the sufficient heating time was found to be 15 minutes.

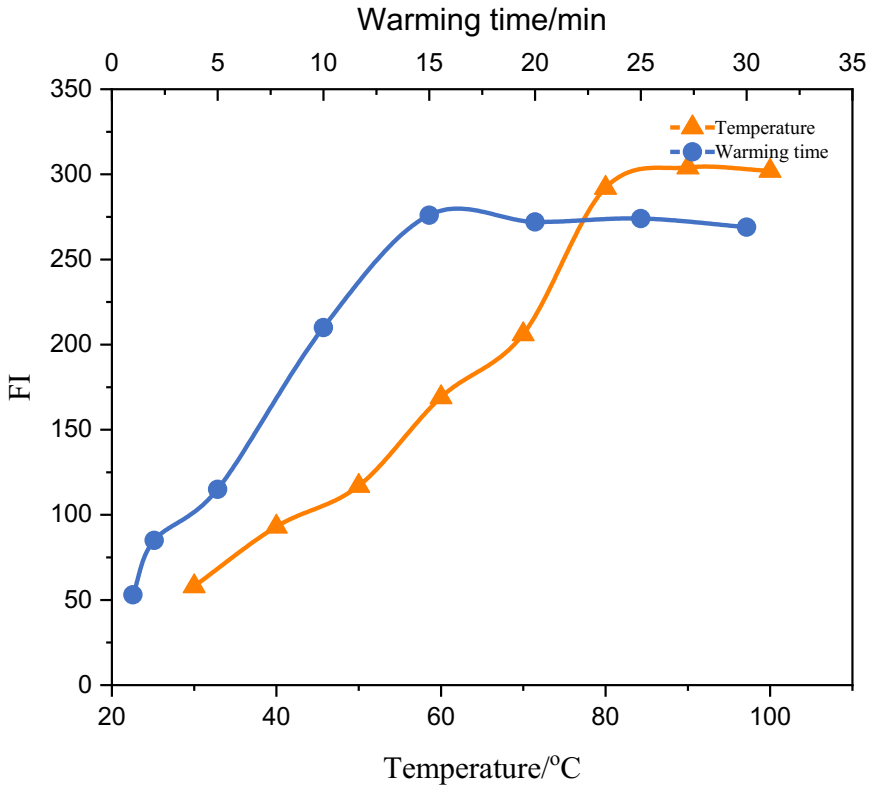

Figure 3-11 Effect of temperature and warming time on the FI of NBD-CLZ product

3.2.4.4 Effect of concentrated HCl volume

According to the literature survey, the high hydroxyl ion concentration of the experimental condition (pH 9.0) causes an interfering problem by reacting with NBD-Cl to form NBD-OH compound, which is responsible for increasing the background signal. This problem can be overcome by lowering the pH of the reaction mixture to less than 1 without influencing the NBD-CLZ product by

adding concentrated HCl volume following the cooling step. Various HCl volumes has been used within the range (0.1-1.0 mL). The optimal HCl volume was found to be 0.6 mL.

3.2.4.5 Diluting solvents Effect

To select the solvent that produces the maximum FI of NBD-CLZ product, various diluting solvents have been examined, such as acetonitrile, 1,4-dioxan acetone, methanol, butanol, ethyl acetate, DMF, DMSO, ethanol, and D.W. The highest FI was attained when using acetone as dilution solvent, as illustrated in *Figure 3-12*.

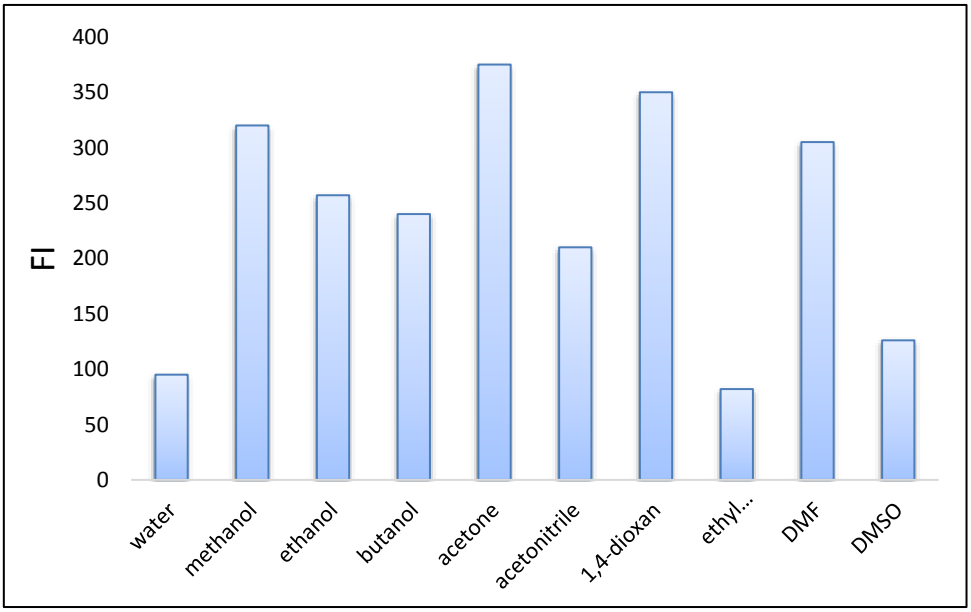

Figure 3-12 Diluting solvents effect on the FI of NBD-CLZ product

3.2.5 Validation of method

The suggested approach has been validated in accordance with (ICH) recommendations[227].

3.2.5.1 Calibration curve (recommended procedure)

An appropriate portion of the working standard solution (10 µg mL^{-1}) were carefully transferred to a series of 10 mL calibrated flasks to prepare a solutions

with final CLZ concentrations over the range (80-900 ng mL^{-1}).Followed by 1.5 mL of reagent (NBD-Cl) together with 1 mL of borate buffer (pH 9.0). The reaction mixture was mixed well and heated in a thermostatically controlled water bath for 15 min at 80 °C, then refrigerated for 5 min. After that, 0.6 mL of concentrated HCl was added to acidify the mixture. The flask contents were then diluted to the mark using methanol. The fluorescence intensity of the resulted product was measured at 540 nm when excited at 469 nm. The same procedure was performed without CLZ to obtain blank solution. The calibration graph was produced via plotting the increment in the fluorescence intensity of NBD-CLZ product with the respect to CLZ concentration *Figure 3-13 (a) and (b)* The regression equation of the calibration graph was derived.

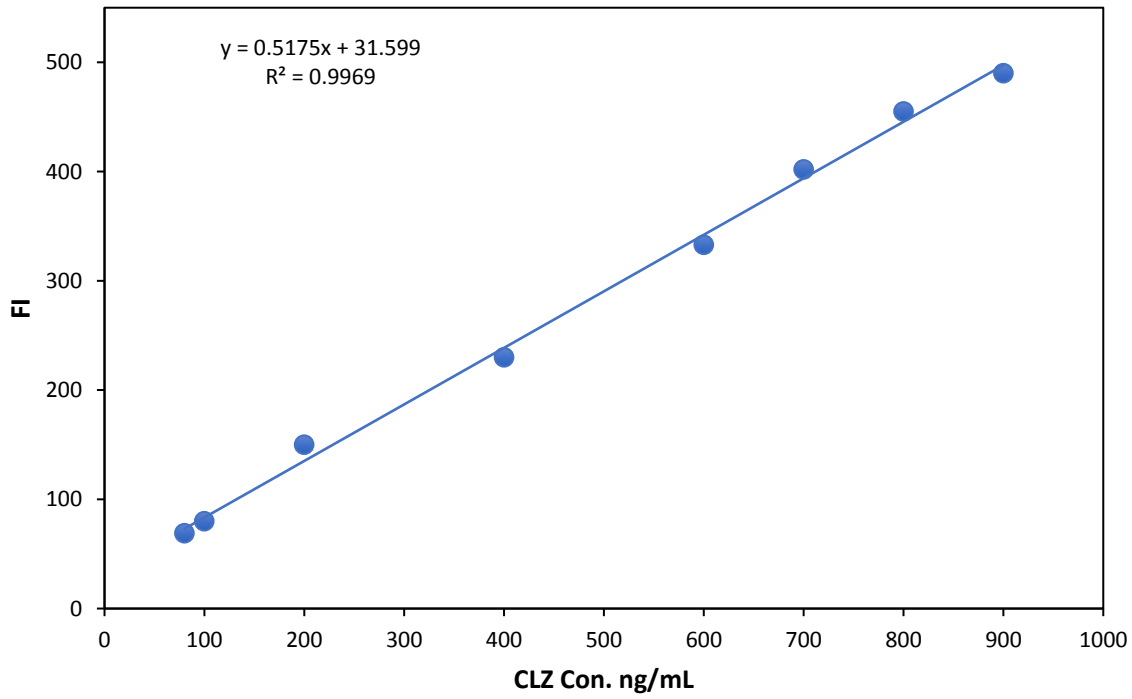

Figure 3-13 (a) Calibration curve of clozapine

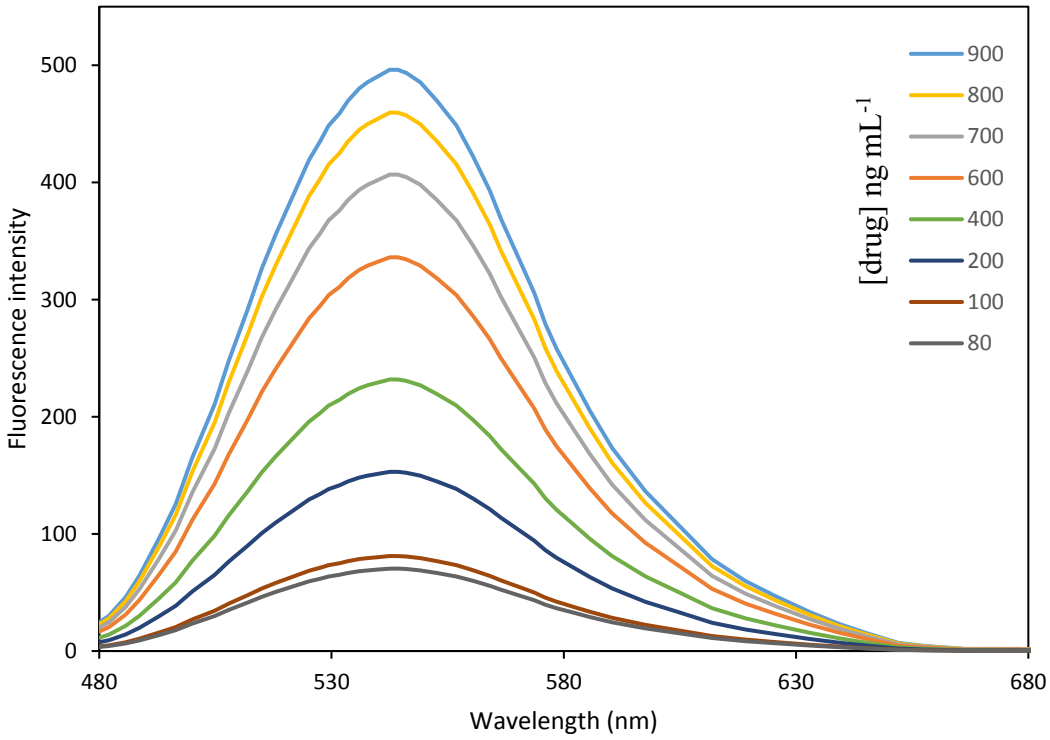

Figure 3-13 (b) Calibration curve of clozapine in dependence to scan spectra

Analysis of variance (ANOVA) was calculated for calibration curve, in which the value of $F_{statistic}$ (F=1908.93) is larger than $F_{significance}$ ($F^{1}_{6} = 5.987$), indicating there is a non-significance difference at confidence level 95% due to the regression and error around regression (residual), So these results are approaching to the ideal state (linearity) as illustrated in *Table 3-9*.

Table 3-9 Results of ANOVA analysis for linear regression equation

Source	*DF	*SS	***MS	F statistic	F significance	
Regression	1	195604.1	195604.1	1908.93	5.987	
Residual	6	614.807	102.46			
Total	7	196218.9				
	Coefficients	Standard Error	t Stat	P-value	Lower CL:95%	Upper CL:95%
Intercept	31.599	6.6431	4.7566	0.003137	15.34	47.85
Slope	0.5175	0.0118	43.691	5.987	0.488	0.546

*Df=Degree of freedom, **SS=Sum of Square, ***MS=Mean of Square, CL = confidence level

3.2.5.2 Linearity and range

The linear regression equation of the analyzed data was given in the following formula:

$F = 0.5175\ C + 31.598$

Where F represent fluorescence intensity, C represent CLZ concentration in ng mL^{-1}.

The linear concentration of the calibration graph ranged from 80-900 ng mL^{-1} of CLZ. The resulted data were summarized in *Table 3-10*.

Table 3-10 Analytical parameters of the suggested approach.

Parameter	suggested method
λ_{exc} (nm)	469
λ_{emi}(nm)	540
Concentration range (ng mL^{-1})	80-900
Slope	0.5175
SD of Slope	0.0146
Determination coefficient (r^2)	0.9969
Correlation coefficient (r)	0.9984
Intercept	31.6
SD of intercept	8.74
LOD* (ng mL^{-1})	14.16
LOQ** (ng mL^{-1})	42.92

****LOQ:** Limit of quantitation. ***LOD:** Limit of detection

3.2.5.3 Limit of detection (LOD) and Limit of quantitation (LOQ)

LOD and LOQ of the suggested approach were obtained by calculating the standard deviation (S.D) of seven blank solution. The obtained S.D value was substituted in the equations supplied by the ICH Q2 (R1) guidelines, where

$$LOD = \frac{3.3\,S}{b}, \qquad LOQ = \frac{10\,S}{b}$$

where S denotes to S.D, while b denotes to slope of the calibration graph's regression line. As mentioned in *Table 3-10*, The small LOD and LOQ values indicate that the suggested approach is highly sensitive.

3.2.5.4 Accuracy

The suggested approach's accuracy has been determined by measuring the fluorescence intensity of the NBD-CLZ product using three concentration level within the calibration graph (100, 200, 300 ng mL^{-1}) by performing five replications of each selected concentration. As detailed in *Table 3-11*, the obtained results were analyzed to obtain percent recovery (Re%) whose values indicate the suggested approach is highly accurate.

Table 3-11 Accuracy data of the suggested approach

Sample	Concentrations ng mL^{-1}	Recovery%* ± SD
1	100	100.09 ± 1.51
2	200	99.13 ± 1.48
3	300	99.45 ± 1.58

* Mean of five determinations

3.2.5.5 Precision

The precision of the suggested approach has been represented as inter-day precision (Reproducibility) and intra-day precision (Repeatability). Three CLZ concentration (150, 200, and 300 ng mL^{-1}) was selected to test the precision of the suggested approach. Each concentration was analyzed at consecutive time during the day to obtain repeatability and at different day to obtain reproducibility. As illustrated in *Table 3-12*, the low value of relative standard deviation (R.S.D.% less than 2) indicate that the suggested approach is highly precise.

Table 3-12 Intra- and inter-day precisions of the suggested approach.

Concentration ng mL^{-1}	**Intra-day precision**		**Inter-day precision**	
	Recovery%*	**R.S.D.%**	**Recovery%***	**R.S.D.%**
100	100.87	1.77	100.48	1.60
200	99.32	0.84	99.71	1.42
300	99.83	1.04	100.22	1.02

* Mean of five determinations

3.2.5.6 Robustness

The robustness describes the stability of the analytical method under a slight change in some experimental factors. In this work, four experimental factors (warming time, Temperature, pH, and reagent volume) was slightly changed to test the robustness of the suggested approach. As mentioned in *Table 3-13*, the obtained values of percent recovery and R.S.D.% implies that slight changes in experimental conditions have no considerable effect on the quantification of CLZ.

Table 3-13 Robustness evaluation for the suggested approach.

Experimental parameters	**Recovery%* ± R.S.D.%**
Warming time (min)	
13	97.77 ± 1.44
15	100.29 ± 1.12
17	98.55 ± 1.13
Temperature (^{o}C)	
77	100.29 ± 1.23
80	99.71 ± 1.42
83	100.48 ± 1.52
Buffer pH	
8.8	98.35 ± 1.55
9	99.32 ± 1.45
9.2	97.19 ± 1.45

Reagent volume (mL)	
1.3	99.71 ± 0.96
1.5	100.09 ± 0.96
1.7	99.32 ± 1.35

* Mean of five determinations.

3.2.5.7 Application

3.2.5.7.1 Application in the pharmaceutical vial

The suggested approach has been successfully used for quantifying of clozapine in pharmaceutical tablets. The resulted data have been compared with the result produced from reported method using student's t and f test at confidence level equal to 95%[230]. *Table 3-14,* illustrate that the t and f values of the suggested approach were less than relevant tabulated values, implying that the reported method and the suggested approach were not statistically different.

Table 3-14 Statistical comparison of data resulted by suggested approach with those of the reported one for determination of CLZ in pharmaceutical tablets.

Pharmaceutical preparation	**Proposed method**		**Reported method**	
Clozapex (100 mg) tablets	Added conc. (ng mL^{-1})	Found%	Added conc. (ng mL^{-1})	Found%
	20	99.6	20	98.94
	40	101	30	99
	60	97.9	60	102
	80	98.5	70	101.4
	100	100.7	80	98.45
Mean ± S.D		99.54 ± 1.34		99.95 ± 1.61
Variance		1.81		2.62
***t* value**		0.44 (2.30)*		
f value		1.44 (6.38)*		

*The value between bracket represent the corresponding f and t tubulated values

3.2.5.7.2 Application in the spiked human plasma

Five CLZ concentration (100, 150, 200, 250, 300 ng mL^{-1}) were successfully determined in spiked fresh human plasma. The obtained values of recovery percent (Re%) were mentioned in *Table 3-15*.

Table 3-15 Application of the suggested approach for determination of CLZ in human plasma

Added conc. (ng mL^{-1})	Found conc. (ng mL^{-1})	Recovery% *± SD
100	101.25	101.25 ± 1.58
150	150.34	100.22 ± 1.81
200	194.78	97.39 ± 2.30
250	248.50	99.40 ± 2.38
300	294.49	98.16 ± 0.85

*: Mean of five determinations.

3.3. Determination of amlodipine besylate and sitagliptin using O-phthalaldehyde as fluorogenic derivatization reagent.

3.3.1 Assigning the fluorescence spectrum of OPA-2ME-Drug fluorophore

O-Phthalaldehyde (OPA) is the most popular fluorogenic agent that widely used for detection a nanogram of compounds with primary amine moiety. Primary amines form a highly fluorescent adducts when reacted with O-Phthalaldehyde (OPA) and a thiol compound (like 2-mercaptoethanol) through condensation reaction under basic conditions. It is used in a very sensitive fluorescent reagent for assaying sulfhydryls, many biogenic amines, peptides, and proteins in nanogram quantities in body fluids. The reaction is essentially complete within 5.0-40.0 minute. The fluorescence intensity of reaction product is attributed to the formation of isoindole group which trigger the compound to give fluorescence

intensity. The produced fluorophores usually excited within the range 330-390 nm with emission 436-480 nm[231-237].

OPA was utilized for determination of amlodipine besylate and sitagliptin via a click-like three-component labeling of primary amine substituted compound (drug) with O-phthalaldehyde and 2-mercaptoethanol (as fluorophore stabilizer agent). The resulting N-fused aromatic isoindole moiety provides a high fluorescence intensity *Figure 3-14*, enabling fast, sensitive, and accurate measurement across a very broad range of drug concentrations. *Figure 3-15* and *3-16* illustrate the fluorescence spectrum of OPA-2ME-AMB and OPA-2ME-STA fluorophores using drugs concentration 500 ng mL^{-1}. The formed fluorophores exhibit excitation wavelength at 378 and 335 nm with emission wavelengths 475 and 458 nm for AMB and STA respectively.

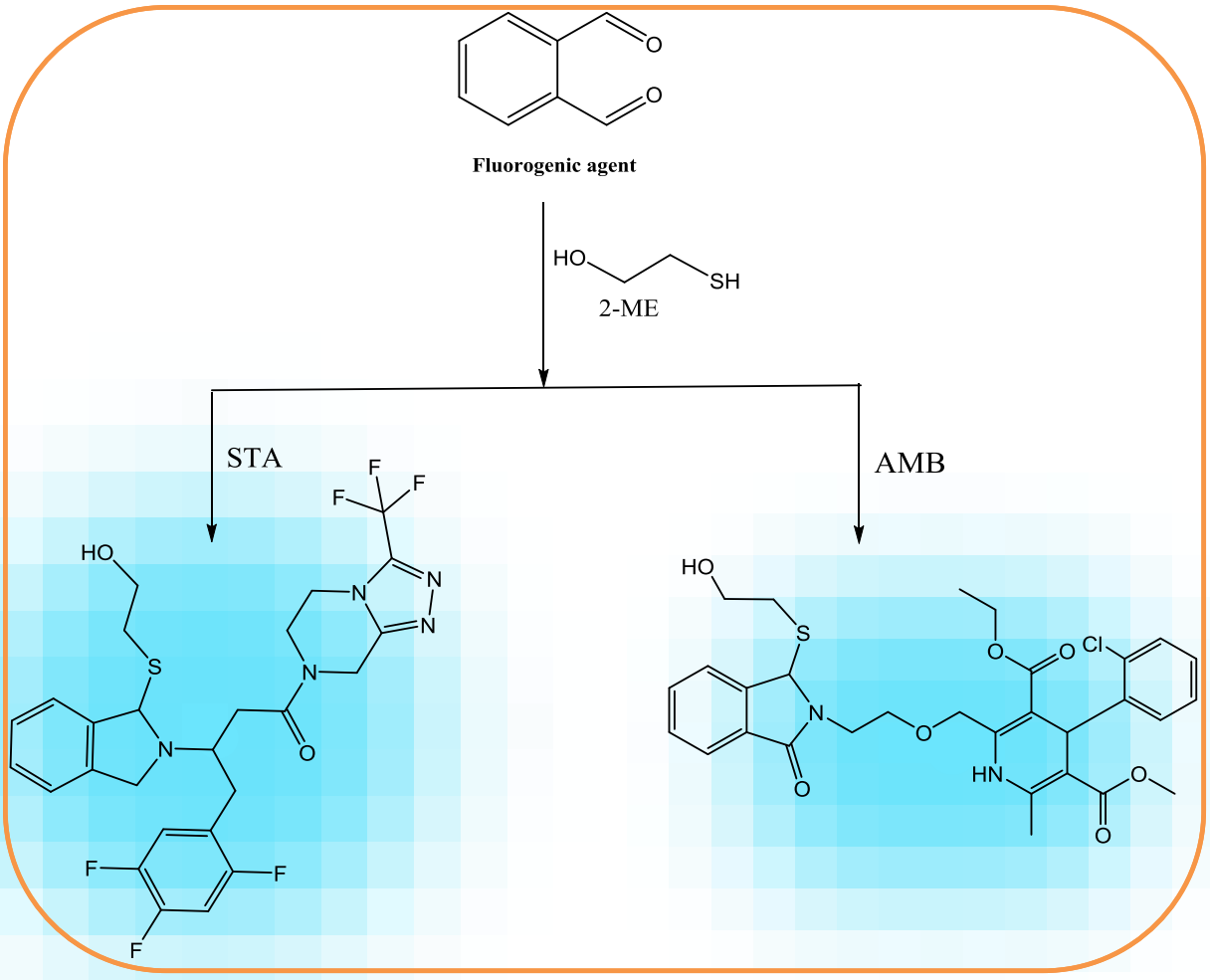

Figure 3-14. The suggested pathway of reaction between OPA with amlodipine and sitagliptin in the presence of 2-ME.

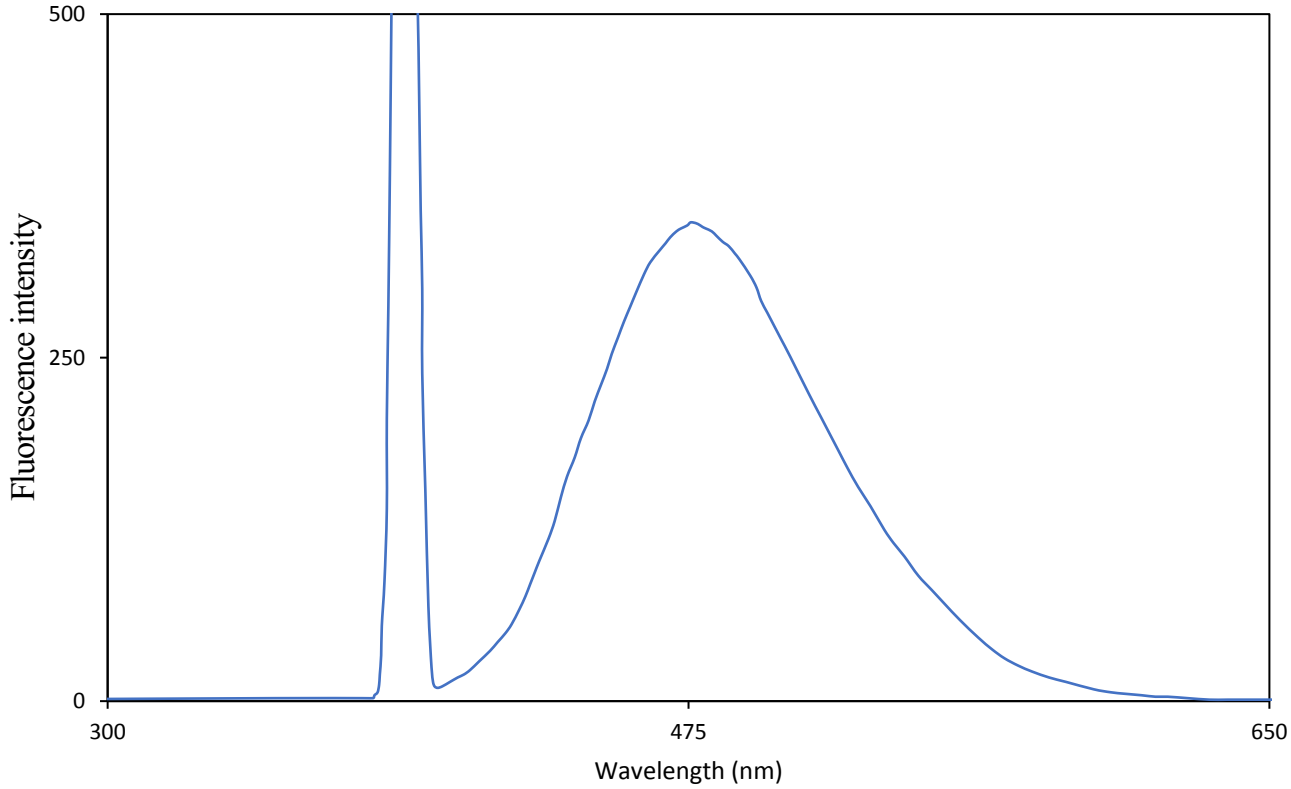

Figure 3-15. Excitation and emission spectra of AMB-2ME-OPA product using optimal experimental condition.

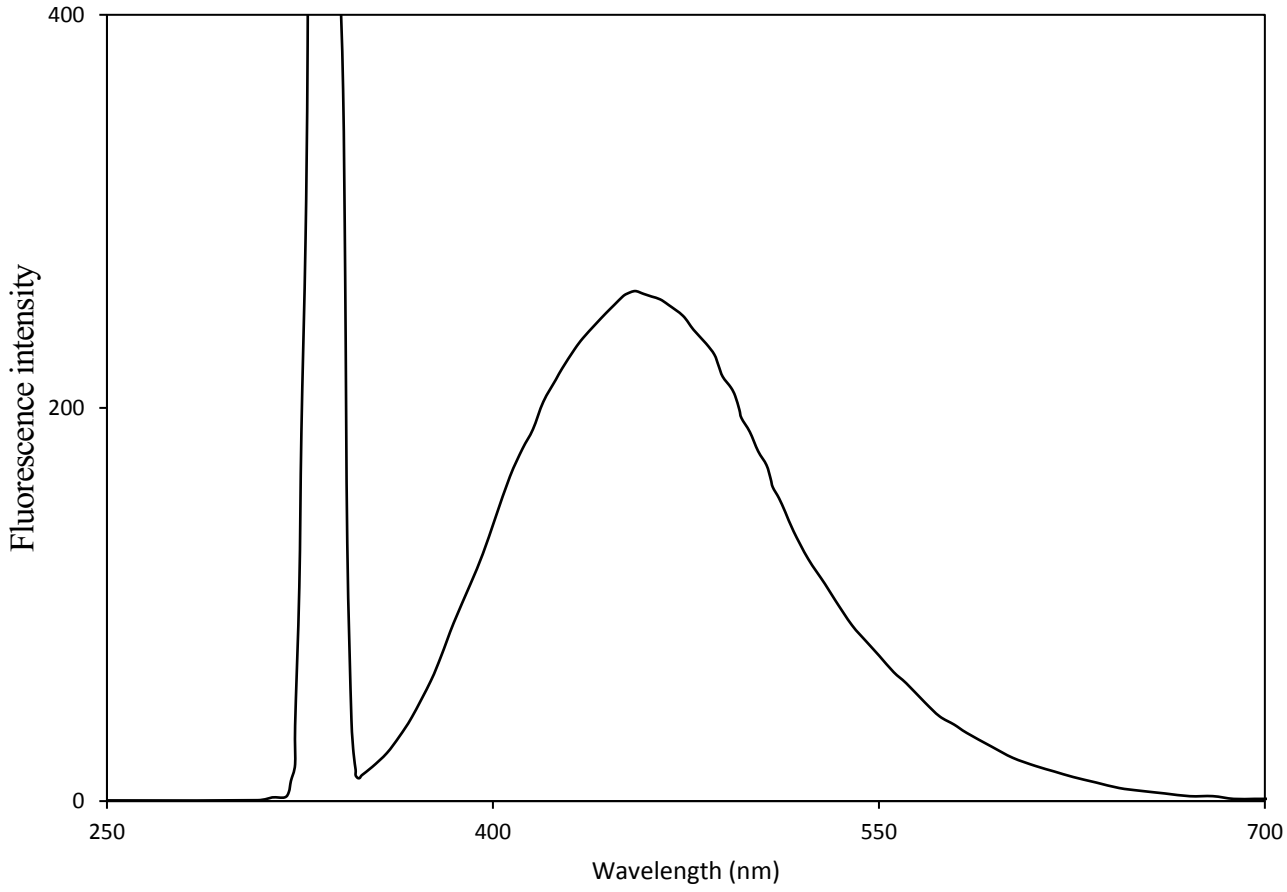

Figure 3-16. Excitation and emission spectra of STA-2ME-OPA product using optimal experimental condition.

3.3.2 Optimization of experimental conditions of OPA-2ME-AMB fluorophore

There are several experimental factors of the subjected approach that affect either on the stability or on the fluorescence intensity of OPA-2ME-AMB fluorophore. These variables have been properly investigated and optimized. Each factor has been studied independently while the other factors kept constant.

3.3.2.1 Effect of pH and buffer's volume

The pH of the reaction mixture solution significantly affects on the fluorescence intensity of the formed fluorophore. One of the most widely used methods for forming a stable isoindole ring is to react OPA with two nucleophiles (2ME and primary amine). The reaction is usually carried out in alkaline media (pH 8.0-12.0) to ensure the conversion of 2ME to thiolate ion (active nucleophile). For this reason, the pH of the reaction mixture solution was studied in the range of 7.5-12.0 using a 0.2 M borate buffer solution. As shown in *Figure 3-18*, the fluorescent intensity of the formed OPA-2ME-MET fluorophore increases as a function of solution pH until it reaches a maximum value at pH= 10.0 and no longer increases. Otherwise, it decreased gradually owing to background compound formation. In fact, the formation of this compound is attributed to a mechanism in which at higher pH values, the OH^- ion competes with the thiolate ion to attack the OPA carbonyl, resulting in isoindole ring formation with two substituted OH groups[238] *Figure 3-17*.

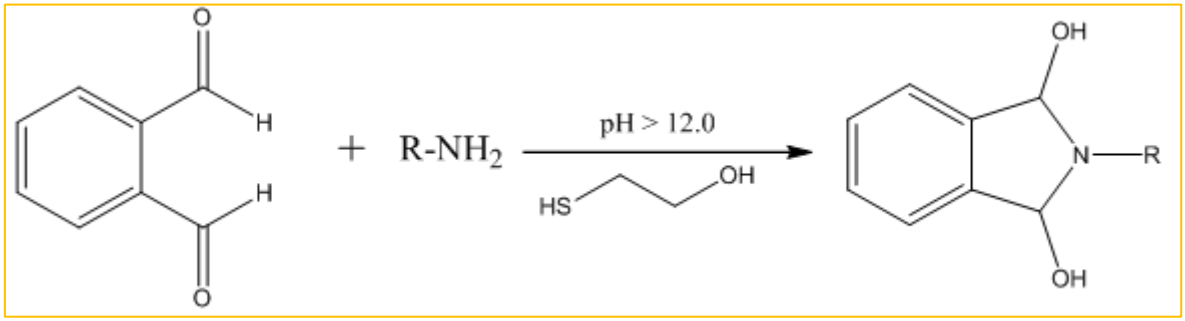

Figure 3-17. Formation of background compound in higher alkali condition.

The influence of borate buffer volume on the FI of the formed fluorophore was also studied in the range of (0.2-3.0 mL) at (pH = 9.8). As showing in *Figure 3-18*, the maximum FI was reached at 2.0 mL which selected as optimal buffer volume.

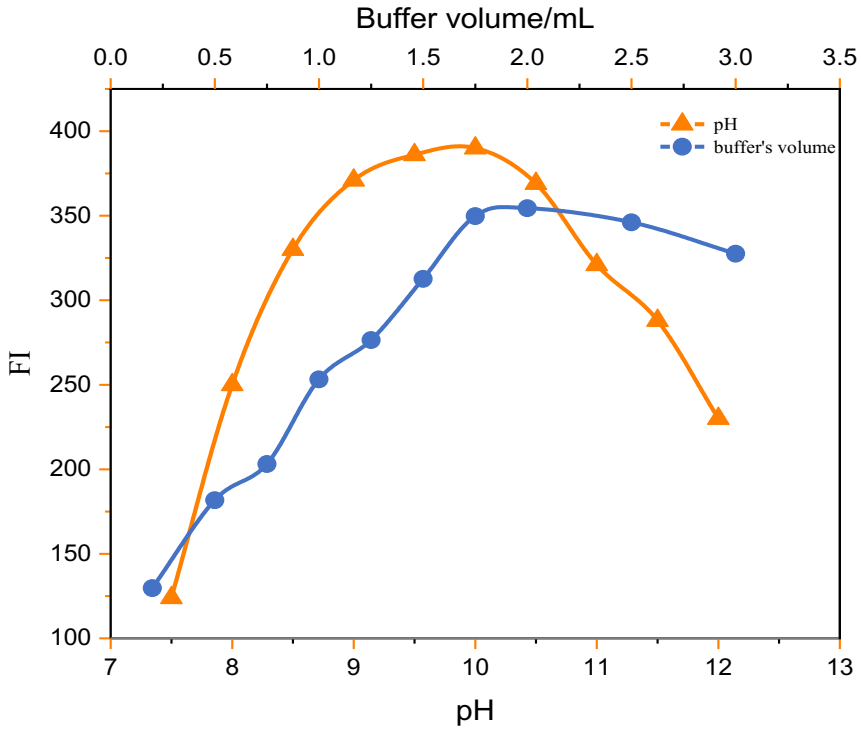

Figure 3-18. Effect of pH and buffer's volume on the FI of the formed fluorophore

3.3.2.2 Effect of OPA volume

The effect of reagent volume on the fluorescence intensity of the formed fluorophore has been studied in the range (0.2-3.0 mL) using 0.1% w/v OPA solution. It was noticed that the fluorescence intensity increases as the reagent volume increase until reach a steady state region from (1.25-1.75 mL), followed by marked decrease. As a consequence, 1.5 mL of OPA was selected optimal reagent volume as detailed in *Figure 3-19*.

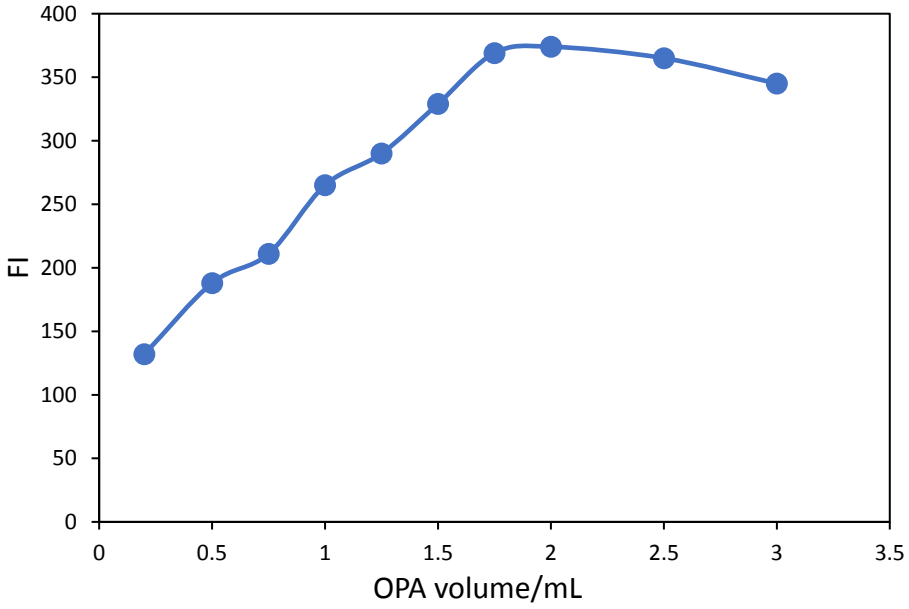

Figure 3-19. Effect of OPA volume on the FI of the formed fluorophore

3.3.2.3 Effect of 2-ME volume

According to the literature, the formation of isoindole compounds from the reaction of OPA with primary amine is usually unstable where the FI is decrease to the halve of its original value after 10 min period. This problem can be overcome by adding an active thiol compound like 2-mercaptoethanol before the OPA addition step[239]. For this reason, different volumes of 2-ME 0.5 % w/v within the range (0.1-1.5 mL) were used. It was found that the fluorescence intensity of the formed fluorophore increases gradually with the volume of 2-ME until reach a steady state region (0.7-1.2 mL) through which the FI remain unchanged, indicating that the formed fluorophore became stable enough and give maximum FI. Hence, 0.8 mL of 2-ME solution was selected as optimal volume *Figure 3-20*.

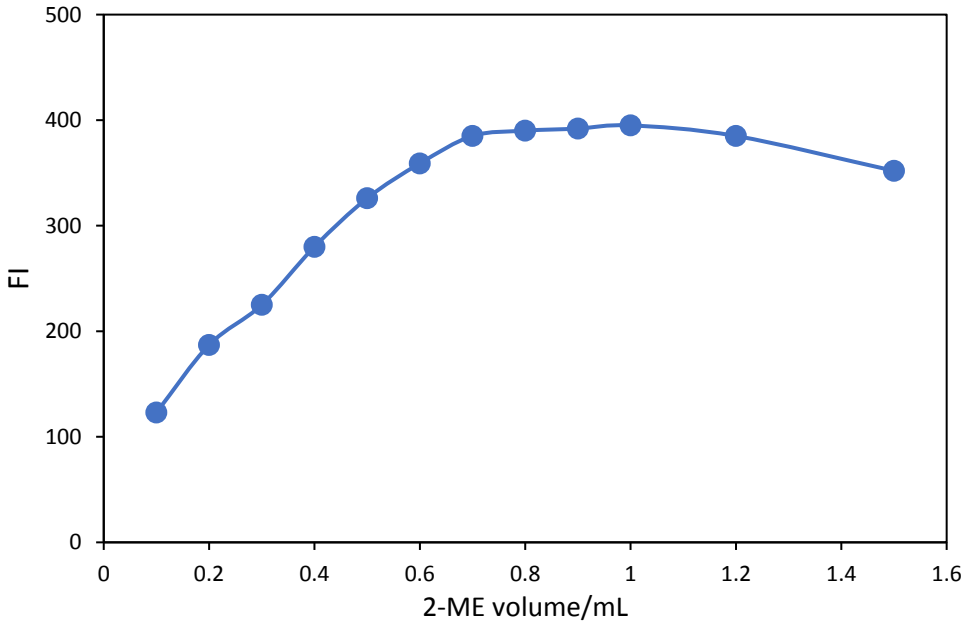

Figure 3-20. Effect of 2-ME volume on the FI of the formed fluorophore

3.3.2.4 Effect of time after addition of 2-ME

It was found that the time after addition 2-ME was significantly affect on the fluorescence intensity of the formed fluorophore, however the formation of thiolate ion requires sufficient time to complete. As shown in *Figure 3-21*, five minutes was selected as optimal time.

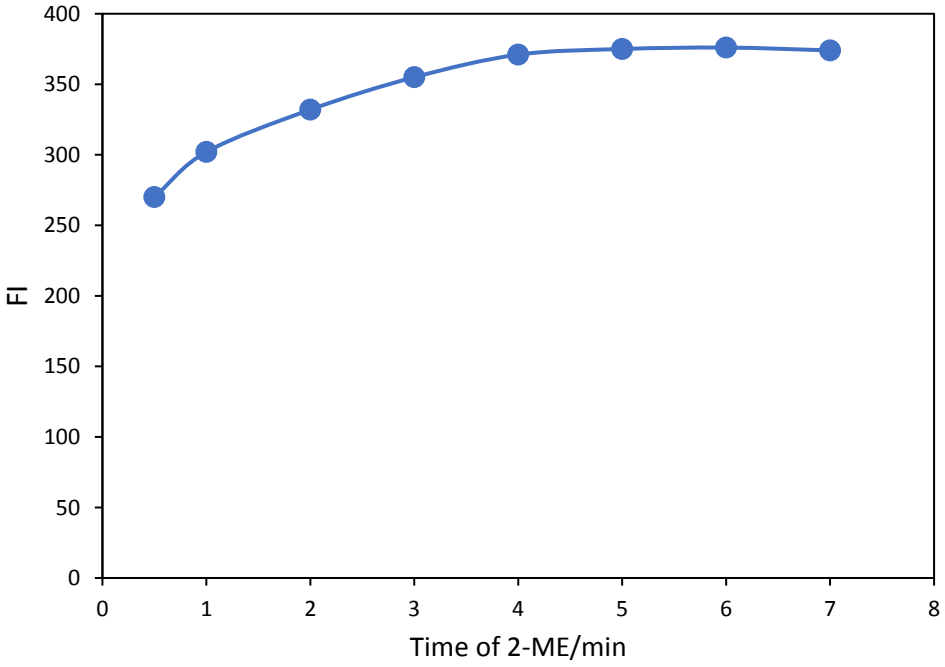

Figure 3-21. Effect of time after addition of 2-ME on the FI of the formed fluorophore

3.3.2.5 Effect of reaction time

Various time intervals within the range (2.0-45.0 min) were tested. It was noticed that the FI increase with the respect to the reaction time up to 30 min, after which the FI remains unchanged up to 90 min. Hence, allowing the reaction mixture to stand for 35 min is sufficient to complete the reaction *Figure 3-22*.

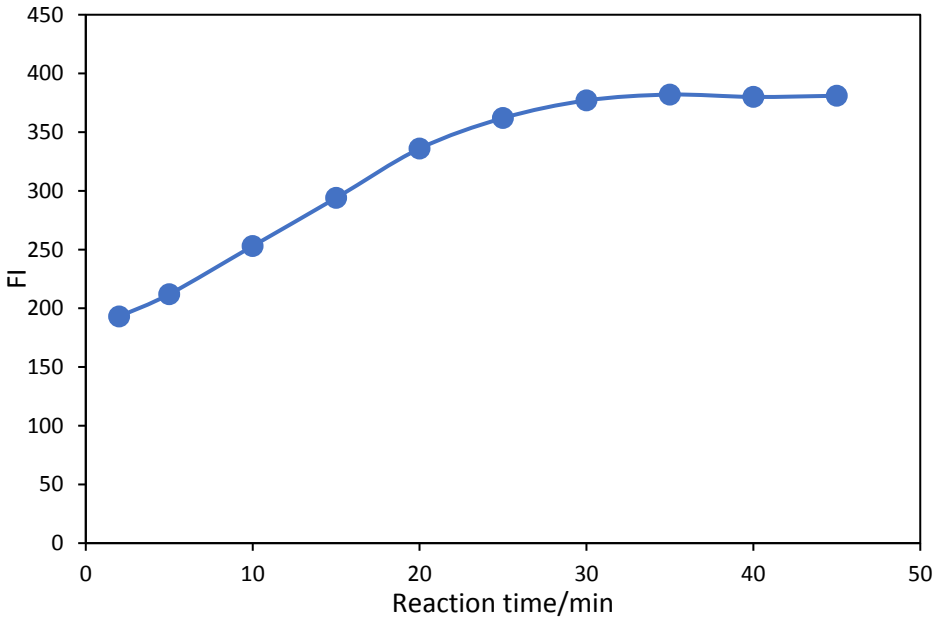

Figure 3-22. Effect of reaction time on the FI of the formed fluorophore

3.3.2.5 Diluting solvents Effect

To select the solvent that obtains the highest fluorescence intensity of the formed fluorophore, different diluting solvents have been tested, such as acetonitrile, 1,4-dioxan acetone, methanol, butanol, ethyl acetate, DMF, DMSO, ethanol, and D.W. It was found that the dilution of the reaction mixture with methanol give maximum FI.

3.3.3 Validation of method

The developed method has been validated according to International Conference on Harmonization (ICH) guidelines.

3.3.3.1 Construction of calibration curve (Recommended procedure)

Aliquots of AMB working standard solutions were quantitatively transferred using micropipette into a series of 10 ml calibrated flasks to prepare a final AMB concentration within the range (125-1400 ng mL^{-1}). Then, 2 mL of 0.2 M borate buffer solution (pH = 9.8) together with 0.8 mL of 1 %v/v 2-ME were added for each flask and mixed well. The reaction mixture was allowed to stand for 5 min. Thereafter, 1.5 mL of 0.1% w/v OPA was added and mixed gently. The reaction mixture was left again for 35 min at room temperature. The solution in each flask was diluted to the mark using methanol. The fluorescence intensity of the resulted solutions were measured at 475 nm when excited at 378 nm. The values of the FI were plotted *vs* final AMB concentration to obtain calibration curve whose linear regression equation was derived simultaneously *Figure 3-23 (a) and (b)*.

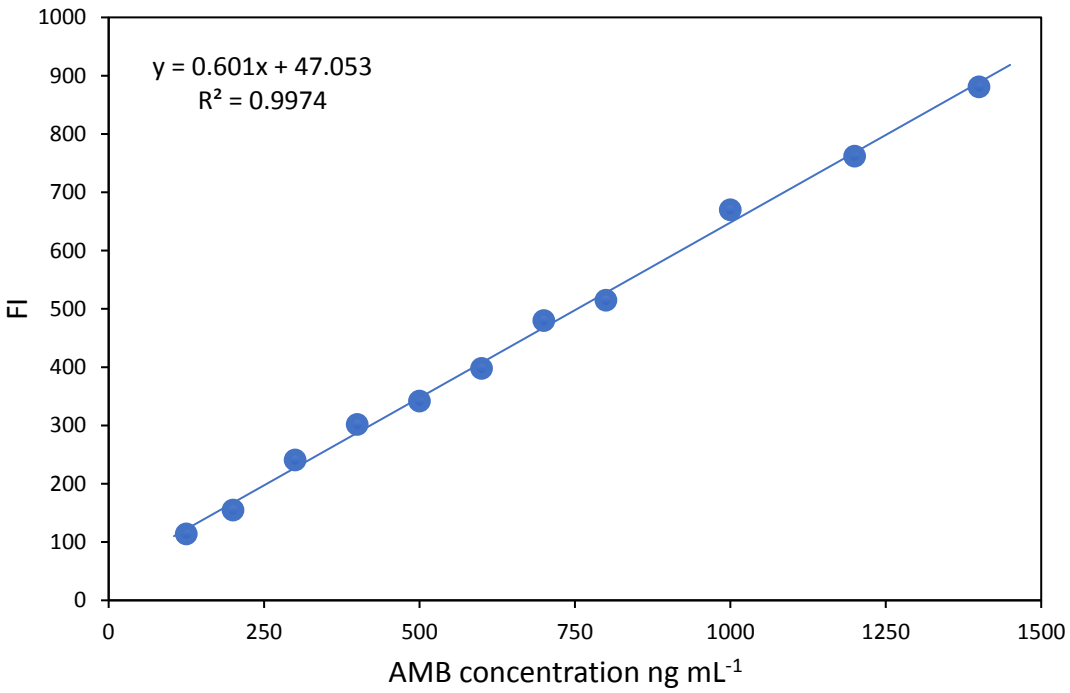

Figure 3-23 (a). Calibration curve of AMB drug

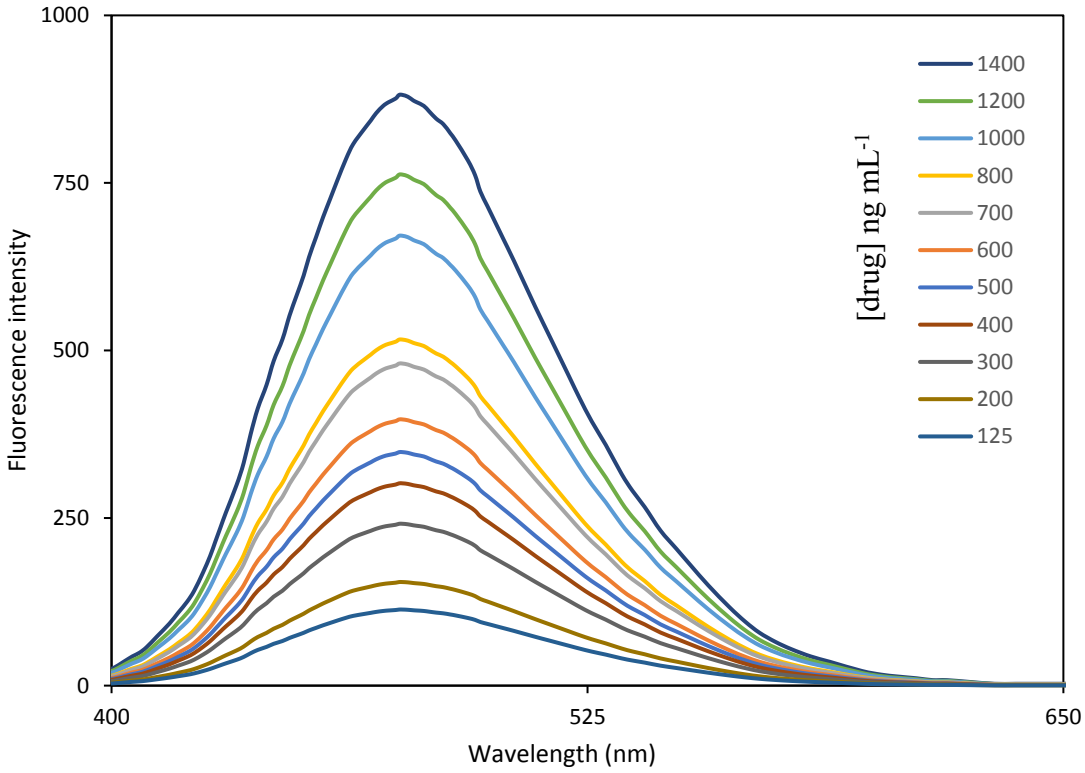

Figure 3-23 (b). Calibration curve of MET drug in dependence to scan spectra

Analysis of variance (ANOVA) was calculated for calibration curve, in which the value of $F_{statistic}$ (F=3390.13) is larger than $F_{significance}$ ($F^{1}_{9} = 5.117$), indicating there is a non-significance difference at confidence level 95% due to the regression and error around regression (residual), So these results are approaching to the ideal state (linearity) as illustrated in *Table 3-16* .

Table 3-16. Results of ANOVA analysis for linear regression equation

Source	*DF	**SS	***MS	F statistic	F significance	
Regression	1	614137.2	614137.24	3390.13	5.117	
Residual	9	1630.39	181.15			
Total	10	615767.6				
Parameter	Value	Standard Error	t Stat	P-value	Lower CL:95%	Upper CL:95%
Intercept	47.052937	7.901720	5.954771	0.000214	29.17	64.92
Slope	0.6010266	0.010322	58.22483	5.117	0.577	0.624

*Df=Degree of freedom, **SS=Sum of Square, ***MS=Mean of Square, CL=confidence level

3.3.3.2 Linearity and range

The linear regression equation of the analyzed data was given in the following formula:

$F = 0.601\ C + 47.053$

Where F represent fluorescence intensity, C represent AMB concentration in ng mL^{-1}. The linear concentration of the calibration graph ranged from 125-1400 ng mL^{-1} of AMB. The resulted data were summarized in *Table 3-17*.

Table 3-17 Analytical parameters of the suggested approach.

Parameter	suggested method
λ_{exc} (nm)	378
λ_{emi}(nm)	475
Concentration range (ng mL^{-1})	125-1400
Slope	0.601
SD of Slope	0.0103
Determination coefficient (r^2)	0.9974
Correlation coefficient (r)	0.9986
Intercept	47.05
SD of intercept	7.90
LOD* (ng mL^{-1})	31.29
LOQ** (ng mL^{-1})	94.84

****LOQ:** Limit of quantitation. ***LOD:** Limit of detection

3.3.3.3 limit of detection (LOD) and Limit of quantitation (LOQ)

LOD and LOQ of the suggested approach were obtained by calculating the standard deviation (S.D) of ten blank solution. The obtained S.D value was substituted in the equations supplied by the ICH Q2 (R1) guidelines. As

mentioned in *Table 3-17*, The small LOD and LOQ values indicate that the suggested approach is highly sensitive.

3.3.3.4 Accuracy

The suggested approach's accuracy has been determined by measuring the fluorescence intensity of the AMB-2ME-OPA fluorophore using three concentration level within the calibration graph (300, 600, 1000 ng mL^{-1}) by performing five replications of each selected concentration. As detailed in *Table 3-18*, the obtained results were analyzed to obtain percent recovery (Re%) whose values indicate that the suggested approach is highly accurate.

Table 3-18. Accuracy data of the suggested approach

Sample	Concentrations ng mL^{-1}	Recovery%* ± SD
1	300	101.13 ± 3.43
2	600	98.04 ± 3.20
3	1000	102.55 ± 3.36

* Mean of five determinations

3.3.3.5 Precision

The precision of the suggested approach has been represented as inter-day precision (Reproducibility) and intra-day precision (Repeatability). Three AMB concentration (250, 500, and 1000 ng mL^{-1}) was selected to test the precision of the suggested approach. Each concentration was analyzed at consecutive time during the day to obtain repeatability and at different day to obtain reproducibility. As illustrated in *Table 3-19*, the low value of relative standard deviation (R.S.D.% less than 2) indicate that the suggested approach is highly precise.

Table 3-19. Intra- and inter-day precisions of the suggested approach.

Concentration ng mL^{-1}	**Intra-day precision**		**Inter-day precision**	
	Recovery%*	**R.S.D.%**	**Recovery%***	**R.S.D.%**
250	97.80	1.36	98.60	0.98
500	101.14	1.04	99.01	1.11
1000	100.85	0.67	101.92	0.91

* Mean of five determinations

3.3.3.6 Robustness

The robustness describes the stability of the analytical method under a slight change in some experimental factors. In this work, three experimental factors (OPA volume, pH, and 2-ME volume) was slightly changed to test the robustness of the suggested approach. As mentioned in *Table 3-20*, the obtained values of percent recovery and R.S.D.% implies that slight changes in experimental conditions have no considerable effect on the quantification of AMB.

Table 3-20. Robustness evaluation for the suggested approach.

Experimental parameters	**Recovery%* ± R.S.D.%**
OPA volume (mL)	
1.3	98.68 ± 1.37
1.5	100.48 ± 1.23
1.7	100.74 ± 0.86
Buffer pH	
9.6	97.08 ± 1.05
9.8	99.81 ± 1.18
10	101.2 ± 0.86
2-ME volume (mL)	
1.3	101.94 ± 1.60
1.5	98.81 ± 1.06
1.7	99.41 ± 1.14

* Mean of five determinations.

3.3.3.7 Application

3.3.3.7.1 Application in the pharmaceutical vial

The suggested approach has been successfully used for quantifying of amlodipine in pharmaceutical *Tablet*s. The resulted data have been compared with the result produced from reported method using student's t and f test at confidence level equal to 95%[240]. *Table 3-21* illustrate that the t and f values of the suggested approach were less than relevant tabulated values, implying that the reported method and the suggested approach were not statistically different.

Table 3-21. Statistical comparison of data resulted by suggested approach with those of the reported one for determination of AMB in pharmaceutical *Tablet*s.

Pharmaceutical preparation	**Labeled contain mg/*Tablet***	**Recovery**	
		Proposed method	**Reported method**
Amtas	5	101.2	99.2
Amlopres	5	100.8	100.2
Amlovas	5	100.4	99.8
Amlopin	5	102.5	100.5
Amdepin	5	99.6	100.3
Mean ± S.D		100.9 ± 1.07	100 ± 0.51
Variance		1.15	0.265
***t* value**		1.69 (2.3)*	
f value		4.33 (6.38)*	

*The value between bracket represent the corresponding f and t tubulated values

3.3.3.7.2 Application in the spiked human plasma

Five AMB concentration (250, 500, 750, 1000, 1250 ng mL^{-1}) were successfully determined in spiked fresh human plasma. The obtained values of recovery percent (Re%) were mentioned in *Table 3-22*.

Table 3-22. Application of the suggested approach for determination of AMB in human plasma

Added conc. (ng mL^{-1})	Found conc. (ng mL^{-1})	Recovery% *± SD
250	256.81	102.72 ± 3.05
500	508.39	101.67 ± 4.92
750	751.65	100.22 ± 5.11
1000	119.87	101.98 ± 3.80
1250	799.40	100.14 ± 4.5

*: Mean of five determinations.

3.3.4. Optimization of experimental conditions of OPA-2ME-STA fluorophore

There are several experimental factors of the subjected approach that affect either on the stability or on the fluorescence intensity of OPA-2ME-STA fluorophore. These variables have been properly investigated and optimized. Each factor has been studied independently while the other factors kept constant.

3.3.4.1 Effect of pH and buffer's volume

The pH of the reaction mixture solution significantly affects on the fluorescent intensity of the formed fluorophore. The pH of the solution was studied in the range of 7.5-12.0 using a 0.2 M borate buffer solution. It was found that the FI of the formed OPA-2ME-MET fluorophore increases gradually with the respect to solution pH until it reaches a maximum fluorescence intensity at pH = 10.5 above which no longer increases. Otherwise, it decreased gradually owing to background compound formation *Figure 3-24*.

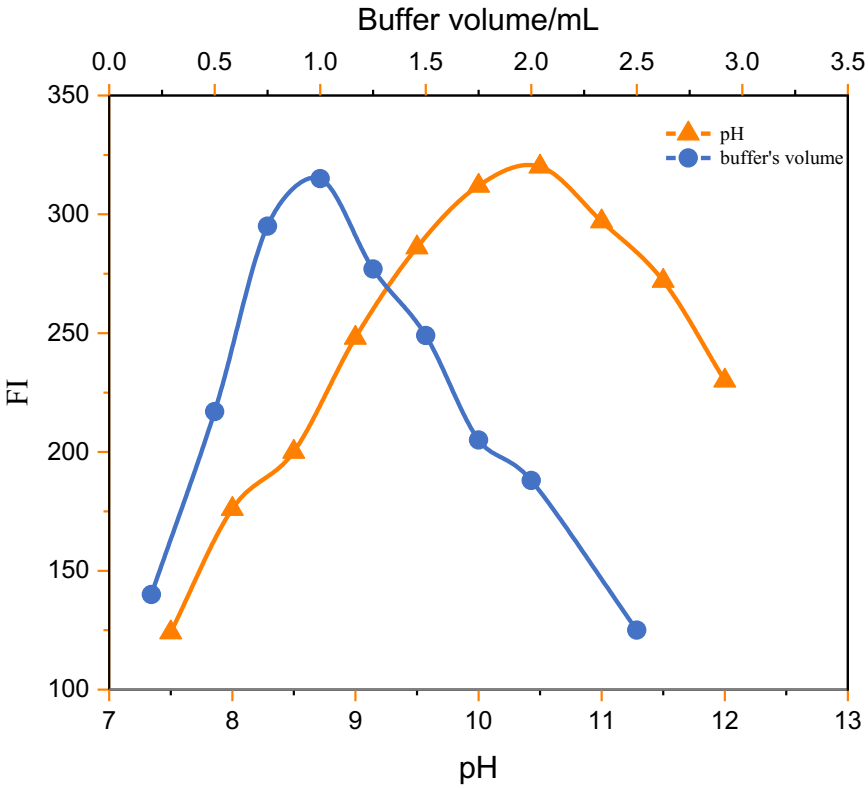

Figure 3-24. Effect of pH and buffer's volume on the FI of the formed fluorophore

The optimal borate buffer volume was also studied in the range (0.2-2.5 mL) at (pH = 10.5). As showing in *Figure 3-24*, the maximum FI was reached at 1.0 mL which selected as optimal buffer' volume.

3.3.4.2 Effect of OPA volume

The effect of reagent volume on the fluorescence intensity of the formed fluorophore has been studied in the range (0.2-2.5 mL) using 0.1% w/v OPA solution. It was noticed that the fluorescence intensity increases as the reagent volume increase until reach a steady state region from (1.25-1.75 mL), followed by marked decrease. As a consequence, 1.5 mL of OPA was selected optimal reagent volume as detailed in *Figure 3-25*.

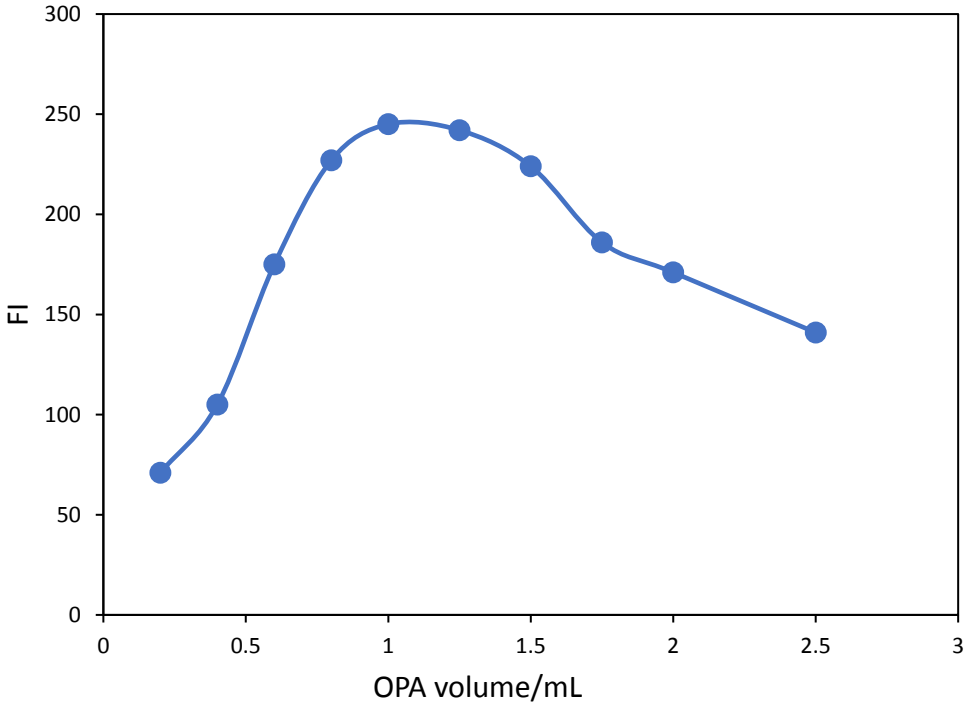

Figure 3-25. Effect of OPA volume on the FI of the formed fluorophore

3.3.4.3 Effect of 2-ME volume

Because 2-ME was used as fluorophore stabilizer agent different volumes of 2-ME 0.5 % w/v within the range (0.1-1.5 mL) were used. It was found that the fluorescence intensity of the formed fluorophore increases gradually with the volume of 2-ME until reach a steady state region (0.8-1.5 mL) through which the FI remain unchanged, indicating that the formed fluorophore became stable enough and give maximum FI. Hence, 1.0 mL of 2-ME solution was selected as optimal volume *Figure 3-26*.

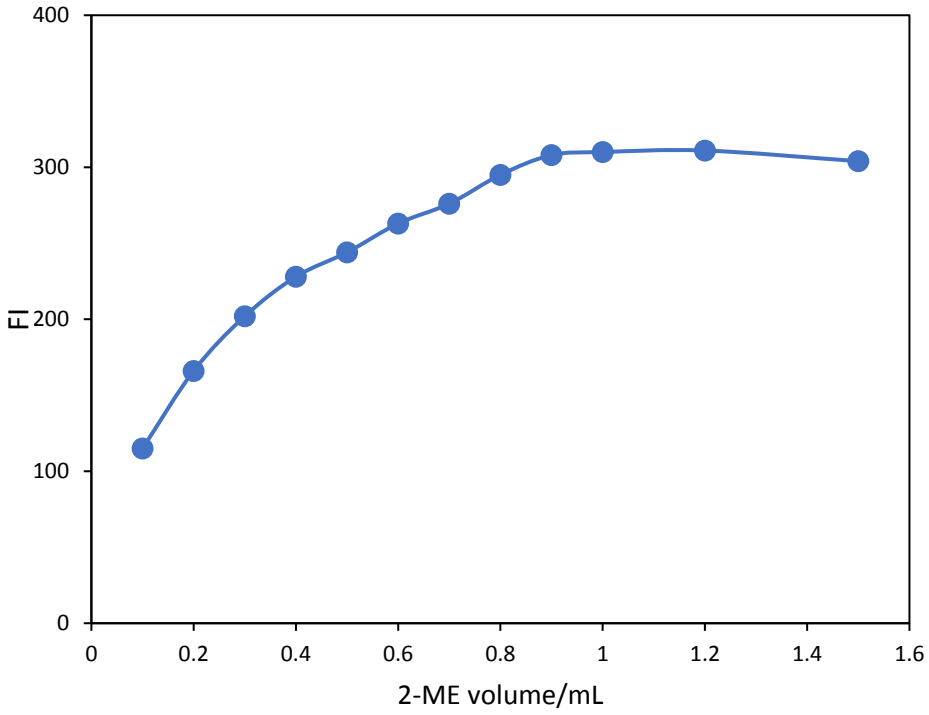

Figure 3-26. Effect of 2-ME volume on the FI of the formed fluorophore

3.3.4.4 Effect of time after addition of 2-ME

It was found that the time after addition 2-ME was significantly affect on the fluorescence intensity of the formed fluorophore, however the formation of thiolate ion requires sufficient time to complete. As shown in *Figure 3-27*, five minutes was selected as optimal time.

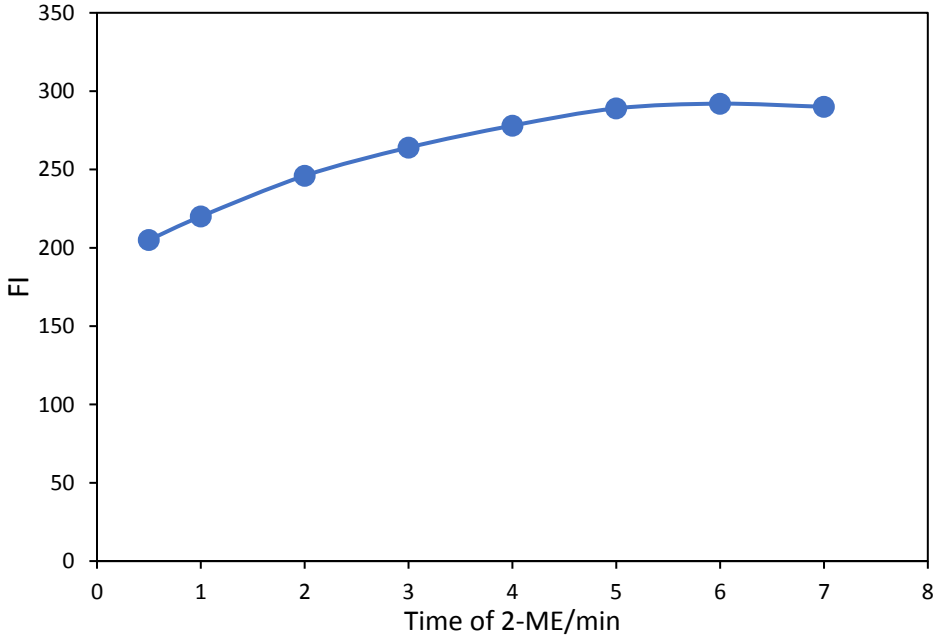

Figure 3-27. Effect of time after addition of 2-ME on the FI of the formed fluorophore.

3.3.4.5 Effect of reaction time

Various time intervals within the range (2.0-45.0 min) were tested. It was noticed that the FI increase with the respect to the reaction time up to 30 min, after which the FI remains unchanged up to 90 min. Hence, allowing the reaction mixture to stand for 35 min is sufficient to complete the reaction *Figure 3-28*.

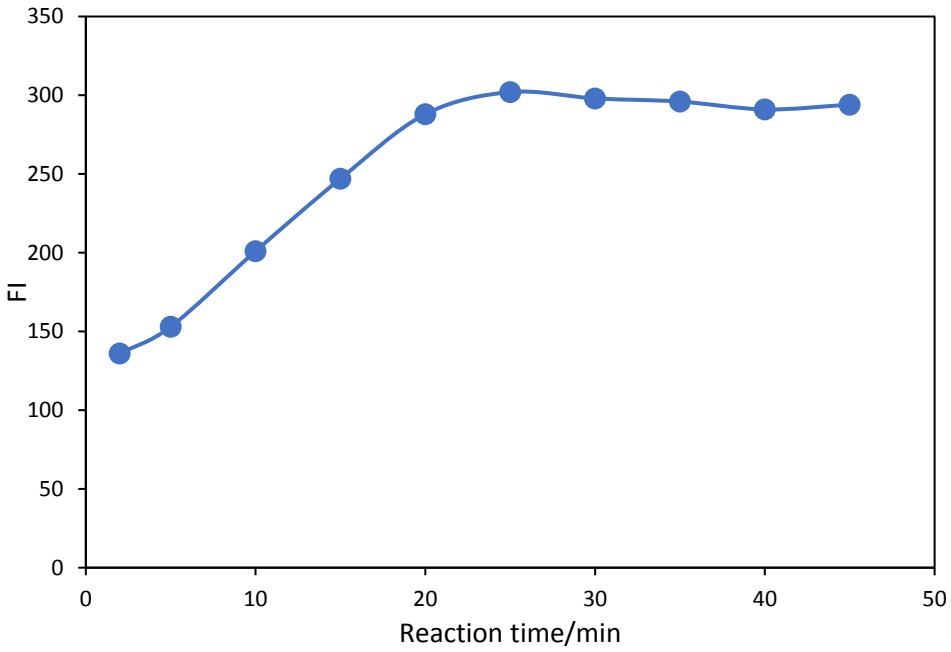

Figure 3-28. Effect of reaction time on the FI of the formed fluorophore

3.3.4.6 Diluting solvents Effect

To select the solvent that obtains the highest fluorescence intensity of the formed fluorophore, different diluting solvents have been tested, such as acetonitrile, 1,4-dioxan acetone, methanol, butanol, ethyl acetate, DMF, DMSO, ethanol, and D.W. It was found that the dilution of the reaction mixture with methanol give maximum FI.

3.3.5 Validation of method

The developed method has been validated according to International Conference on Harmonization (ICH) guidelines.

3.3.5.1 Construction of calibration curve (Recommended procedure)

To a set of 10 mL volumetric flasks, appropriate aliquots of the working standard solution (10 µg mL^{-1}) were accurately transferred using a micropipette to prepare solutions with drug concentration ranging from (275-1650 ng mL^{-1}), Then, 1 mL of 0.2 M borate buffer solution (pH = 10.5) together with 1.0 mL of 1 %v/v 2-ME were added for each flask and mixed well. The reaction mixture was allowed to stand for 5 min. Thereafter, 1.0 mL of 0.1% w/v OPA was added and mixed gently. The reaction mixture was left again for 25 min at room temperature. The solution in each flask was diluted to the mark using methanol. The fluorescence intensity of the resulted solutions were measured at 458 nm when excited at 335 nm. The values of the FI were plotted *vs* final STA concentration to obtain calibration curve whose linear regression equation was derived simultaneously *Figure 3-29 (a) and (b)*.

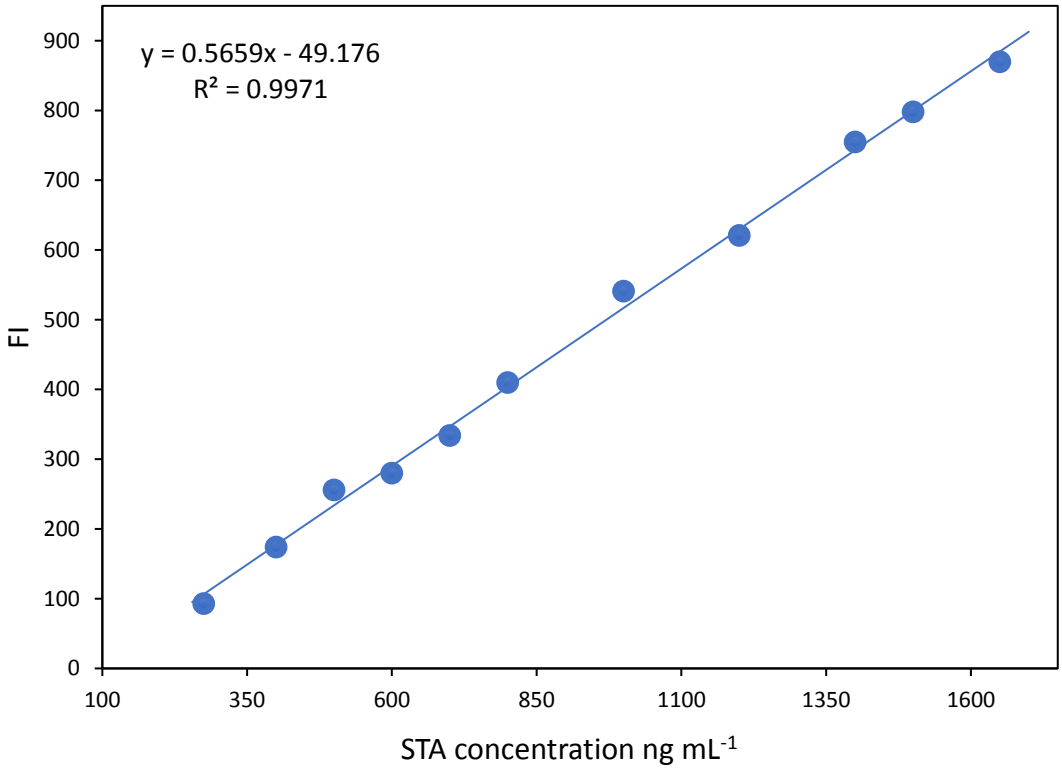

Figure 3-29 (a). Calibration curve of STA drug

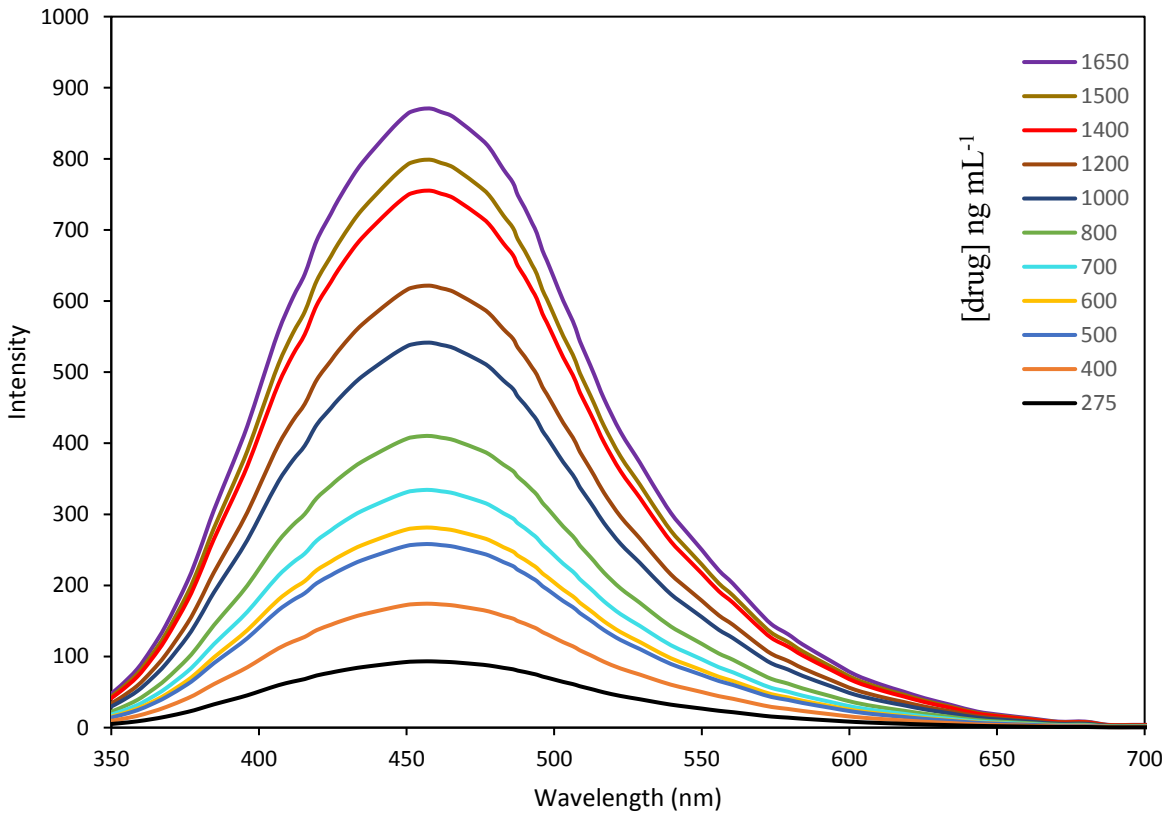

Figure 3-29 (b). Calibration curve of STA drug according to scan spectra

Analysis of variance (ANOVA) for calibration curve was calculated, in which the value of $F_{statistic}$ (F=3144.27) is larger than $F_{significance}$ ($F^{1}_{9} = 5.117$), indicating there is a non-significance difference at confidence level 95% due to the regression and error around regression (residual), So these results are approaching to the ideal state (linearity) as illustrated in *Table 3-23*.

Table 3-23. Results of ANOVA analysis for linear regression equation

Source	*DF	**SS	***MS	F statistic	F significance	
Regression	1	708229.5	708229.5	3144.274	5.117	
Residual	9	2027.198	225.2442			
Total	10	710256.7				
Parameter	Value	Standard Error	t Stat	P-value	Lower CL:95%	Upper CL:95%
Intercept	-49.175	10.250	-4.797	0.000977	-72.36	-25.98
Slope	0.5658	0.0100	56.073	5.117	0.5430	0.5887

*Df=Degree of freedom,**SS=Sum of Square,***MS=Mean of Square, CL=confidence level

3.3.5.2 Linearity and range

The linear regression equation of the analyzed data was given in the following formula:

$F = 0.5658\ C - 49.175$

Where F represent fluorescence intensity, C represent STA concentration in ng mL^{-1}. The linear concentration of the calibration graph ranged from 275-1650 ng mL^{-1} of STA. The resulted data were summarized in *Table 3-24*.

Table 3-24. Analytical parameters of the suggested approach.

Parameter	suggested method
λ_{exc} (nm)	335
λ_{emi}(nm)	458
Concentration range (ng mL^{-1})	275-1650
Slope	0.5658
SD of Slope	0.010
Determination coefficient (r^2)	0.9971
Correlation coefficient (r)	0.9985
Intercept	-49.175
SD of intercept	10.25
LOD* (ng mL^{-1})	58.94
LOQ** (ng mL^{-1})	178.62

****LOQ:** Limit of quantitation. ***LOD:** Limit of detection

3.3.5.3 limit of detection (LOD) and Limit of quantitation (LOQ)

LOD and LOQ of the suggested approach were obtained by calculating the standard deviation (S.D) of ten blank solution. The obtained S.D value was substituted in the equations supplied by the ICH Q2 (R1) guidelines. As

mentioned in *Table 3-24*, The small LOD and LOQ values indicate that the suggested approach is highly sensitive.

3.3.5.4 Accuracy

The suggested approach's accuracy has been determined by measuring the fluorescence intensity of the STA-2ME-OPA fluorophore using three concentration level within the calibration graph (500, 1000, 1500 ng mL^{-1}) by performing five replications of each selected concentration. As detailed in *Table 3-25,* the obtained results were analyzed to obtain percent recovery (Re%) whose values indicate that the suggested approach is highly accurate.

Table 3-25. Accuracy data of the suggested approach

Sample	Concentrations ng mL^{-1}	Recovery%* ± SD
1	500	102.20 ± 3.16
2	1000	101.39 ± 3.64
3	1500	99.14 ± 3.84

* Mean of five determinations

3.3.5.5 Precision

The precision of the suggested approach has been represented as inter-day precision (Reproducibility) and intra-day precision (Repeatability). Three STA concentration (500, 1000, and 1500 ng mL^{-1}) was selected to test the precision of the suggested approach. Each concentration was analyzed at consecutive time during the day to obtain repeatability and at different day to obtain reproducibility. As illustrated in *Table 3-26*, the low value of relative standard deviation (R.S.D.% less than 2) indicate that the suggested approach is highly precise.

Table 3-26. Intra- and inter-day precisions of the suggested approach.

Concentration ng mL^{-1}	**Intra-day precision**		**Inter-day precision**	
	Recovery%*	**R.S.D.%**	**Recovery%***	**R.S.D.%**
500	101.56	1.20	99.16	1.16
1000	101.03	0.76	98.95	0.56
1500	100.85	0.67	98.38	0.44

* Mean of five determinations

3.3.5.6 Robustness

The robustness describes the stability of the analytical method under a slight change in some experimental factors. In this work, three experimental factors (OPA volume, pH, and 2-ME volume) was slightly changed to test the robustness of the suggested approach. As mentioned in *Table 3-27*, the obtained values of percent recovery and R.S.D.% implies that slight changes in experimental conditions have no considerable effect on the quantification of STA.

Table 3-27. Robustness evaluation for the suggested approach.

Experimental parameters	**Recovery%* ± R.S.D.%**
OPA volume (mL)	
0.9	98.35 ± 0.63
1.0	101.07 ± 0.93
1.1	102.34 ± 0.55
Buffer pH	
10.3	101.60 ± 0.74
10.5	102.73 ± 0.61
10.7	97.96 ± 0.60
2-ME volume (mL)	
0.9	101.35 ± 0.75
1.0	101.56 ± 0.69
1.1	99.16 ± 0.69

* Mean of five determinations.

3.3.5.7 Application

3.3.5.7.1 Application in the pharmaceutical vial

The suggested approach has been successfully used for quantifying of STA in pharmaceutical tablets. The resulted data have been compared with the result produced from reported and official methods using student's t and f test at confidence level equal to 95%[241]. *Table 3-28*, illustrate that the t and f values of the suggested approach were less than relevant tabulated values, implying that the reported or official method and the suggested approach were not statistically different.

Table 3-28. Statistical comparison of data resulted by suggested approach with those of the reported and official method for determination of STA in pharmaceutical tablets.

Parameter	Proposed method	Reported method	Official method
Recovery%	100.7	100.19	100.5
S.D	1.25	1.02	1.39
Variance	1.57	1.05	1.93
Observation (n)	5	5	5
t test	$t_{critical}$ = 2.3 (p= 0.05)	0.7	0.2
f test	$f_{critical}$ = 6.39 (p= 0.05)	1.49	0.81

3.3.5.7.2 Application in the spiked human plasma

Five STA concentration (300, 500, 750, 1000, 1500 ng mL^{-1}) were successfully determined in spiked fresh human plasma. The obtained values of recovery percent (Re%) were mentioned in *Table 3-29*.

Table 3-29. Application of the suggested approach for determination of STA in human plasma

Added conc. (ng mL^{-1})	Found conc. (ng mL^{-1})	Recovery% *± SD
300	301.42	100.47 ± 2.07
500	506.76	101.42 ± 2.38
750	758.74	101.16 ± 3.11
1000	1012.15	101.23 ± 3.84
1500	1509.41	100.62 ± 4.94

*: Mean of five determinations.

3.4. Determination of metformin hydrochloride using 3,6-Dibromo-9,10-phenanthrenequinone as fluorogenic derivatization reagent.

3.4.1 Assigning the fluorescence spectrum of PQ-2Br-MET fluorophore

The literature survey of analytical fluorogenic derivatization reagent exhibits that mono and bi-guanide-containing compounds undergoes condensation reaction with 9,10-phenanthrenequinone or its derivatives like PQ-2Br to produce fluorescent product[242] *Figure 3-30*. This reaction was utilized for quantification of metformin hydrochloride in spiked human plasma and Diabetic COVID-19 patients administered metformin medication. *Figure 3-31,* illustrate the fluorescence spectrum of PQ-2Br-MET fluorophores using drugs concentration 500 ng mL^{-1}. The formed fluorophores exhibit excitation wavelength at 253 nm with emission wavelengths 420 nm.

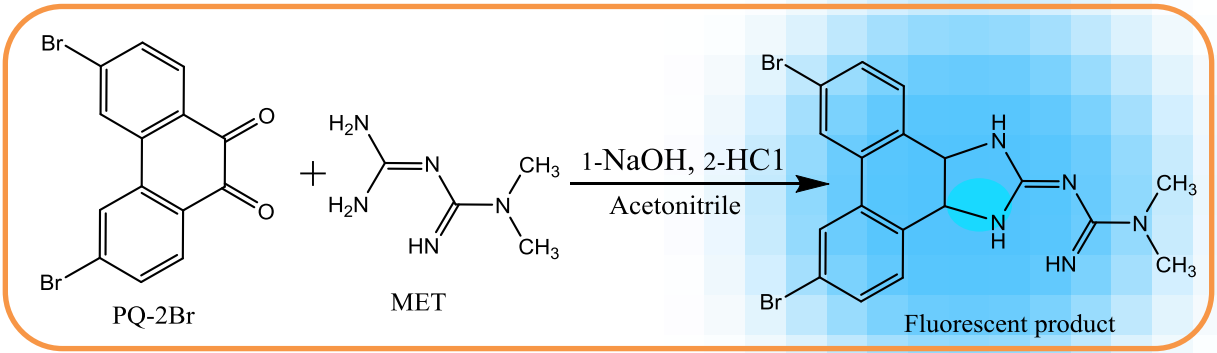

Figure 3-30. The suggested pathway of reaction between MET and PQ-2Br

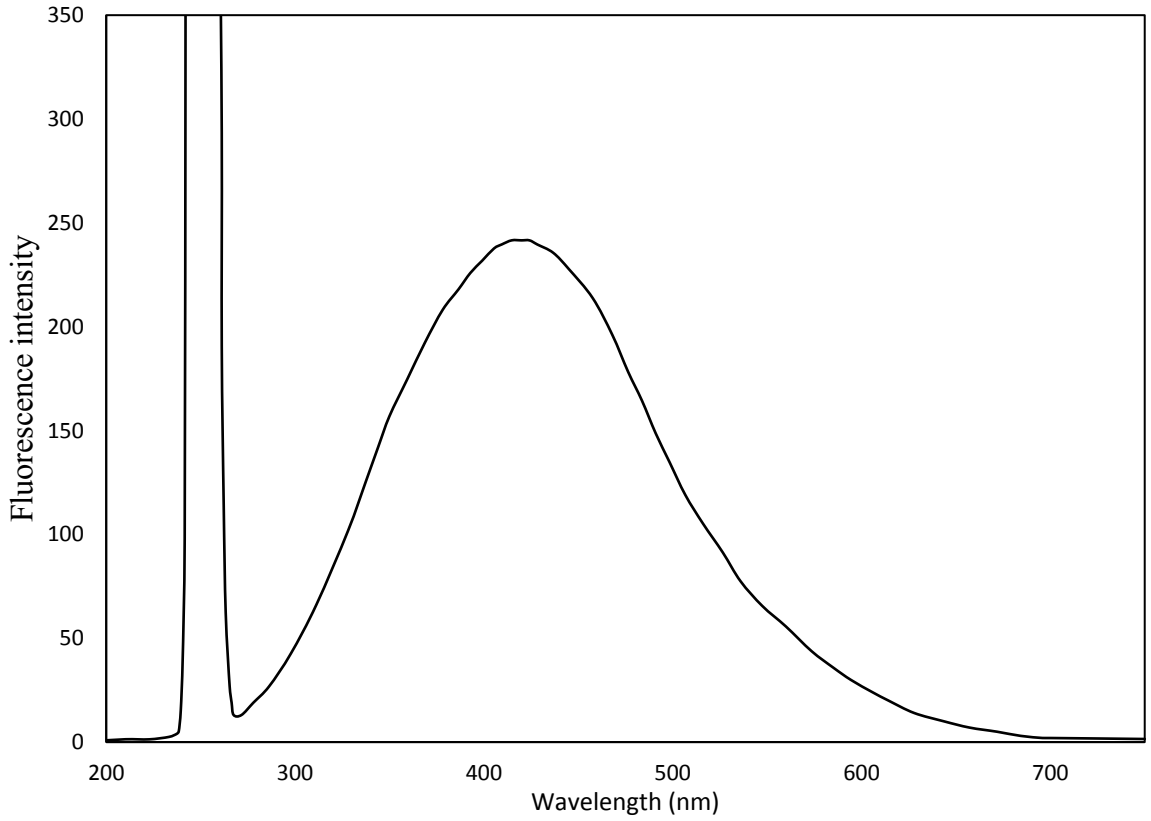

Figure 3-31. Excitation and emission spectra of PQ-2Br- MET product using optimal experimental condition

3.4.2 Optimization of experimental conditions of PQ-2Br-MET fluorophore

The experimental parameters of the suggested method that affect the stability and FI of the PQ-2Br-MET fluorophore were carefully estimated and optimized. Each parameter was investigated individually while the other parameters remained unchanged.

3.4.2.1 Effect of diluting solvent

The FI of the formed fluorophore was monitored after using different solvents to dilute the reaction product. It was found that the reaction is relatively more likely to occur in acetonitrile. As a result, acetonitrile was selected as the solvent of choice as illustrated in *Figure 3-32*

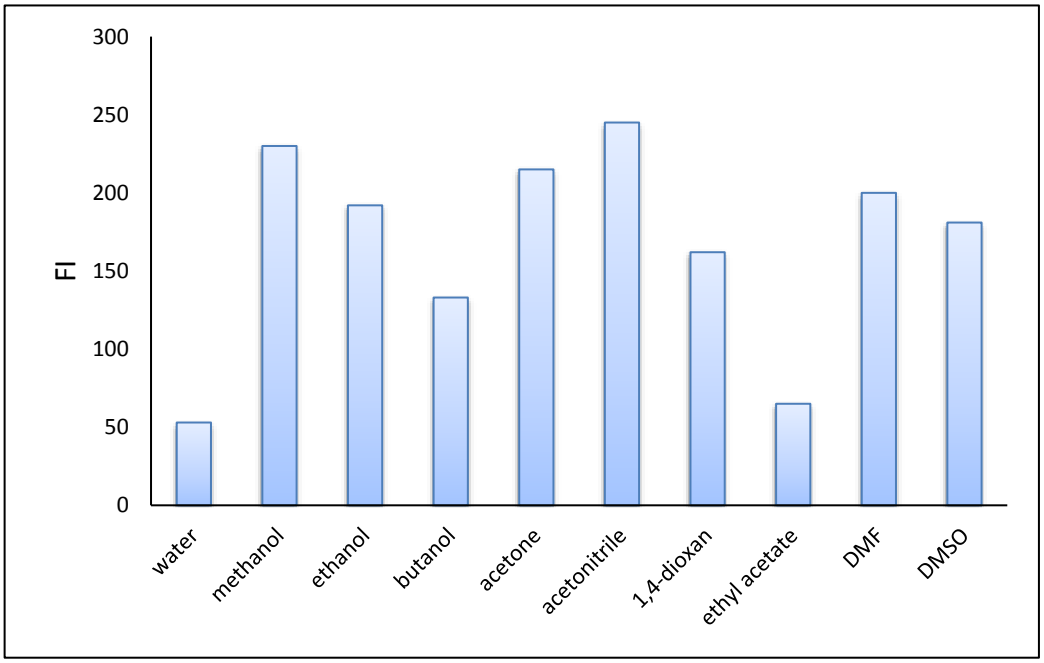

Figure 3-32 Effect of diluting solvents on the FI of PQ-2Br-MET fluorophore

3.4.2.2 Effect of reagent volume

Different volumes of 15 µg mL^{-1} PQ-2Br within the range (0.1-2.0 mL) were used and, as observed in *Figure 3-33*, the fluorescence intensity increased with respect to the reagent volume until reaching a steady state region (0.6-1.0 mL) and there was no further increase in fluorescence intensity. As a result, 0.80 mL of reagent solution was used for subsequent experiments.

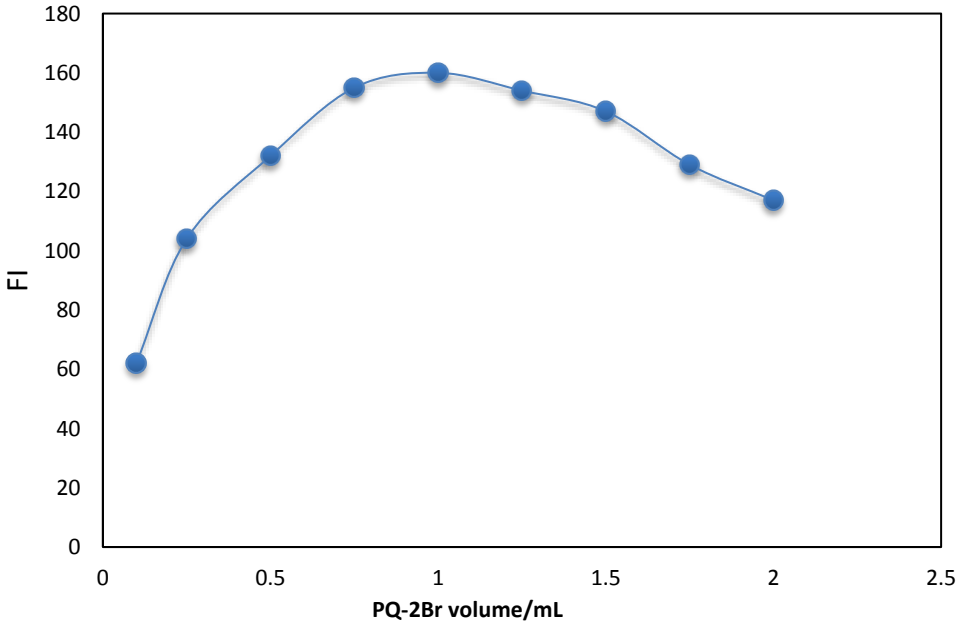

Figure 3-33. Effect of reagent volume on the FI of PQ-2Br-MET fluorophore

3.4.2.3 Effect of NaOH volume

The reaction of PQ-2Br reagent with guanidine-containing compounds are performed in alkalified solution. In fact, the nucleophilicity of amino groups of guanidine moiety increase in alkaline media. For this reason, different volume within the range of (0.25-2.5 mL) of 0.2 M sodium hydroxide were used. A maximum fluorescence intensity was attained at 1.25 mL, so this volume was selected as optimal NaOH volume as detailed in *Figure 3-34*.

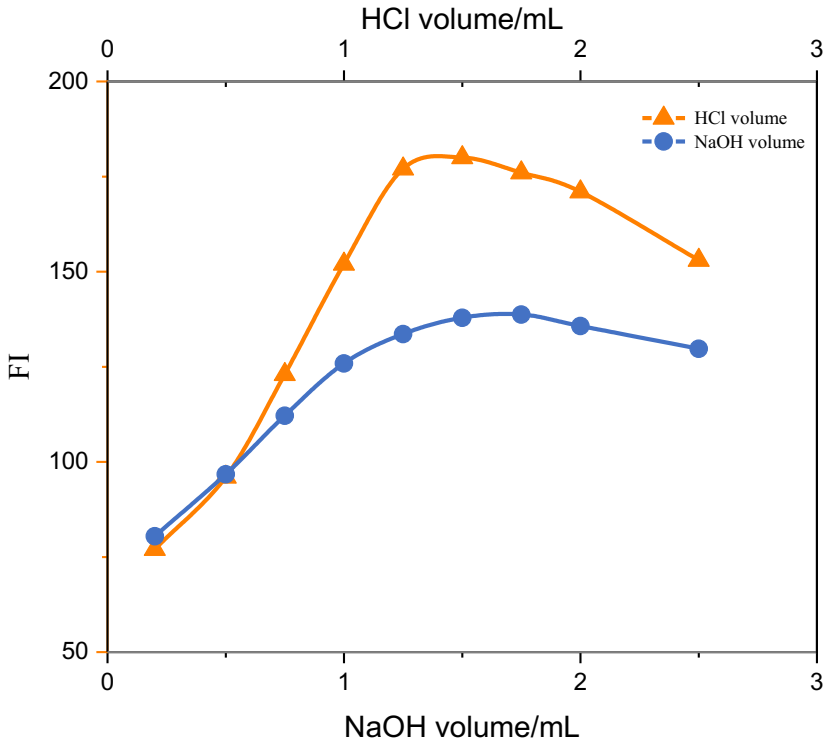

Figure 3-34. Effect of NaOH and HCl volumes on the FI of PQ-2Br-MET fluorophore.

3.4.2.4 Effect of HCl volume

It was reported that the reaction of guanide-containing compounds with PQ reagent was carried out in alkaline media to produce fluorescent or non-fluorescent compounds. In the case of the monoguanide substituted compound, a non-fluorescent product was formed. However, acidification of the reaction product solution leads to acid hydrolysis of the formed product into a fluorescent metabolite. On the other hand, diguanide substituted compounds produce fluorescent products in alkaline media and become more stable in acidic media[243-

[247]. This fact facilitates the quantification of biguanide compounds in a mixture of them in alkaline media. Because the basic media of NaOH require equimolar of HCl to neutralize i.e. 10 mg (0.25 mmole) or (1.25 mL of 0.2 M) of NaOH require 0.25 mmole (1.25 mL of 0.2 M) of HCl to be neutralized, several volume of 0.2 M HCl covering the range (0.2-3.0 mL) were used. Monitoring the FI of the formed fluorophore indicated that the FI was higher than its value in a neutral and acidic medium as illustrated in *Figure 3-34*, so 1.5 mL was selected as the optimal HCl volume.

3.4.2.5 Effect of temperature & reaction time

The optimal temperature necessary to obtain maximum FI of the formed fluorophore was found to be in the range of (30-40) ºC. Out of this range, the FI decreased gradually. As a result, 35 ºC was selected as the temperature of choice. The sufficient time interval required to complete the reaction was also studied in the range of (2.0-20 min). *Figure 3-35*, illustrates that 15 min is the optimal time to complete the reaction.

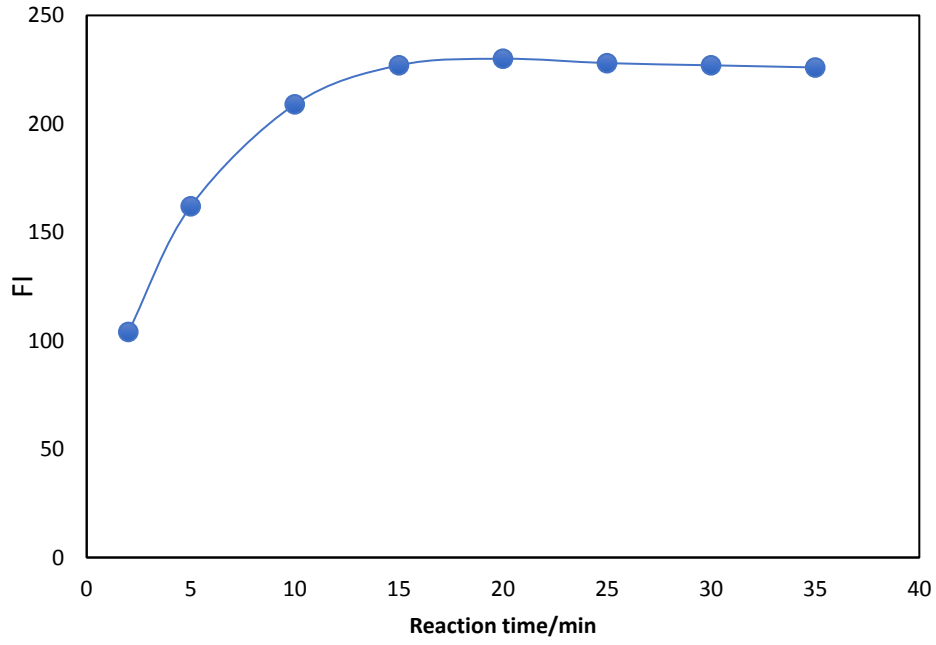

Figure 3-35. Effect of reaction time on the FI of PQ-2Br-MET fluorophore.

3.4.3 Validation of method

The developed method has been validated according to International Conference on Harmonization (ICH) guidelines.

3.4.3.1 Construction of calibration curve (Recommended procedure)

To a series of 10 mL volumetric flasks, appropriate aliquots of the working standard solution (10 µg mL^{-1}) were accurately transferred using a micropipette to prepare solutions with drug concentration ranging from (70-1300 ng mL^{-1}), Then, 1.25 mL of 0.2 M methanolic NaOH together with 0.75 mL of 20 µg mL^{-1} PQ-2Br reagent were added to each flask and mixed well. The reaction mixture was allowed to stand for 15 min in thermostatically water bath at 35 °C. Thereafter, 1.5 mL of 0.2 M HCl was added and mixed gently. The solution in each flask was diluted to the mark using acetonitrile. The fluorescence intensity of the resulted solutions were measured at 420 nm when excited at 253 nm. The values of the FI were plotted *vs* final MET concentration to obtain calibration curve whose linear regression equation was derived simultaneously *Figure 3-36 (a) and (b)*.

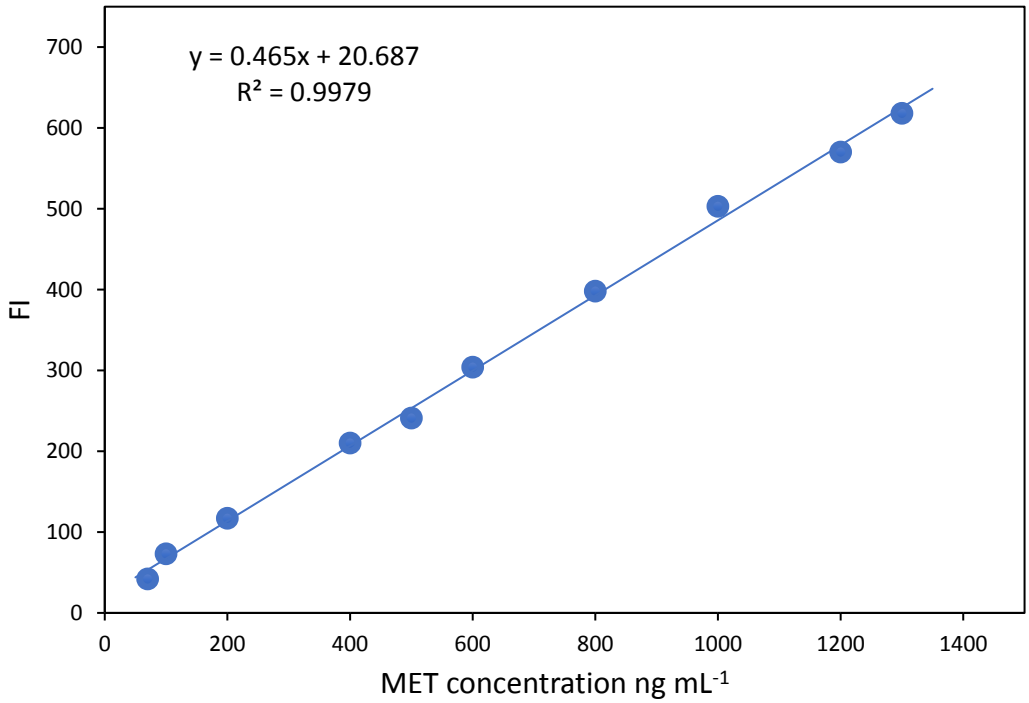

Figure 3-36(a). Calibration curve of MET drug

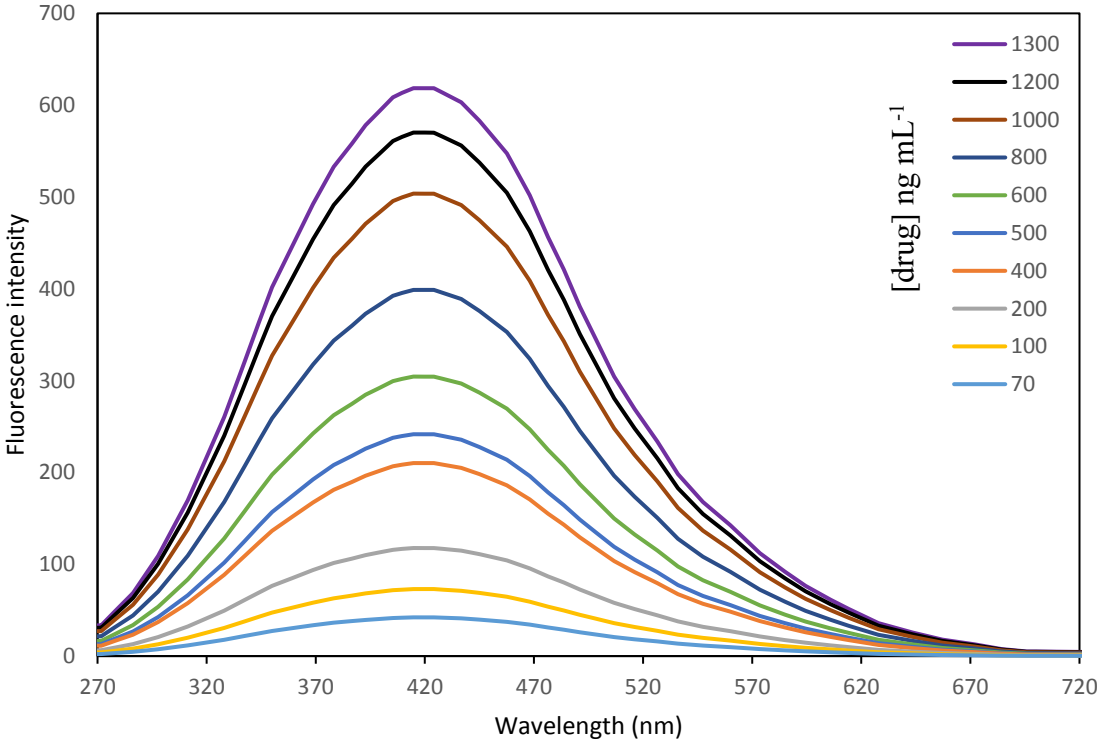

Figure 3-36(b). Calibration curve of MET drug according to scan spectra.

Analysis of variance (ANOVA) for calibration curve was calculated, in which the value of $F_{statistic}$ (F= 3846.04) is larger than $F_{significance}$ ($F^{1}_{8} = 5.318$), indicating there is a non-significance difference at confidence level 95% due to the regression and error around regression (residual), So these results are approaching to the ideal state (linearity) as illustrated in *Table 3-30*.

Table 3-30. Results of ANOVA analysis for linear regression equation

Source	*DF	**SS	***MS	F statistic	F significance	
Regression	1	386634.17	386634.17	3846.04	5.318	
Residual	8	804.22	100.52			
Total	9	387438.4				
Parameter	Value	Standard Error	t Stat	P-value	Lower CL:95%	Upper CL:95%
Intercept	20.6869	5.60859	3.688	0.0061440	7.753	33.620
Slope	0.4650	0.00749	62.016	5.318	0.447	0.482

*Df=Degree of freedom, **SS=Sum of Square, ***MS=Mean of Square, CL=confidence level

3.4.3.2 Linearity and range

The linear regression equation of the analyzed data was given in the following formula:

$F = 0.465\ C + 20.687$

Where F represent fluorescence intensity, C represent MET concentration in ng mL^{-1}. The linear concentration of the calibration graph ranged from 70-1300 ng mL^{-1} of MET. The resulted data were summarized in *Table 3-31*.

Table 3-31. Analytical parameters of the suggested approach.

Parameter	suggested method
λ_{exc} (nm)	253
λ_{emi}(nm)	420
Concentration range (ng mL^{-1})	70-1300
Slope	0.465
SD of Slope	0.0075
Determination coefficient (r^2)	0.9979
Correlation coefficient (r)	0.9989
Intercept	20.687
SD of intercept	5.60
LOD* (ng mL^{-1})	19.5
LOQ** (ng mL^{-1})	59.11

****LOQ:** Limit of quantitation. ***LOD:** Limit of detection

3.4.3.3 limit of detection (LOD) and Limit of quantitation (LOQ)

LOD and LOQ of the suggested approach were obtained by calculating the standard deviation (S.D) of ten blank solution. The obtained S.D value was substituted in the equations supplied by the ICH Q2 (R1) guidelines. As

mentioned in *Table 3-31*, The small LOD and LOQ values indicate that the suggested approach is highly sensitive.

3.4.3.4 Accuracy

The suggested approach's accuracy has been determined by measuring the fluorescence intensity of the MET-PQ-2Br fluorophore using three concentration level within the calibration graph (250, 500, 1000 ng mL^{-1}) by performing five replications of each selected concentration. As detailed in *Table 3-32*, the obtained results were analyzed to obtain percent recovery (Re%) whose values indicate that the suggested approach is highly accurate.

Table 3-32. Accuracy data of the suggested approach

Sample	**Concentrations ng mL^{-1}**	**Recovery%* ± SD**
1	250	101.77 ± 2.23
2	500	99.66 ± 3.04
3	1000	102.39 ± 3.70

* Mean of five determinations

3.4.3.5 Precision

The precision of the suggested approach has been represented as inter-day precision (Reproducibility) and intra-day precision (Repeatability). Three AMB concentration (100, 500, and 1000 ng mL^{-1}) was selected to test the precision of the suggested approach. Each concentration was analyzed at consecutive time during the day to obtain repeatability and at different day to obtain reproducibility. As illustrated in *Table 3-33*, the low value of relative standard deviation (R.S.D.% less than 2) indicate that the suggested approach is highly precise.

Table 3-33. Intra- and inter-day precisions of the suggested approach.

Concentration ng mL^{-1}	**Intra-day precision**		**Inter-day precision**	
	Recovery%*	**R.S.D.%**	**Recovery%***	**R.S.D.%**
100	103.03	1.66	102.17	1.91
500	100.43	0.75	101.46	0.59
1000	102.69	0.62	103.07	0.67

* Mean of five determinations

3.4.3.6 Robustness

The robustness describes the stability of the analytical method under a slight change in some experimental factors. In this work, three experimental factors (NaOH volume, PQ-2Br volume, and reaction time) was slightly changed to test the robustness of the suggested approach. As mentioned in *Table 3-34*, the obtained values of Re% and R.S.D.% implies that slight changes in experimental conditions have no considerable effect on the quantification of MET.

Table 3-34. Robustness evaluation for the suggested approach.

Experimental parameters	**Recovery%* ± R.S.D.%**
NaOH volume (mL)	
1.3	99.58 ± 0.42
1.5	100.84 ± 0.81
1.7	100.41 ± 0.83
PQ-2Br volume (mL)	
0.6	102.85 ± 0.54
0.8	101.93 ± 0.51
1.0	101.65 ± 0.89
Reaction time (min)	
13	101.19 ± 0.77
15	100.67 ± 0.83
17	99.64 ± 0.40

* Mean of five determinations.

3.4.3.7 Application in the spiked human plasma

Five MET concentration (200, 400, 600, 800, 1000 ng mL^{-1}) were successfully determined in spiked fresh human plasma. The obtained values of recovery percent (Re%) were mentioned in *Table 3-35*.

Table 3-35. Application of the suggested approach for determination of MET in human plasma

Added conc. (ng mL^{-1})	**Found conc. (ng mL^{-1})**	**Recovery% *± SD**
200	205.40	102.70 ± 1.92
400	411.85	102.85 ± 2.23
600	613.57	102.26 ± 1.58
800	815.72	101.96 ± 3.39
1000	1031.64	103.16 ± 3.91

*: Mean of five determinations.

3.5 Clinical study

The current study is divided into two parts: the first one aims to evaluate the biomarkers like (D-dimer, LDH, GPT, and TG) in positive COVID-19 patients compared to healthy individuals. The second aims to investigate and evaluate the effect of remdesivir as a first-line antiviral drug on the patients with both positive COVID-19 and type 2 diabetic mellitus and those with only positive COVID-19 infection using biomarkers like (plasma metformin, D-dimer, LDH, GPT, and TG).

3.5.1 Inclusion and exclusion criteria

Only participants over the age of 20 years with confirmed SARS-CoA-2 infection were included in this study. However, patients with severe liver and kidney problems were excluded from this study, whether or not they had confirmed COVID-19 infection. Moreover, Patients having pneumonia on radiographic imaging with oxygen saturation ($SpO_2 < 90\%$) needing external oxygen support, were also excluded as they have severe COVID-19 infection. Liver and kidney functions tests were routinely monitored as precautionary laboratory examination for hospitalized patients with confirmed COVID-19 infection.

3.5.2 Statistical Analysis

The obtained data was statistically analyzed using the "Statistical Package for Social Sciences" (SPSS) software (version 26.0). The obtained data was presented as (Means ± SD). Analysis of variance (one way- ANOVA) was used to make a statistical comparison either within patient groups or with the control group by testing the significance level of differences in means between more than two groups. A probability (P) value less than 0.05 is considered statistically significant.

3.5.3 Characteristics of both Control and Patients Groups

The current study was conducted on three groups: (1) Patients with both positive COVID-19 and type 2 diabetic mellitus treated with remdesivir drug, (2) patients with positive COVID-19 without diabetic mellitus treated with remdesivir drug, (3) healthy individuals group (control). Despite the laboratory tests such as a throat swab used to detect COVID-19 infection, suspected COVID-19 infection was confirmed by radiographic imaging using computed tomography (CT scan), which is considered an effective and diagnostic tool providing accurate, fast, noninvasive, and painless scanning, enabling the detection of tiny nodules inside the lungs. *Table 3-36* illustrate the information of all patients and control groups required for the present study.

Table 3-36 The initial information for all patients and control group of the current study

Parameters	Ref. value	Diabetic-Covid-19 patients Mean ± SD N= 36	Non-Diabetic Covid-19 patients Mean ± SD N= 30	Control Mean ± SD N= 30
Age (years)	-------	43 - 66	35 - 59	24 - 61
BMI (kg/m^2)	18.5-24.9	28 ± 5.63	27 ± 6.88	26 ± 6.24
D-dimer (ng/mL)	< 500	4293± 2140	4438 ± 2064	387 ± 162
LDH (u/l)	> 250	564 ± 229	461 ± 202	176 ± 31
GPT IU/L	< 40	47 ± 26	51 ± 25	36 ± 9
s.TG mg/dL	< 150	175 ± 25.9	168 ± 30	153 ± 26
Plasma metformin ng/mL	----------	933 ± 131	-------	------

3.5.4. Biochemical Studies

The levels of biomarkers (D-dimer, LDH, GPT, TG, and Plasma metformin) were determined in COVID-19 patients before and after remdesivir administration and in the control group. The obtained data were analyzed with "Fisher's Least Significant Difference (LSD)," a type of post hoc test that compares multiple groups.

3.5.4.1. Results of D-dimer in COVID-19 Patients and Control Subjects

D-dimer was measured in 30 COVID-19 patients before and after remdesivir administration and in 30 control healthy group. As illustrated in *Table 3-37*, the D-dimer levels of patients groups (GP1 and GP2) were compared either with each other or with the control group.

Table 3-37 Statistical analysis of obtained data of D-dimer levels in patients and control groups

Groups	N	Mean ± SD	CL 95%		Compared groups		P value
			Lower	Upper			
GP1	30	4438 ± 2064	3667	5209	GP1	GP2	<0.001
						GC	<0.001
GP2	30	1685 ± 1120	1267	2103	GP2	GC	<0.001
GC	30	387 ± 162	326	447			

GP1: Patients group before remdesivir administration. GP2: Patients group after remdesivir administration. GC: Control group.

COVID-19 Patients group had high D-dimer levels, whether they were before or after drug administration as compared to control group (GP1: 4438 ± 2064, GP2: 1685 ± 1120).

When any damage occurs in the blood vessel wall, the coagulation cascade proteins will be activated and the coagulation process will begin. As the coagulation process proceeds, the soluble blood protein fibrinogen is converted to

fibrin, which then aggregates into cross-linked fibrin, leading to the formation of an insoluble gel and then forming a blood clot. On the other hand, a reverse process called fibrinolysis will occur in which the blood clot is degraded to a fibrin degradation product. One of the most clinical products of this process is called D-dimer, which is present in the blood after fibrinolysis and is comprised of two fibrin protein fragments joined by a cross-link, forming a protein dimer. D-dimer levels are utilized as a predictive biomarker for the blood disorder, in coagulation disorders associated with COVID-19, and disseminated intravascular coagulation[248-252]. A systematic analysis published in August 2020 found that COVID-19 patients presenting with high D-dimer values were at increased risk of severe disease and mortality[253, 254]. Patients with acute COVID-19 typically appeared D-dimer increase, either as a result of the acute lung injury itself or as a result of the common thromboembolic complications associated with COVID-19[255].

In addition to thrombosis and pulmonary embolism, D-dimer might be a manifestation of severe virus infection. A virus infection may develop into sepsis and induce coagulation dysfunction, which was common in serious disease progression. Moreover, the increase of D-dimer may be an indirect manifestation of inflammatory reaction, as inflammatory cytokines could cause the imbalance of coagulation and fibrinolysis in the alveoli, which may activate the fibrinolysis system, and then increase the level of D-dimer[256, 257]. And D-dimer greater than 1 μg/ml was found a risk factor of poor prognosis for patients with COVID-19[258]. The most common reason cited in the literature for the elevation of D-dimer includes viremia and the cytokine storm syndrome, in which the rise in pro-inflammatory cytokines (IL-2, IL-6, IL-8, IL-17, TNF-α) are inadequately controlled by the anti-inflammatory factors which overwhelm the coagulation cascade. Hypoxia itself leads to activation of hypoxia-inducible transcription factor-dependent signaling pathway, predisposing to thrombosis. The disease

most commonly affects elderly and comorbid patients. Advancing age and common comorbidities such as hypertension, diabetes mellitus, and cardiovascular diseases can predispose the patients to thrombosis[259,260].

3.5.4.2. Results of LDH in COVID-19 Patients and Control Subjects

LDH was measured in 30 COVID-19 patients before and after remdesivir administration and in 30 control healthy group. As shown in *Table 3-38*, the LDH levels of patients groups (GP1 and GP2) were compared either with each other or with the control group.

Table 3-38 Statistical analysis of obtained data of LDH levels in patients and control groups

Groups	N	Mean ± SD	CL 95%		Compared groups		P value
			Lower	Upper			
GP1	30	461 ± 202	385	537	GP1	GP2	<0.001
						GC	<0.001
GP2	30	256 ± 96	220	292	GP2	GC	0.02
GC	30	176 ± 31	164	188			

GP1: Patients group before remdesivir administration. GP2: Patients group after remdesivir administration. GC: Control group.

COVID-19 Patients group had high LDH levels, whether they were before or after drug administration as compared to control group (GP1: 461 ± 202, GP2: 256 ± 96).

Lactate dehydrogenase (LDH) is an enzyme that is present in almost all living cells. under oxygen-insufficient conditions, LDH catalyzes the reversible reaction that convert the final product of glycolysis, pyruvate, to lactate and back, just as it catalyzes the conversion of NAD^+ to NADH and back. Breakdown of tissues release LDH, and therefore, increase LDH levels in the damaged tissues. Such a damage occur in red blood cell causes a hemolysis which detected by using LDH

levels therefore it can be used as indicative biomarker for hemolysis. Despite the fact that LDH was utilized as a biomarker of cardiac damage since the 1960s, A variety of organ damage, reduced oxygenation, and activation of the glycolytic pathway also result in abnormal LDH levels[261-263]. Severe infections can result in a damage to cytokine-mediated tissue which causes to release of LDH. Because LDH is found in lung tissue, people with severe COVID-19 infections can be expected to release greater amounts of LDH in the circulation, as a severe form of interstitial pneumonia, that frequently progresses to acute respiratory distress syndrome. LDH levels are also increase in thrombotic microangiopathy, which is linked to myocardial damage and renal failure. For this reason, there was a necessity to show the relation between LDH levels and severity of Covid-19 pneumonia. In the current study, LDH level was utilized as a biomarker for evaluating clinical severity and monitoring treatment response in COVID-19 pneumonia. It was found that decrease or increase of serum LDH level was effective tool for indicative of radiographic progress or improvement [264-267].

3.5.4.3. Results of GPT in COVID-19 Patients and Control Subjects

Alanine Aminotransferase (ALT) (GPT) was measured in 30 COVID-19 patients before and after remdesivir administration and in 30 control healthy group. As shown in *Table 3-39*, the GPT levels of patients groups (GP1 and GP2) were compared either with each other or with the control group. COVID-19 Patients group had high GPT levels, whether they were before or after drug administration as compared to control group (GP1: 51 ± 25, GP2: 64 ± 24).

Table 3-39 Statistical analysis of obtained data of GPT levels in patients and control groups

Groups	N	Mean ± SD	CL 95%		Compared groups		P value
			Lower	Upper			
GP1	30	51 ± 25	42	60	GP1	GP2	0.021
						GC	0.007

GP2	30	64 ± 24	54	73	GP2	GC	<0.001
GC	30	36 ± 9	33	40			

GP1: Patients group before remdesivir administration. GP2: Patients group after remdesivir administration. GC: Control group.

3.5.4.5. Results of s.TG in COVID-19 Patients and Control Subjects

Serum triglyceride (s.TG) was measured in 30 COVID-19 patients before and after remdesivir administration and in 30 control healthy group. As shown in *Table 3-40*, the TG levels of patients groups (GP1 and GP2) were compared either with each other or with the control group.

Table 3-40 Statistical analysis of obtained data of TG levels in patients and control groups

Groups	N	Mean ± SD	CL 95%		Compared groups		P value
			Lower	Upper			
GP1	30	168 ± 30	157	180	GP1	GP2	<0.047
						GC	<0.039
GP2	30	183 ± 27	173	193	GP2	GC	<0.001
GC	30	153 ± 26	143	163			

GP1: Patients group before remdesivir administration. GP2: Patients group after remdesivir administration. GC: Control group.

COVID-19 Patients group had high TG levels, whether they were before or after drug administration as compared to control group (GP1: 168 ± 30, GP2: 183 ± 27).

3.5.4.6. Results of biomarkers levels of Diabetic-COVID-19 Patients and Control Subjects

The levels of different biomarkers such as (D-dimer, LDH, GPT, TG, and plasma metformin) were measured in 36 COVID19-Diabetic patients before and after remdesivir administration. *Table 3-41,* illustrates the levels of these markers in

patients groups before and after remdesivir administration (GP1 and GP2) with a comparison of these groups either with each other or with the control group. As observed in the COVID-19 patients, the COVID19-Diabetic patients have also high levels of D-dimer and LDH before remdesivir administration. After remdesivir administration, the levels of D-dimer and LDH were decreased significantly. On the other hand, the levels of GPT, TG, and plasma metformin were increased significantly.

A study carried out on 193 COVID-19 patients, diabetic individuals (48 patients) had higher D-dimer levels than non-diabetic ones[(268)]. In last study of 28 COVID-19 patients with underlying diabetes, the level of D-dimer in patients admitted to the ICU was significantly different from that of the non-ICU patients (Table 7)[(269)].

Table 3-41 Statistical analysis of obtained data of biomarkers levels in Diabetic-COVID-19 patients and control groups

Biomarker	Groups	N	Mean ± SD	CL 95%		Compared groups		P value
				Lower	Upper			
D-dimer	GP1	36	4293 ± 2140	3563	5024	GP1	GP2	0.002
							GC	<0.001
	GP2	36	3043 ± 1785	2439	3647	GP2	GC	<0.001
	GC	30	387 ± 162	326	447			
LDH	GP1	36	564 ± 229	486	641	GP1	GP2	<0.001
							GC	<0.001
	GP2	36	377 ± 164	321	432	GP2	GC	<0.001
	GC	30	176 ± 31	164	188			
GPT	GP1	36	47 ± 26	38	56	GP1	GP2	0.008
							GC	0.06
	GP2	36	61 ± 25	52	70	GP2	GC	<0.001
	GC	30	36 ± 9	33	40			
TG	GP1	36	175 ± 25	166	183	GP1	GP2	<0.001
							GC	<0.001
	GP2	36	196 ± 24	187	204	GP2	GC	<0.001
	GC	30	153 ± 26	143	163			
Metformin	GP1	10	993 ± 131	--	--	GP1	GP2	0.003
	GP2	10	1206 ± 168	--	--			

GP1: Patients group before remdesivir administration. GP2: Patients group after remdesivir administration. GC: Control group.

3.5.5. Analysis of variance (ANOVA)

Tables 3-42 and 3-43, illustrate the analysis of variance (ANOVA) for the obtained data of biomarkers levels for COVID-19 and Diabetic-COVID-19 patients respectively.

Table 3-42, Analysis of variance (ANOVA) for the obtained data of biomarkers levels for COVID-19 patients

		Sum of Squares	df	Mean Square	F	Sig.
D-dimer	Between Groups	256838917	2	128419458	69.483	<0.001
	Within Groups	160794679	87	1848214		
	Total	417633597	89			
LDH	Between Groups	1296903	2	648451	37.830	<0.001
	Within Groups	1491269	87	17141		
	Total	2788172	89			
GPT	Between Groups	11449	2	5724	12.973	<0.001
	Within Groups	38391	87	441		
	Total	49840	89			
TG	Between Groups	13622	2	6811	8.459	<0.001
	Within Groups	70050	87	805		
	Total	83672	89			

Table 3-43, Analysis of variance (ANOVA) for the obtained data of biomarkers levels for Diabetic COVID-19 patients

		Sum of Squares	df	Mean Square	F	Sig.
D-dimer	Between Groups	256160741	2	128080370	46.017	<0.001
	Within Groups	275548850	99	2783321		
	Total	531709592	101			
LDH	Between Groups	2459269	2	1229634	43.105	<0.001
	Within Groups	2824134	99	28526		
	Total	5283404	101			
GPT	Between Groups	10406	2	5203	10.280	<0.001
	Within Groups	50111	99	506		
	Total	60518	101			
TG	Between Groups	29957	2	14978	22.590	<0.001
	Within Groups	65643	99	663		
	Total	95600	101			

GP1: Patients group before remdesivir administration. GP2: Patients group after remdesivir administration. GC: Control group.

3.5.6. Comparison of results between COVID-19 and diabetic-COVID-19 patients

Table 3-44, explain the comparison of result between non-diabetic COVID-19 and diabetics-COVID-19 patients in the term of recovery time period and biomarkers levels.

Table 3-44 Comparison of biomarkers results between diabetic and non-diabetic COVID-19 patients

Biomarker	Non-diabetic COVID-19 patients (Mean ± SD)		Diabetics COVID-19 patients (Mean ± SD)	
	Before T.R[a]	After T.R	Before T.R	After T.R
D-dimer	4438 ± 2064	1685 ± 1120	4293 ± 2140	3043 ± 1785
LDH	461 ± 202	256 ± 96	564 ± 229	377 ± 164
GPT	51 ± 25	64 ± 24	47 ± 26	61 ± 25
TG	168 ± 30	183 ± 27	175 ± 25	196 ± 24
metformin	----	----	993 ± 131	1206 ± 168
Recovery time period	8 – 11 days		14 – 17 days	

[a] Treatment with remdesivir

According to the results, non-diabetic patients treated with remdesivir showed a faster recovery, than those placed in the diabetic category having COVID-19 complication. The results of biomarkers that were measured during lab examination depicted that remdesivir showed therapeutic effectiveness in both diabetic and non-diabetic COVID-19 patients. Furthermore, the effectiveness of remdesivir was not associated with complications of diabetes mellitus. However, the recovery rate was slow in diabetic patients as compared to non-diabetic patients. The clinical range of COVID-19 is wide, going from gentle flu like manifestations to intense respiratory conditions, organ dysfunctioning, and

demise. Constant irritation, expanded coagulation action, compromised immunity, and direct pancreatic harm brought about by SARS-CoV-2 are on the whole potential components underlying the diabetes-COVID-19 affiliation. The concurrence of two worldwide pandemics such as COVID-19 and diabetes mellitus have major threatful clinical outcomes and ramifications for bleakness and mortality[270]. It is basic for clinicians to focus and draw their concentration on people suffering from diabetes mellitus accompanying Covid-19 infection to increase the understanding about the metabolic factors related to disease severity, and to remain acknowledged about disease progression, and potential Covid-19 medication therapies. Finally, and most importantly, we accentuate the significance of ideal inoculations for people with diabetes mellitus where the end goal leads towards Covid-19 vaccination which is the topmost priority in order to jeopardize the chances of viral infection[271]. Patients with diabetes mellitus are more susceptible to COVID-19 infection, resulting an intense respiratory condition. The coronavirus can increase the chances of hyperglycemia in individuals infected with this infection. The coronavirus can increase the risk of hyperglycemia in diabetic individuals[272]. The hyperglycemia, in association with other harmful factors, may change immunological and provocative reactions, leading towards lethal outcomes[273]. During treatment with remdesivir a specialist or attendant should intently do your screening. During the administration of remdesivir the individual patients have to tell the physician or medical caretaker about any adverse reaction that he may experience, including chills or shuddering, sickness, spewing, exorbitant perspiring, difficulty in standing, rash, wheezing or difficulty in breathing, abnormal heartbeat, inflammation or expanding of the face, throat, tongue, lips, or eyes. If any of these effects persist, your physician should diminish or cease your treatment[274].

(4.1) Conclusions and Future Prospects

(4.1.1) Conclusions

1- The prescribed spectrofluorometric methods provide a simple, rapid and precise methods for the estimation of drugs in their pharmaceutical dosage form and spiked fresh human plasma without interferences from plasma matrix or common excipients.

2- The developed methods showed promising selectivity, sensitivity, good linear ranges, excellent quantitative recoveries, and low detection limits with (R.S.D%) were less than 2 % for reproducibility and repeatability analysis.

3- Unlike chromatographic methods, which require costly hazardous solvents and sample pretreatment, these procedures are simple and low cost, allowing them to be used in routine analysis of studied drugs in the quality control and clinical laboratories.

4- The results for assaying the D-dimer and LDH levels in COVID-19 patients indicate that these biomarkers can be used as effective tools to diagnosis COVID-19 infection.

5- Remdesivir drug improve the levels of D-dimer and LDH in both Diabetic and non-Diabetic-COVID-19 patients with the increase in the levels of GPT, TG, and plasma metformin.

(4.1.2) Future Prospects

1. Synchronous fluorescence spectrofluorimetric method for the simultaneous determination of the previous studied drugs in its dosage form and fresh human plasma.
2. Fabricate a new microchip with fluorescence sensor for each drug (Lab on Chip) for detection of the studied drug in real sample.
3. Developing cloud point extraction technique for preconcentration of the studied drug in trace level-containing solution

References

1. Lakowicz, J.R., 1983. Protein fluorescence. In Principles of fluorescence spectroscopy (pp. 341-381). Springer, Boston, MA.
2. Itagaki, H., 2000. Fluorescence spectroscopy. Experimental Methods in Polymer Science, Academic Press, San Diego, CA, pp.155-260.
3. GUARDIGLI, M. 2012. Markus Sauer, Johan Hofkens, and Jörg Enderlein: Handbook of fluorescence spectroscopy and imaging: from ensemble to single molecules. Analytical and Bioanalytical Chemistry, 403, 1-2.
4. Skoog Douglas, A., West Donald, M., Holler, F.J. and Crouch Stanley, R., 2014. Fundamentals of analytical chemistry. Chem. Listy, 108, pp.694-696.
5. Ronda, C.R. ed., 2007. Luminescence: from theory to applications. John Wiley & Sons.
6. Lakowicz, J.R. ed., 2006. Principles of fluorescence spectroscopy. Boston, MA: springer US.
7. Valeur, B. and Berberan-Santos, M.N., 2012. Molecular fluorescence: principles and applications. John Wiley & Sons.
8. Gryczynski, Z.K. and Gryczynski, I., 2019. Practical fluorescence spectroscopy. CRC Press.
9. Bajpai, D.N., 2001. Advanced Physical Chemistry. S. Chand Publishing.
10. Rhys Williams, A. T., 1984. Fluorescence derivatization in liquid chromatography. Perkin-Elmer Ltd.
11. Wild, D. ed., 2013. The immunoassay handbook: theory and applications of ligand binding, ELISA and related techniques. Newnes.
12. Wick, G., Traill, K.N. and Schauenstein, K., 1982. Immunofluorescence technology. Sole distributors for the USA and Canada, Elsevier Science Pub. Co..
13. Pedras, B. and Avó, J.M.R. eds., 2019. Fluorescence in industry (Vol. 18). Springer.

14. Hof, M., Hutterer, R. and Fidler, V. eds., 2004. Fluorescence spectroscopy in biology: advanced methods and their applications to membranes, proteins, DNA, and cells (Vol. 3). Springer Science & Business Media.
15. Albani, J.R., 2008. Principles and applications of fluorescence spectroscopy. John Wiley & Sons.
16. Geddes, C.D. ed., 2017. Reviews in Fluorescence 2016. Springer International Publishing.
17. Engelborghs, Y. and Visser, A.J.W.G., 2014. Fluorescence Spectroscopy and Microscopy. Methods in molecular biology, 1076.
18. Nahata, A., 2011. Spectrofluorimetry as an analytical tool. Pharm Anal Acta, 2(8), pp.1-2.
19. Cox, G. ed., 2019. Fundamentals of fluorescence imaging. CRC Press.
20. Jameson, D.M., 2014. Introduction to fluorescence. Taylor & Francis.
21. Jickells, S. and Negrusz, A., 2008. Clarke's analytical forensic toxicology. In Annales de Toxicologie Analytique (Vol. 20, No. 4, pp. 233-234). EDP Sciences.
22. Wang, Q., Huang, H., Ning, B., Li, M. and He, L., 2016. A highly sensitive and selective spectrofluorimetric method for the determination of nitrite in food products. Food analytical methods, 9(5), pp.1293-1300.
23. Ranaweera, R.K., Gilmore, A.M., Capone, D.L., Bastian, S.E. and Jeffery, D.W., 2021. Spectrofluorometric analysis combined with machine learning for geographical and varietal authentication, and prediction of phenolic compound concentrations in red wine. Food Chemistry, 361, p.130149.
24. Hentschel, B.T., 1998. Spectrofluorometric quantification of neutral and polar lipids suggests a food-related recruitment bottleneck for juveniles of a deposit-feeding polychaete population. Limnology and oceanography, 43(3), pp.543-549.

25. Bose, A., Thomas, I. and Abraham, E., 2018. Fluorescence spectroscopy and its applications: A Review. International journal of advances in pharmaceutical analysis, 8, pp.01-08.
26. Johansson, J., 1993. Fluorescence spectroscopy for medical and environmental diagnostics, sweden.
27. Marcu, L., 2012. Fluorescence lifetime techniques in medical applications. Annals of biomedical engineering, 40(2), pp.304-331.
28. El-Emam, A.A., Hansen, S.H., Moustafa, M.A., El-Ashry, S.M. and El-Sherbiny, D.T., 2004. Determination of lisinopril in dosage forms and spiked human plasma through derivatization with 7-chloro-4-nitrobenzo-2-oxa-1, 3-diazole (NBD-Cl) followed by spectrophotometry or HPLC with fluorimetric detection. Journal of Pharmaceutical and Biomedical Analysis, 34(1), pp.35-44.
29. Haggag, R.S., Gawad, D.A., Belal, S.F. and Elbardisy, H.M., 2016. Spectrophotometric determination of the sulfhydryl containing drug mesna. Bulletin of Faculty of Pharmacy, Cairo University, 54(1), pp.21-32.
30. Ibrahim, F.A., El-Yazbi, A.F., Wagih, M.M. and Barary, M.A., 2017. Sensitive inexpensive spectrophotometric and spectrofluorimetric analysis of ezogabine, levetiracetam and topiramate in tablet formulations using Hantzsch condensation reaction. Spectrochimica Acta Part A: Molecular and Biomolecular Spectroscopy, 184, pp.47-60.
31. Al-Majed, A.A. and Al-Zehouri, J., 2001. Use of 7-fluoro-4-nitrobenzo-2-oxo-1, 3-diazole (NBD-F) for the determination of ramipril in tablets and spiked human plasma. Il Farmaco, 56(4), pp.291-296.
32. Hakim, A., Hossain, F., Jahan, I. and Ahmed, M.J., A Simple Spectrofluorimetric Method for the Determination of Cadmium at Ultra-trace Levels in some Real, Environmental, Biological, Tobacco, Food, Fertilizer, and Soil Samples Using 2', 3, 4', 5, 7-pentahydroxyflavone.

33. Ahmed, M.J., Islam, M.T. and Farhana, F., 2019. A highly sensitive and selective spectrofluorimetric method for the determination of cerium at pico-trace levels in some real, environmental, biological, soil, food and bone samples using 2-(α-pyridyl)-thioquinaldinamide. RSC advances, 9(44), pp.25609-25626.
34. Hossain, F., Begum, S., Jahan, I. and Ahmed, M.J., 2020. A Rapid Spectrofluorometric Method for the Determination of Aluminum at Nano-trace Levels in some Real, Environmental, Biological, Hemodialysis, Food, Pharmaceutical, and Soil Samples Using 2', 3, 4', 5, 7-pentahydroxyflavone. Analytical Sciences, p.19P443.
35. Khan, P., Idrees, D., Moxley, M.A., Corbett, J.A., Ahmad, F., von Figura, G., Sly, W.S., Waheed, A. and Hassan, M., 2014. Luminol-based chemiluminescent signals: clinical and non-clinical application and future uses. Applied biochemistry and biotechnology, 173(2), pp.333-355.
36. Gooch, J.P., 2019. Biosensors for the forensic detection of body fluids (Doctoral dissertation, King's College London.(
37. Campaña, A.M.G., Barrero, F.A. and Ceba, M.R., 1992. Spectrofluorimetric determination of boron in soils, plants and natural waters with Alizarin Red S. Analyst, 117(7), pp.1189-1191.
38. Vedrina-Dragojević, I., Dragojević, D. and Čadež, S., 1997. Spectrofluorimetric method for the determination of the total mercury content in sediment and soil. Analytica chimica acta, 355(2-3), pp.151-156.
39. Ahmed, M.J., Islam, M.T. and Hossain, F., 2018. A highly sensitive and selective spectrofluorimetric method for the determination of manganese at nanotrace levels in some real, environmental, biological, soil, food and pharmaceutical samples using 2-(α-pyridyl)-thioquinaldinamide. RSC advances, 8(10), pp.5509-5522.

40. Vilchez, J., Blanc, R. and Navalón, A., 1997. Simultaneous spectrofluorimetric determination of 1-naphthylacetic acid and 1-naphthalenacetamide in commercial formulations and soil samples. Talanta, 45(1), pp.105-111.
41. Sánchez, F.G. and Gallardo, A.A., 1992. Spectrofluorimetric determination of the insecticide azinphos-methyl in cultivated soils following generation of a fluorophore by hydrolysis. Analyst, 117(2), pp.195-198.
42. Andrade-Eiroa, A., Canle, M. and Cerda, V., 2013. Environmental applications of excitation-emission spectrofluorimetry: an in-depth review I. Applied Spectroscopy Reviews, 48(1), pp.1-49.
43. Poglazova, M.N., Mitskevich, I.N. and Kuzhinovsky, V.A., 1996. A spectrofluorimetric method for the determination of total bacterial counts in environmental samples. Journal of microbiological methods, 24(3), pp.211-218.
44. Sharma, A. and Schulman, S.G., 1999. Introduction to fluorescence spectroscopy (Vol. 13). New York: Wiley.
45. Wiederschain, G.Y., 2011. The Molecular Probes handbook. A guide to fluorescent probes and labeling technologies. Biochemistry (Moscow), 76(11), pp.1276-1277.
46. Knapp, D.R., 1979. Handbook of analytical derivatization reactions. John Wiley & Sons.
47. Zaikin, V. and Halket, J.M., 2009. A handbook of derivatives for mass spectrometry. IM publications.
48. Evershed, R.P., Blau, K. and Halket, J.M., 1993. Handbook of derivatives for chromatography. Advances in silylation. New York: Wiley, pp.51-108.
49. Fitton, A. Ogden, & Hill, J., 1970. Selected derivatives of organic compounds : a guidebook of techniques and reliable preparations. London, Chapman and Hall.
50. Demchenko, A.P., 2020. Introduction to Fluorescence Sensing: Volume 1: Materials and Devices, Springer Cham.

51. Baghdady, Y.Z. and Schug, K.A., 2016. Review of in situ derivatization techniques for enhanced bioanalysis using liquid chromatography with mass spectrometry. Journal of separation science, 39(1), pp.102-114.
52. Gell, C., Brockwell, D. and Smith, A., 2006. Handbook of single molecule fluorescence spectroscopy. Oxford University Press on Demand.
53. Hedegaard, S.F., Derbas, M.S., Lind, T.K., Kasimova, M.R., Christensen, M.V., Michaelsen, M.H., Campbell, R.A., Jorgensen, L., Franzyk, H., Cárdenas, M. and Nielsen, H.M., 2018. Fluorophore labeling of a cell-penetrating peptide significantly alters the mode and degree of biomembrane interaction. Scientific Reports, 8(1), pp.1-14.
54. Boutorine, A.S., Novopashina, D.S., Krasheninina, O.A., Nozeret, K. and Venyaminova, A.G., 2013. Fluorescent probes for nucleic acid visualization in fixed and live cells. Molecules, 18(12), pp.15357-15397.
55. Rajarao, G.K., Nekhotiaeva, N. and Good, L., 2002. Peptide-mediated delivery of green fluorescent protein into yeasts and bacteria. FEMS microbiology letters, 215(2), pp.267-272.
56. Bark, S.J. and Hahn, K.M., 2000. Fluorescent indicators of peptide cleavage in the trafficking compartments of living cells: Peptides site-specifically labeled with two dyes. Methods, 20(4), pp.429-435.
57. LODISH, H., BERK, A., KAISER, C. A., KRIEGER, M., BRETSCHER, A., PLOEGH, H., AMON, A. & SCOTT, M. P. 2012. Molecular Cell Biology, W. H. Freeman.
58. Proudnikov, D. and Mirzabekov, A., 1996. Chemical methods of DNA and RNA fluorescent labeling. Nucleic acids research, 24(22), pp.4535-4542.
59. CARSON, S., MILLER, H. B., WITHEROW, D. S. & SROUGI, M. C. 2019. Part V. Modulation of Gene Expression. In: CARSON, S., MILLER, H. B., WITHEROW, D. S. & SROUGI, M. C. (eds.) Molecular Biology Techniques (Fourth Edition). Academic Press.

60. Beddard, G.S. and West, M.A. eds., 1981. Fluorescent probes. Academic Press.

61. Ramarao, M.K., Murphy, E.A., Shen, M.W., Wang, Y., Bushell, K.N., Huang, N., Pan, N., Williams, C. and Clark, J.D., 2005. A fluorescence-based assay for fatty acid amide hydrolase compatible with high-throughput screening. Analytical biochemistry, 343(1), pp.143-151.

62. Chan, J., Dodani, S.C. and Chang, C.J., 2012. Reaction-based small-molecule fluorescent probes for chemoselective bioimaging. Nature chemistry, 4(12), pp.973-984.

63. Ploem, J.S., 1999. Fluorescence microscopy. Fluorescent and Luminescent Probes for Biological Activity. WT Mason, editor. Academic Press, London, pp.3-13.

64. Rönnberg, A.L., Hansson, C., Drakenberg, T. and Håkanson, R., 1984. Reaction of histamine with o-phthalaldehyde: isolation and analysis of the fluorophore. Analytical Biochemistry, 139(2), pp.329-337.

65. Nussler, A.K., Glanemann, M., Schirmeier, A., Liu, L. and Nüssler, N.C., 2006. Fluorometric measurement of nitrite/nitrate by 2, 3-diaminonaphthalene. Nature protocols, 1(5), pp.2223-2226.

66. Bartos, J. and Pesez, M., 1979. Colorimetric and fluorimetric determination of aldehydes and ketones. Pure Appl Chem, 51(8), pp.1803-14.

67. Robert-Peillard, F., Chottier, C., Coulomb, B. and Boudenne, J.L., 2015. Simple and ultrasensitive microplate method for spectrofluorimetric determination of trace resorcinol. Microchemical Journal, 122, pp.5-9.

68. Ahluwalia, V.K., 2010. Intermediates for organic synthesis. IK International Pvt Ltd.

69. Sethna, S. and Phadke, R., 2004. The Pechmann Reaction. Organic Reactions, 7, J. Wiley & Sons, Inc. New York. pp.1-58.

70. Mills, T., 1978. Application of fluorometry to the analytical problems concerning marijuana in biological materials (Doctoral dissertation, Georgia Institute of Technology.(

71. Matuszewski, B.K. and Bayne, W.F., 1989. Fluorogenic reaction between adenine derivatives and chloroacetaldehyde and its application to the determination of 9-(2-chloro-6-fluorobenzyl) adenine in human plasma. Analytica chimica acta, 227, pp.189-202.

72. Stratford, M.R. and Dennis, M.F., 1994. Determination of adenine nucleotides by fluorescence detection using high-performance liquid chromatography and post-column derivatisation with chloroacetaldehyde. Journal of Chromatography B: Biomedical Sciences and Applications, 662(1), pp.15-20.

73. Kawamoto, Y., Shinozuka, K., Kunitomo, M. and Haginaka, J., 1998. Determination of ATP and its metabolites released from rat caudal artery by isocratic ion-pair reversed-phase high-performance liquid chromatography. Analytical biochemistry, 262(1), pp.33-38.

74. Ilutiu-Varvara, D.A., Radulescu, D. and Donca, V., 2017. Benfothiamine administration in patients with dilated cardiomyopathy and advanced heart failure with chronic diuretic treatment. Studia Universitatis Babes-Bolyai, Chemia, 62(1.(

75. Edwards, K.A., Tu-Maung, N., Cheng, K., Wang, B., Baeumner, A.J. and Kraft, C.E., 2017. Thiamine assays—advances, challenges, and caveats. ChemistryOpen, 6(2), pp.178-191.

76. Lu, J. and Frank, E.L., 2008. Rapid HPLC measurement of thiamine and its phosphate esters in whole blood. Clinical chemistry, 54(5), pp.901-906.

77. Pradhan, T., Jung, H.S., Jang, J.H., Kim, T.W., Kang, C. and Kim, J.S., 2014. Chemical sensing of neurotransmitters. Chemical Society Reviews, 43(13), pp.4684-4713.

78. Lange, W.E. and Bell, S.A., 1966. Fluorometric determination of acetylsalicylic acid and salicylic acid in blood. Journal of Pharmaceutical Sciences, 55(4), pp.386-389.
79. Shane, N. and Stillman, R., 1971. Fluorometric determination of salicylic acid in buffered aspirin products. Journal of Pharmaceutical Sciences, 60(1), pp.114-116.
80. Xu, B., Li, K., Qiao, J., Liungai, Z., Chen, C. and Lu, Y., 2017. UV photoconversion of environmental oestrogen diethylstilbestrol and its persistence in surface water under sunlight. Water research, 127, pp.77-85.
81. Coly, A. and Aaron, J.J., 1998. Fluorimetric analysis of pesticides: Methods, recent developments and applications. Talanta, 46(5), pp.815-843.
82. Grinberg, N. and Rodriguez, S. eds., 2019. Ewing's analytical instrumentation handbook. CRC Press.
83. McCleverty, J.A. and Meyer. T. J., 2003. Comprehensive coordination chemistry II. Amsterdam: Elsevier.
84. Bergel, F., 1964. Chelating agents and metal chelates: Edited by F. P. Dwyer and Mellor. D. P, Academic Press, New York.
85. Tsutsui, M., Levy, M.N., Nakamura, A., Ichikawa, M. and Mori, K., 1970. Reactions of Metal π-Complexes. In Introduction to Metal π-Complex Chemistry (pp. 119-170). Springer, Boston, MA.
86. Dai, Z., Ai, T., Zhou, Q. and Zhang, H., 2021. Design, Synthesis, and Application of Novel π-Conjugated Materials. Frontiers in Chemistry, 8, p.634698.
87. Yurish, S., 2018. Advances in Sensors: Reviews, Vol. 6. Lulu. International Frequency Sensor Association.
88. Geddes, C.D. and Lakowicz, J.R. eds., 2007. Advanced concepts in fluorescence sensing: Part A: Small molecule sensing (Vol. 9). Springer Science & Business Media.

89. Ji, S., Wu, W., Wu, W., Song, P., Han, K., Wang, Z., Liu, S., Guo, H. and Zhao, J., 2010. Tuning the luminescence lifetimes of ruthenium (II) polypyridine complexes and its application in luminescent oxygen sensing. Journal of Materials Chemistry, 20(10), pp.1953-1963.

90. Violante, A., Huang, P.M. and Gadd, G.M. eds., 2007. Biophysico-chemical processes of heavy metals and metalloids in soil environments. John Wiley & Sons.

91. Nishibayashi, Y., 2019. Transition Metal-Dinitrogen Complexes: Preparation and Reactivity. John Wiley & Sons.

92. Tsvirko, M., Meshkova, S., Chebotarska, I., Kiriiak, G. and Gorodnyuk, V., 2007, August. Fluorescent properties of some transition metals complexes with the new podand containing hydrazide groups. In Journal of Physics: Conference Series (Vol. 79, No. 1, p. 012027). IOP Publishing.

93. Philip, S., Thomas, P.S. and Mohanan, K., 2019. Synthesis, characterization, fluorescence imaging, and cytotoxicity studies of a uracil-based azo derivative and its metal complexes. Journal of the Chinese Chemical Society, 66(1), pp.21-30.

94. Strianese, M. and Pellecchia, C., 2016. Metal complexes as fluorescent probes for sensing biologically relevant gas molecules. Coordination Chemistry Reviews, 318, pp.16-28.

95. White, T.A., Arachchige, S.M., Sedai, B. and Brewer, K.J., 2010. Emission spectroscopy as a probe into photoinduced intramolecular electron transfer in polyazine bridged Ru (II), Rh (III) supramolecular complexes. Materials, 3(8), pp.4328-4354.

96. Şen, P., Hirel, C., Andraud, C., Aronica, C., Bretonnière, Y., Mohammed, A., Ågren, H., Minaev, B., Minaeva, V., Baryshnikov, G. and Lee, H.H., 2010. Fluorescence and FTIR spectra analysis of trans-A2B2-substituted di-and tetra-phenyl porphyrins. Materials, 3(8), pp.4446-4475.

97. Prasad, P., Gupta, A. and Sasmal, P.K., 2021. Aggregation-induced emission active metal complexes: a promising strategy to tackle bacterial infections. Chemical Communications, 57(2), pp.174-186.
98. Mao, Z., Liu, J., Kang, T.S., Wang, W., Han, Q.B., Wang, C.M., Leung, C.H. and Ma, D.L., 2016. An Ir (III) complex chemosensor for the detection of thiols. Science and Technology of advanced MaTerialS, 17(1), pp.109-114.
99. Sun, J., Wu, Y., Xiao, D., Lin, X. and Li, H., 2014. Spectrofluorimetric determination of aluminum ions via complexation with luteolin in absolute ethanol. Luminescence, 29(5), pp.456-461.
100. Kasprzak, M.M., Erxleben, A. and Ochocki, J., 2015. Properties and applications of flavonoid metal complexes. Rsc Advances, 5(57), pp.45853-45877.
101. Monago-Maraña, O., Durán-Merás, I., Galeano-Díaz, T. and de la Peña, A.M., 2016. Fluorescence properties of flavonoid compounds. Quantification in paprika samples using spectrofluorimetry coupled to second order chemometric tools. Food Chemistry, 196, pp.1058-1065.
102. Gutierrez, A.C. and Gehlen, M.H., 2002. Time resolved fluorescence spectroscopy of quercetin and morin complexes with Al3+. Spectrochimica Acta Part A: Molecular and Biomolecular Spectroscopy, 58(1), pp.83-89.
103. Phillips, D.A., Soroka, K., Vithanage, R.S. and Dasgupta, P.K., 1986. Enhancement and quenching of fluorescence of metal chelates of 8-hydroxyquinoline-5-sulfonic acid. Microchimica Acta, 88(3), pp.207-220.
104. Prat, M.D., Compañó, R., Beltrán, J.L. and Codony, R., 1994. Fluorescence of metal complexes of 8-hydroxyquinoline derivatives in aqueous micellar media. Journal of Fluorescence, 4(4), pp.279-281.
105. Kawakami, J., Ohta, M., Yamauchi, Y. and Ohzeki, K., 2003. 8-Hydroxyquinoline derivative as a fluorescent chemosensor for zinc ion. Analytical sciences, 19(10), pp.1353-1354.

106. Soroka, K., Vithanage, R.S., Phillips, D.A., Walker, B. and Dasgupta, P.K., 1987. Fluorescence properties of metal complexes of 8-hydroxyquinoline-5-sulfonic acid and chromatographic applications. Analytical Chemistry, 59(4), pp.629-636.

107. Minta, A., Kao, J.P. and Tsien, R.Y., 1989. Fluorescent indicators for cytosolic calcium based on rhodamine and fluorescein chromophores. Journal of Biological Chemistry, 264(14), pp.8171-8178.

108. Lim, M.H., Wong, B.A., Pitcock Jr, W.H., Mokshagundam, D., Baik, M.H. and Lippard, S.J., 2006. Direct nitric oxide detection in aqueous solution by copper (II) fluorescein complexes. Journal of the American Chemical Society, 128(44), pp.14364-14373.

109. Mohammad, H., Islam, A.S.M., Prodhan, C. and Ali, M., 2019. A fluorescein-based chemosensor for "turn-on" detection of Hg 2+ and the resultant complex as a fluorescent sensor for S 2− in semi-aqueous medium with cell-imaging application: experimental and computational studies. New Journal of Chemistry, 43(14), pp.5297-5307.

110. Aoki, I., Saito, A. and Watanabe, K., 1989. The Fluorometric Determination of Magnesium with 2, 2′-Dihydroxy-4, 4′-dimethylazobenzene. Bulletin of the Chemical Society of Japan, 62(6), pp.2084-2086.

111. Wang, J. and Ha, C.S., 2010. 2, 2′-Dihydroxyazobenzene-based fluorescent system for the colorimetric 'turn-on'sensing of cyanide. Tetrahedron, 66(10), pp.1846-1851.

112. Khopkar, S.M., 1998. Basic concepts of analytical chemistry. New Age International.

113. Knoeck, J. and Buchholz, J.A., 1971. Structure, bonding, and fluorescence of bivalent metal chelates of o, o'-dihydroxyazobenzene. Talanta, 18(9), pp.895-903.

114. Kohn, K.W., 1961. Determination of tetracyclines by extraction of fluorescent complexes. Application to biological materials. Analytical Chemistry, 33(7), pp.862-866.
115. Berthon, G., Brion, M. and Lambs, L., 1983. Metal ion-tetracycline interactions in biological fluids. 2. Potentiometric study of magnesium complexes with tetracycline, oxytetracycline, doxycycline, and minocycline, and discussion of their possible influence on the bioavailability of these antibiotics in blood plasma. Journal of inorganic biochemistry, 19(1), pp.1-18.
116. Carlotti, B., Cesaretti, A. and Elisei, F., 2012. Complexes of tetracyclines with divalent metal cations investigated by stationary and femtosecond-pulsed techniques. Physical chemistry chemical physics, 14(2), pp.823-834.
117. Granados, J.A.O., Thangarasu, P., Singh, N. and Vázquez-Ramos, J.M., 2019. Tetracycline and its quantum dots for recognition of Al3+ and application in milk developing cells bio-imaging. Food chemistry, 278, pp.523-532.
118. Šober, M., 2016. Optimisation of Europium Sensitized Fluorescence Assay for Detection of Tetracycline Antibiotics. International Journal of Collaborative Research on Internal Medicine & Public Health, 8(8.(
119. Takahashi, Y., Tanaka, D.A.P., Matsunaga, H. and Suzuki, T.M., 2002. Switching of terbium (III)-sensitized luminescence by ligand exchange reaction: determination of catecholamines. Chemistry letters, 31(7), pp.722-723.
120. Chandrasekaran, S. ed., 2016. Click reactions in organic synthesis. John Wiley & Sons.
121. Lahann, J. ed., 2009. Click chemistry for biotechnology and materials science. John Wiley & Sons.
122. Witczak, Z.J. and Bielski, R., 2013. Click chemistry in glycoscience: New developments and strategies. John Wiley & Sons.
123. Shaik, S., 2016. Chemistry as a Game of Molecular Construction. The Bond-Click. John Wiley and Sons.

124. Chen. Y. and Tong. Z. R., 2017. Click Chemistry: Approaches, Applications, and Challenges, Nova Science.
125. Košmrlj, J. ed., 2012. Click triazoles (Vol. 28). Springer.
126. Quadrelli, P. ed., 2019. Modern applications of cycloaddition chemistry. Elsevier.
127. Ulrich, H., 2009. Cumulenes in click reactions. John Wiley & Sons.
128. Cserép, G.B., Herner, A. and Kele, P., 2015. Bioorthogonal fluorescent labels: A review on combined forces. Methods and applications in fluorescence, 3(4), p.042001.
129. Le Droumaguet, C., Wang, C. and Wang, Q., 2010. Fluorogenic click reaction. Chemical Society Reviews, 39(4), pp.1233-1239.
130. Sabnis, R.W., 2015. Handbook of fluorescent dyes and probes. John Wiley & Sons.
131. Stewart, J.T. and Lotti, D.M., 1971. Fluorometric determination of amphetamines with 3-carboxy-7-hydroxycoumarin. Journal of Pharmaceutical Sciences, 60(3), pp.461-463.
132. Stewart, J.T. and Lotti, D.M., 1970. Fluorimetric determination of some aliphatic and cyclic amines with 3-carboxy-7-hydroxycoumarin. Analytica Chimica Acta, 52(2), pp.390-393.
133. Pashkova, A., Moskovets, E. and Karger, B.L., 2004. Coumarin tags for improved analysis of peptides by MALDI-TOF MS and MS/MS. 1. Enhancement in MALDI MS signal intensities. Analytical chemistry, 76(15), pp.4550-4557.
134. Mizukami, S., Hori, Y. and Kikuchi, K., 2014. Small-molecule-based protein-labeling technology in live cell studies: probe-design concepts and applications. Accounts of Chemical Research, 47(1), pp.247-256.
135. Poole, L.B., Zeng, B.B., Knaggs, S.A., Yakubu, M. and King, S.B., 2005. Synthesis of chemical probes to map sulfenic acid modifications on proteins. Bioconjugate chemistry, 16(6), pp.1624-1628.

136. Santa, T., 2014. Recent advances in development and application of derivatization reagents having a benzofurazan structure: a brief overview. Biomedical Chromatography, 28(6), pp.760-766.
137. Al-Majed, A.A., 2000. Specific spectrofluorometric quantification of D-penicillamine in bulk and dosage forms after derivatization with 4-fluoro-7-nitrobenzo-2-oxa-1, 3-diazole. Analytica chimica acta, 408(1-2), pp.169-175.
138. Omar, M.A., Anwer, E.F. and El-Deen, D.A.N., 2020. Spectrofluorimetric approach for determination of tranexamic acid in pure form and pharmaceutical formulations; Application in human plasma. Spectrochimica Acta Part A: Molecular and Biomolecular Spectroscopy, 239, p.118510.
139. Toyo'oka, T., 2012. Development of Benzofurazan− bearing Fluorescence Labeling Reagents for Separation and Detection in High− performance Liquid Chromatography. Chromatography, 33(1), pp.1-17.
140. Nikonov, G.N. and Bobrov, S., 2008. 1, 2, 5-Oxadiazoles. In Comprehensive Heterocyclic Chemistry III. PP. 315-395. Elsevier.
141. Henneken, H., Lindahl, R., Östin, A., Vogel, M., Levin, J.O. and Karst, U., 2003. Diffusive sampling of methyl isocyanate using 4-nitro-7-piperazinobenzo-2-oxa-1, 3-diazole (NBDPZ) as derivatizing agent. Journal of environmental monitoring, 5(1), pp.100-105.
142. Levi, V. and González Flecha, F.L., 2003. Labeling of proteins with fluorescent probes: photophysical characterization of dansylated bovine serum albumin. Biochemistry and Molecular Biology Education, 31(5), pp.333-336.
143. Santa, T., 2011. Derivatization reagents in liquid chromatography/electrospray ionization tandem mass spectrometry. Biomedical Chromatography, 25(1-2), pp.1-10.
144. Xiao, Y., Guo, Y., Dang, R., Yan, X., Xu, P. and Jiang, P., 2017. A dansyl-based fluorescent probe for the highly selective detection of cysteine based on a d-PeT switching mechanism. RSC advances, 7(34), pp.21050-21053.

145. Silva, M., 2005. Quantitation by HPLC of amines as dansyl derivatives. In Journal of Chromatography Library (Vol. 70, pp. 445-470). Elsevier.
146. Danger, G. and Ross, D., 2008. Chiral separation with gradient elution isotachophoresis for future in situ extraterrestrial analysis. Electrophoresis, 29(19), pp.4036-4044.
147. Lau, S.K., Zaccardo, F., Little, M. and Banks, P., 1998. Nanomolar derivatizations with 5-carboxyfluorescein succinimidyl ester for fluorescence detection in capillary electrophoresis. Journal of Chromatography A, 809(1-2), pp.203-210.
148. Sergeev, N.V., Brevnov, M.G. and Furtado, M.R., Life Technologies Corp, 2011. Identification of Nucleic Acids. U.S. Patent Application 13/106,736.
149. Hirabayashi, K., Hanaoka, K., Shimonishi, M., Terai, T., Komatsu, T., Ueno, T. and Nagano, T., 2011. Selective two-step labeling of proteins with an off/on fluorescent probe. Chemistry–A European Journal, 17(52), pp.14763-14771.
150. RAJASEKAR, M. 2021. Recent development in fluorescein derivatives. Journal of Molecular Structure, 1224, 129085.
151. Matsuno, T., Fujirebio Inc, 2015. Method for detecting target nucleic acid using molecular beacon-type probe. U.S. Patent Application 14/389,629.
152. Riggs, J.L., Seiwald, R.J., Burckhalter, J.H., Downs, C.M. and Metcalf, T.G., 1958. Isothiocyanate compounds as fluorescent labeling agents for immune serum. The American journal of pathology, 34(6), p.1081.
153. Amir, R.J., Albertazzi, L., Willis, J., Khan, A., Kang, T. and Hawker, C.J., 2011. Multifunctional trackable dendritic scaffolds and delivery agents. Angewandte Chemie International Edition, 50(15), pp.3425-3429.
154. Onoue, S., Liu, B., Nemoto, Y., Hirose, M. and Yajima, T., 2006. Chemical synthesis and application of C-terminally 5-carboxyfluorescein-labelled thymopentin as a fluorescent probe for thymopoietin receptor. Analytical sciences, 22(12), pp.1531-1535.

155. BREEUWER, P., DROCOURT, J., ROMBOUTS, F. M. & ABEE, T. 1996. A Novel Method for Continuous Determination of the Intracellular pH in Bacteria with the Internally Conjugated Fluorescent Probe 5 (and 6-)-Carboxyfluorescein Succinimidyl Ester. Applied and Environmental Microbiology, 62, 178-183.
156. Cihlar, T. and Ho, E.S., 2000. Fluorescence-based assay for the interaction of small molecules with the human renal organic anion transporter 1. Analytical biochemistry, 283(1), pp.49-55.
157. Dandliker, W.B., Hicks, A.N., Levison, S.A. and Brawn, R.J., 1977. A fluorescein-labeled derivative of estradiol with binding affinity towards cellular receptors. Biochemical and Biophysical Research Communications, 74(2), pp.538-544.
158. Rink, W.M. and Thomas, F., 2018. Decoration of Coiled-Coil Peptides with N-Cysteine Peptide Thioesters As Cyclic Peptide Precursors Using Copper-Catalyzed Azide–Alkyne Cycloaddition (CuAAC) Click Reaction. Organic Letters, 20(23), pp.7493-7497.
159. Guerra, C.E., 2006. Analysis of oligonucleotide microarrays by 3′ end labeling using fluorescent nucleotides and terminal transferase. Biotechniques, 41(1), pp.53-56.
160. Nishioka, T., Yuan, J., Yamamoto, Y., Sumitomo, K., Wang, Z., Hashino, K., Hosoya, C., Ikawa, K., Wang, G. and Matsumoto, K., 2006. New luminescent europium (III) chelates for DNA labeling. Inorganic chemistry, 45(10), pp.4088-4096.
161. Kitamura, K., Itoh, H., Sakurai, K., Dan, S. and Inoue, M., 2018. Target identification of yaku'amide B and its two distinct activities against mitochondrial FoF1-ATP synthase. Journal of the American Chemical Society, 140(38), pp.12189-12199.
162. Wu, C.W., Yarbrough, L.R. and Wu, F.Y., 1976. N-(1-pyrene) maleimide: a fluorescent crosslinking reagent. Biochemistry, 15(13), pp.2863-2868.

163. Yamana, K., Iwai, T., Ohtani, Y., Sato, S., Nakamura, M. and Nakano, H., 2002. Bis-pyrene-labeled oligonucleotides: sequence specificity of excimer and monomer fluorescence changes upon hybridization with DNA. Bioconjugate chemistry, 13(6), pp.1266-1273.

164. Kumar, M., Kumar, R., Bhalla, V., Sharma, P.R., Kaur, T. and Qurishi, Y., 2012. Thiacalix [4] arene based fluorescent probe for sensing and imaging of Fe3+ ions. Dalton Transactions, 41(2), pp.408-412.

165. Nikolaus, J., Czapla, S., Möllnitz, K., Höfer, C.T., Herrmann, A., Wessig, P. and Müller, P., 2011. New molecular rods—Characterization of their interaction with membranes. Biochimica et Biophysica Acta (BBA)-Biomembranes, 1808(12), pp.2781-2788.

166. Xia, Y., Wang, M., Demaria, O., Tang, J., Rocchi, P., Qu, F., Iovanna, J.L., Alexopoulou, L. and Peng, L., 2012. A novel bitriazolyl acyclonucleoside endowed with dual antiproliferative and immunomodulatory activity. Journal of medicinal chemistry, 55(11), pp.5642-5646.

167. KONNO, T., KAMATA, T., OHRUI, H. and MEGURO, H., 1993. A Sensitive Fluorometric Assay of Cholinesterase Activity with N-(9-Acridinyl) maleimide. Analytical sciences, 9(6), pp.871-874.

168. Hashida, Y., Umeyama, T., Mihara, J., Imahori, H., Tsujimoto, M., Isoda, S., Takano, M. and Hashida, M., 2012. Development of a novel composite material with carbon nanotubes assisted by self-assembled peptides designed in conjunction with β-sheet formation. Journal of pharmaceutical sciences, 101(9), pp.3398-3412.

169. Kosower, N.S., Kosower, E.M., Newton, G.L. and Ranney, H.M., 1979. Bimane fluorescent labels: labeling of normal human red cells under physiological conditions. Proceedings of the National Academy of Sciences, 76(7), pp.3382-3386.

170. Yano, H., Kuroda, S. and Buchanan, B.B., 2002. Disulfide proteome in the analysis of protein function and structure. PROTEOMICS: International Edition, 2(9), pp.1090-1096.

171. Namba, K., Osawa, A., Nakayama, A., Mera, A., Tano, F., Chuman, Y., Sakuda, E., Taketsugu, T., Sakaguchi, K., Kitamura, N. and Tanino, K., 2015. Synthesis of yellow and red fluorescent 1, 3a, 6a-triazapentalenes and the theoretical investigation of their optical properties. Chemical science, 6(2), pp.1083-1093.

172. Zhanel, G.G., Wiebe, R., Dilay, L., Thomson, K., Rubinstein, E., Hoban, D.J., Noreddin, A.M. and Karlowsky, J.A., 2007. Comparative review of the carbapenems. Drugs, 67(7), pp.1027-1052.

173. Papp-Wallace, K.M., Endimiani, A., Taracila, M.A. and Bonomo, R.A., 2011. Carbapenems: past, present, and future. Antimicrobial agents and chemotherapy, 55(11), pp.4943-4960.

174. Muneer, S., Wang, T., Rintoul, L., Ayoko, G.A., Islam, N. and Izake, E.L., 2020. Development and characterization of meropenem dry powder inhaler formulation for pulmonary drug delivery. International Journal of Pharmaceutics, 587, p.119684.

175. Ferrone, V., Cotellese, R., Di Marco, L., Bacchi, S., Carlucci, M., Cichella, A., Raimondi, P. and Carlucci, G., 2017. Meropenem, levofloxacin and linezolid in human plasma of critical care patients: A fast semi-automated micro-extraction by packed sorbent UHPLC-PDA method for their simultaneous determination. Journal of pharmaceutical and biomedical analysis, 140, pp.266-273.

176. Baldwin, C.M., Lyseng-Williamson, K.A. and Keam, S.J., 2008. Meropenem. Drugs, 68(6), pp.803-838.

177. de Souza Barbosa, F., Pezzi, L.C., Tsao, M., Macedo, S.M.D., de Oliveira, T.F., Schapoval, E.E. and Mendez, A.S., 2020. Stability in clinical use and stress testing of meropenem antibiotic by direct infusion ESI-Q-TOF: Quantitative

method and identification of degradation products. Journal of Pharmaceutical and Biomedical Analysis, 179, p.112973.

178. Roth, T., Fiedler, S., Mihai, S. and Parsch, H., 2017. Determination of meropenem levels in human serum by high-performance liquid chromatography with ultraviolet detection. Biomedical Chromatography, 31(5), p.e3880.
179. Ferrari, D., Ripa, M., Premaschi, S., Banfi, G., Castagna, A. and Locatelli, M., 2019. LC-MS/MS method for simultaneous determination of linezolid, meropenem, piperacillin and teicoplanin in human plasma samples. Journal of Pharmaceutical and Biomedical Analysis, 169, pp.11-18.
180. Raza, A., Ngieng, S.C., Sime, F.B., Cabot, P.J., Roberts, J.A., Popat, A., Kumeria, T. and Falconer, J.R., 2021. Oral meropenem for superbugs: challenges and opportunities. Drug Discovery Today, 26(2), pp.551-560.
181. Sarkar, P., Yarlagadda, V., Ghosh, C. and Haldar, J., 2017. A review on cell wall synthesis inhibitors with an emphasis on glycopeptide antibiotics. Medchemcomm, 8(3), pp.516-533.
182. Fukasawa, M., Sumita, Y., Harabe, E.T., Tanio, T., Nouda, H., Kohzuki, T., Okuda, T., Matsumura, H. and Sunagawa, M., 1992. Stability of meropenem and effect of 1 beta-methyl substitution on its stability in the presence of renal dehydropeptidase I. Antimicrobial Agents and Chemotherapy, 36(7), pp.1577-1579.
183. Nicolau, D.P., 2008. Carbapenems: a potent class of antibiotics. Expert opinion on pharmacotherapy, 9(1), pp.23-37.
184. Kus, J.V., 2014. Infections due to Citrobacter and Enterobacter, Elsevier.
185. Jann, M.W., 1991. Clozapine. Pharmacotherapy: The Journal of Human Pharmacology and Drug Therapy, 11(3), pp.179-195.
186. Choc, M.G., Hsuan, F., Honigfeld, G., Robinson, W.T., Ereshefsky, L., Crismon, M.L., Saklad, S.R., Hirschowitz, J. and Wagner, R., 1990. Single-vs

multiple-dose pharmacokinetics of clozapine in psychiatric patients. Pharmaceutical research, 7(4), pp.347-351.

187. Raggi, M.A., Pucci, V., Bugamelli, F. and Volterra, V., 2001. Comparison of three analytical methods for quality control of clozapine tablets. Journal of AOAC International, 84(2), pp.361-367.
188. Essali, A., Haasan, N.A.H., Li, C. and Rathbone, J., 2009. Clozapine versus typical neuroleptic medication for schizophrenia. Cochrane database of systematic reviews, (1). John Wiley & Sons, Ltd.
189. Siskind, D., McCartney, L., Goldschlager, R. and Kisely, S., 2016. Clozapine v. first-and second-generation antipsychotics in treatment-refractory schizophrenia: systematic review and meta-analysis. The British Journal of Psychiatry, 209(5), pp.385-392.
190. Mitchell, P. B., 2020. in 'Therapeutic drug monitoring of antidepressant and antipsychotic drugs', Vol. 7, p257- 275, Elsevier.
191. Alvir, J.M.J., Lieberman, J.A., Safferman, A.Z., Schwimmer, J.L. and Schaaf, J.A., 1993. Clozapine-induced agranulocytosis--incidence and risk factors in the United States. New England Journal of Medicine, 329(3), pp.162-167.
192. Islam, F., Hain, D., Lewis, D., Law, R., Brown, L., Tanner, J.A. and Mueller, D.J., 2021. The Genetic Determinants of Clozapine-Induced Agranulocytosis: A Systematic Review and Meta-Analysis. Biological Psychiatry, 89(9), p.S341.
193. Tunsirimas, N., Pariwatcharakul, P., Choovanichvong, S. and Ratta-Apha, W., 2019. Clozapine-induced agranulocytosis and leukopenia: incidence, associated factors, and rate of hematologic adverse-effects monitoring in psychiatric out-patient services in Thailand. Asian Journal of Psychiatry, 41, pp.13-16.
194. Rajagopal, S., 2005. Clozapine, agranulocytosis, and benign ethnic neutropenia. Postgraduate medical journal, 81(959), pp.545-546.

195. Hasegawa, M., Cola, P.A. and Meltzer, H.Y., 1994. Plasma clozapine and desmethylclozapine levels in clozapine-induced agranulocytosis. Neuropsychopharmacology, 11(1), pp.45-47.
196. Wiciński, M. and Węclewicz, M.M., 2018. Clozapine-induced agranulocytosis/granulocytopenia: mechanisms and monitoring. Current opinion in hematology, 25(1), pp.22-28.
197. Gerson, S.L. and Meltzer, H., 1992. Mechanisms of clozapine-induced agranulocytosis. Drug Safety, 7(1), pp.17-25.
198. Ng, W., Kennar, R. and Uetrecht, J., 2014. Effect of clozapine and olanzapine on neutrophil kinetics: implications for drug-induced agranulocytosis. Chemical Research in Toxicology, 27(7), pp.1104-1108.
199. Sproule, B.A., Naranjo, C.A., Bremner, K.E. and Hassan, P.C., 1997. Selective serotonin reuptake inhibitors and CNS drug interactions. Clinical pharmacokinetics, 33(6), pp.454-471.
200. Mohamed, N.G., 2011. Simultaneous determination of amlodipine and valsartan. Analytical chemistry insights, 6, pp.ACI-S7282.
201. Madhuri, C., Reddy, Y.V.M., Vattikuti, S.P., Švorc, Ľ., Shim, J. and Madhavi, G., 2019. Trace-level determination of amlodipine besylate by immobilization of palladium-silver bi-metallic nanoparticles on reduced graphene oxide as an electrochemical sensor. Journal of Electroanalytical Chemistry, 847, p.113259.
202. Malesuik, M.D., Cardoso, S.G., Bajerski, L. and Lanzanova, F.A., 2006. Determination of amlodipine in pharmaceutical dosage forms by liquid chromatography and ultraviolet spectrophotometry. Journal of AOAC international, 89(2), pp.359-364.
203. Shama, S.A., Amin, A.S., El Sayed, M.M. and Omara, H.A., 2009. Utility of oxidation–reduction reaction for the spectrophotometric determination of amlodipine besylate. Arabian Journal of Chemistry, 2(1), pp.59-63.
204. Magdy, R., Hemdan, A., Fares, N.V. and Farouk, M., 2019. Determination of amlodipine and atorvastatin mixture by different spectrophotometric methods

with or without regression equations. Spectrochimica Acta Part A: Molecular and Biomolecular Spectroscopy, 210, pp.203-211.

205. Grossman, E. and Messerli, F.H., 2004. Calcium antagonists. Progress in Cardiovascular Diseases, 47(1), pp.34-57.
206. Shokouhi, S. and Sohrabi, M.R., 2021. Net analyte signal and radial basis function neural network for development spectrophotometry method for the simultaneous determination of metformin and sitagliptin in anti-diabetic commercial tablet. Optik, 243, p.167518.
207. https://www.drugs.com/monograph/sitagliptin.html
208. Bolen, S., Feldman, L., Vassy, J., Wilson, L., Yeh, H.C., Marinopoulos, S., Wiley, C., Selvin, E., Wilson, R., Bass, E.B. and Brancati, F.L., 2007. Systematic review: comparative effectiveness and safety of oral medications for type 2 diabetes mellitus. Annals of internal medicine, 147(6), pp.386-399.
209. Pasquini, B., Gotti, R., Villar-Navarro, M., Douša, M., Renai, L., Del Bubba, M., Orlandini, S. and Furlanetto, S., 2021. Analytical quality by design in the development of a solvent-modified micellar electrokinetic chromatography method for the determination of sitagliptin and its related compounds. Journal of Pharmaceutical and Biomedical Analysis, 202, p.114163.
210. El Messaoudi, S., Rongen, G.A., de Boer, R.A. and Riksen, N.P., 2011. The cardioprotective effects of metformin. Current opinion in lipidology, 22(6), pp.445-453.
211. Lakshmi, K.S., Rajesh, T. and Sharma, S., 2009. Simultaneous determination of metformin and pioglitazone by reversed phase HPLC in pharmaceutical dosage forms. International journal of pharmacy and pharmaceutical sciences, 1(2), pp.162-166.
212. Kumar, D., Trivedi, N., and Dixit, R. K., Determination of metformin in rat plasma using high performance liquid chromatography and its application to pharmacokinetic study, International Journal of Current Research, 8, (06), 33101- 33107.

213. Kavitha, D., Sahoo, S.K., Nagamani, M. and Ch, B., 2017. Development and validation of RP HPLC method for determination of metformin and sitagliptin in bulk and pharmaceutical dosage form. Journal of Applied Pharmaceutical Research, 5(2), pp.34-39.

214. Ahmed, N.R., 2020. Determination of Metformin. HCL in Pharmaceutical Formulations, Environmental Water Samples. Biomedical Journal of Scientific & Technical Research, 30(3), pp.23441-23444.

215. Guillory, A.N., Porter, C., Suman, O.E., Zapata-Sirvent, R.L., Finnerty, C.C. and Herndon, D.N., 2018. Modulation of the hypermetabolic response after burn injury. Total burn care, pp.301-306.

216. Sonnett, T.E., Levien, T.L., Neumiller, J.J., Gates, B.J. and Setter, S.M., 2009. Colesevelam hydrochloride for the treatment of type 2 diabetes mellitus. Clinical therapeutics, 31(2), pp.245-259.

217. Gul, W., 2016. Metformin: methods of analysis and its role in lowering the risk of cancer. J Bioequiv Availab, 8(6), pp.254-9.

218. Khurana, R. and Malik, I.S., 2010. Metformin: safety in cardiac patients. Heart, 96(2), pp.99-102.

219. Shrestha, B., Bhuyan, N.R. and Sinha, B.N., 2013. Simultaneous determination of Ceftriaxone and Tazobactam in injectables by UHPLC method. *Pharmaceutical Methods*, *4*(2), pp.46-51.

220. Omar, M.A., Ahmed, H.M., Batakoushy, H.A. and Hamid, M.A.A., 2020. New spectrofluorimetric analysis of empagliflozin in its tablets and human plasma using two level full factorial design. Spectrochimica Acta Part A: Molecular and Biomolecular Spectroscopy, 235, p.118307.

221. El-Olemy, A., Abdelazim, A.H., Ramzy, S., Hasan, M.A., Madkour, A.W., Almrasy, A.A. and Shahin, M., 2021. Application of different spectrofluorimetric approaches for quantitative determination of acetylsalicylic acid and omeprazole in recently approved pharmaceutical preparation and

human plasma. Spectrochimica Acta Part A: Molecular and Biomolecular Spectroscopy, 262, p.120116.

222. Zhou, B., Bentham, J., Di Cesare, M., Bixby, H., Danaei, G., Cowan, M.J., Paciorek, C.J., Singh, G., Hajifathalian, K., Bennett, J.E. and Taddei, C., 2017. Worldwide trends in blood pressure from 1975 to 2015: a pooled analysis of 1479 population-based measurement studies with 19· 1 million participants. The Lancet, 389(10064), pp.37-55.
223. FDA, U. 2020. Coronavirus (COVID-19) update: FDA issues emergency use authorization for potential COVID-19 treatment. Press Announc., 3-5.
224. Food, U. 2020. Drug Administration, Coronavirus (COVID-19) Update: FDA Issues Emergency Use Authorization for Potential COVID-19 Treatment, FDA News Release.
225. Salman, B.I., Hussein, S.A., Ali, M.F. and Marzouq, M.A., 2019. Innovative ultra-sensitive spectrofluorimetric method for nanogram detection of doripenem monohydrate in human plasma, urine and pharmaceutical formulation. Microchemical Journal, 145, pp.959-965.
226. Haggag, R.S., Gawad, D.A., Belal, S.F. and Elbardisy, H.M., 2016. Spectrophotometric determination of the sulfhydryl containing drug mesna. Bulletin of Faculty of Pharmacy, Cairo University, 54(1), pp.21-32.
227. Guideline, I. Q2 (R1), 2005. Validation of analytical procedure: text and methodology. ICH, London 1(20), 05.
228. Miller, J.N., & Miller, J.C. 2010. Statistics and Chemometrics for Analytical Chemistry, 6th Edition, Ellis Horwood imprint.
229. Fayed, A.S., Youssif, R.M., Salama, N.N., Hendawy, H.A. and Elzanfaly, E.S., 2019. Two-wavelength manipulation stability-indicating spectrophotometric methods for determination of meropenem and ertapenem: greenness consolidation and pharmaceutical product application. Chemical Papers, 73(11), pp.2723-2736.

230. Ayman, A., Zeid, A.M., Wahba, M.E.K. and Yasser, E.S., 2020. Analysis of clozapine in its tablets using two novel spectrophotometric reactions targeting its tertiary amino group. Spectrochimica Acta Part A: Molecular and Biomolecular Spectroscopy, 238, p.118447.

231. El-Enany, N.M., El-Sherbiny, D.T., Abdelal, A.A. and Belal, F.F., 2010. Validated spectrofluorimetric method for the determination of lamotrigine in tablets and human plasma through derivatization with o-phthalaldehyde. Journal of fluorescence, 20(2), pp.463-472.

232. Kőrös, Á., Hanczko, R., Jambor, A., Qian, Y., Perl, A. and Molnar-Perl, I., 2007. Analysis of amino acids and biogenic amines in biological tissues as their o-phthalaldehyde/ethanethiol/fluorenylmethyl chloroformate derivatives by high-performance liquid chromatography: A deproteinization study. Journal of Chromatography A, 1149(1), pp.46-55.

233. Yoshitake, M., Sejima, N., Yoshida, H., Todoroki, K., Nohta, H. and Yamaguchi, M., 2007. Selective determination of tryptophan-containing peptides through precolumn derivatization and liquid chromatography using intramolecular fluorescence resonance energy transfer detection. Analytical Sciences, 23(8), pp.949-953.

234. El-Gindy, A., Ashour, A., Abdel-Fattah, L. and Shabana, M.M., 2001. Spectrophotometric, septrofluorimetric and LC determination of lisinopril. Journal of pharmaceutical and biomedical analysis, 25(5-6), pp.913-922.

235. Tzanavaras, P.D., Zacharis, C.K. and Rigas, P., 2008. Novel automated assay for the quality control of mexiletine hydrochloride formulations using sequential injection and on-line dilution. Journal of pharmaceutical and biomedical analysis, 48(4), pp.1254-1260.

236. El-Enany, N.M., El-Sherbiny, D.T., Abdelal, A.A. and Belal, F.F., 2010. Validated spectrofluorimetric method for the determination of lamotrigine in tablets and human plasma through derivatization with o-phthalaldehyde. Journal of fluorescence, 20(2), pp.463-472.

237. Attia, T.Z., Elnady, M. and Derayea, S.M., 2019. A highly sensitive fluorimetric protocol based on isoindole formation for determination of gabapentin. RSC advances, 9(51), pp.29942-29948.
238. Zuman, P., 2004. Reactions of orthophthalaldehyde with nucleophiles. Chemical reviews, 104(7), pp.3217-3238.
239. Shah, J., Jan, M.R. and Shah, S., 2013. Development and validation of a spectrofluorimetric method for the quantification of ceftriaxone in pharmaceutical formulations and plasma. Luminescence, 28(4), pp.516-522.
240. Goyal, R.N. and Bishnoi, S., 2010. Voltammetric determination of amlodipine besylate in human urine and pharmaceuticals. Bioelectrochemistry, 79(2), pp.234-240.
241. El-Bagary, R.I., Elkady, E.F. and Ayoub, B.M., 2011. Spectrophotometric methods for the determination of sitagliptin and vildagliptin in bulk and dosage forms. International journal of biomedical science: IJBS, 7(1), p.55.
242. Abdel-Hay, M.H., Galal, S.M., Bedair, M.M., Gazy, A.A. and Wahbi, A.A.M., 1992. Spectrofluorimetric determination of guanethidine sulphate, guanoxan sulphate and amiloride hydrochloride in tablets and in biological fluids using 9, 10-phenanthraquinone. Talanta, 39(10), pp.1369-1375.
243. Sakaguchi, T., Tanabe, S., Yagi, H., Miyawaki, T. and Saito, A., 1977. Reaction of guanidines with alpha-diketones. IV. The reactivity of guanidine, monosubstituted guanidines, and biguanides and the fluorometric determination of guanidine with 9, 10-phenanthraquinone as a fluorescence reagent (author's transl). Yakugaku zasshi: Journal of the Pharmaceutical Society of Japan, 97(10), pp.1053-1057.
244. TANABE, S. and SAKAGUCHI, T., 1978. Reaction of Guanidines with α-Diketones. VI. Structures of Fluorescent Products of Biguanides with 9, 10-Phenanthraquinone. Chemical and Pharmaceutical Bulletin, 26(2), pp.423-428.
245. Wahba, M.E., 2017. Micellar liquid chromatographic determination of metformin hydrochloride using fluorimetric detection after pre-column

derivatization: application to pharmacokinetic parameters in immediate and sustained release formulations. Luminescence, 32(3), pp.452-459.

246. Tachibana, M., Hayakawa, M. and Furusawa, M., 1982. The spectrofluorometric determination of 9, 10-phenanthrenequinone. Bulletin of the Chemical Society of Japan, 55(11), pp.3520-3522.
247. Tanabe, S., Kobayashi, T. and Kawanabe, K., 1987. Determination of oral hypoglycemic biguanides by high performance liquid chromatography with fluorescence detection. Analytical sciences, 3(1), pp.69-73.
248. Asakura, H. and Ogawa, H., 2021. COVID-19-associated coagulopathy and disseminated intravascular coagulation. *International journal of hematology*, *113*(1), pp.45-57.
249. Khan, F., Tritschler, T., Kahn, S.R. and Rodger, M.A., 2021. Venous thromboembolism. *The lancet*, *398*(10294), pp.64-77.
250. Ponti, G., Maccaferri, M., Ruini, C., Tomasi, A. and Ozben, T., 2020. Biomarkers associated with COVID-19 disease progression. *Critical reviews in clinical laboratory sciences*, *57*(6), pp.389-399.
251. Velavan, T.P. and Meyer, C.G., 2020. Mild versus severe COVID-19: laboratory markers. *International Journal of Infectious Diseases*, *95*, pp.304-307.
252. Wells, P.S., Anderson, D.R., Rodger, M., Forgie, M., Kearon, C., Dreyer, J., Kovacs, G., Mitchell, M., Lewandowski, B. and Kovacs, M.J., 2003. Evaluation of D-dimer in the diagnosis of suspected deep-vein thrombosis. *New England Journal of Medicine*, *349*(13), pp.1227-1235.
253. Querol-Ribelles, J.M., Tenias, J.M., Grau, E., Querol-Borras, J.M., Climent, J.L., Gomez, E. and Martinez, I., 2004. Plasma d-dimer levels correlate with outcomes in patients with community-acquired pneumonia. *Chest*, *126*(4), pp.1087-1092.
254. Shah, S., Shah, K., Patel, S.B., Patel, F.S., Osman, M., Velagapudi, P., Turagam, M.K., Lakkireddy, D. and Garg, J., 2020. Elevated D-dimer levels

are associated with increased risk of mortality in coronavirus disease 2019: a systematic review and meta-analysis. *Cardiology in review*, *28*(6), pp.295-302.

255. Lehmann, A., Prosch, H., Zehetmayer, S., Gysan, M.R., Bernitzky, D., Vonbank, K., Idzko, M. and Gompelmann, D., 2021. Impact of persistent D-dimer elevation following recovery from COVID-19. *PLoS One*, *16*(10), p.e0258351.
256. Tang, N., Bai, H., Chen, X., Gong, J., Li, D. and Sun, Z., 2020. Anticoagulant treatment is associated with decreased mortality in severe coronavirus disease 2019 patients with coagulopathy. *Journal of thrombosis and haemostasis*, *18*(5), pp.1094-1099.
257. Li, X.Y., Du, B., Wang, Y.S., Kang, H.Y.J., Wang, F., Sun, B., Qiu, H.B. and Tong, Z.H., 2020. The keypoints in treatment of the critical coronavirus disease 2019 patient (2). *Chinese journal of tuberculosis and respiratory diseases*, *43*(4), pp.277-281.
258. Zhou, F., Yu, T., Du, R., Fan, G., Liu, Y., Liu, Z., Xiang, J., Wang, Y., Song, B., Gu, X. and Guan, L., 2020. Clinical course and risk factors for mortality of adult inpatients with COVID-19 in Wuhan, China: a retrospective cohort study. *The lancet*, *395*(10229), pp.1054-1062.
259. Wool, G.D. and Miller, J.L., 2021. The impact of COVID-19 disease on platelets and coagulation. *Pathobiology*, *88*(1), pp.15-27.
260. Poudel, A., Poudel, Y., Adhikari, A., Aryal, B.B., Dangol, D., Bajracharya, T., Maharjan, A. and Gautam, R., 2021. D-dimer as a biomarker for assessment of COVID-19 prognosis: D-dimer levels on admission and its role in predicting disease outcome in hospitalized patients with COVID-19. *Plos one*, *16*(8), p.e0256744.
261. Wu, M.Y., Yao, L., Wang, Y., Zhu, X.Y., Wang, X.F., Tang, P.J. and Chen, C., 2020. Clinical evaluation of potential usefulness of serum lactate dehydrogenase (LDH) in 2019 novel coronavirus (COVID-19) pneumonia. *Respiratory Research*, *21*(1), pp.1-6.

262. Wang, L., Yang, L.M., Pei, S.F., Chong, Y.Z., Guo, Y., Gao, X.L., Tang, Q.Y., Li, Y. and Feng, F.M., 2021. CRP, SAA, LDH, and DD predict poor prognosis of coronavirus disease (COVID-19): a meta-analysis from 7739 patients. *Scandinavian Journal of Clinical and Laboratory Investigation*, *81*(8), pp.679-686.

263. Henry, B.M., Aggarwal, G., Wong, J., Benoit, S., Vikse, J., Plebani, M. and Lippi, G., 2020. Lactate dehydrogenase levels predict coronavirus disease 2019 (COVID-19) severity and mortality: A pooled analysis. *The American journal of emergency medicine*, *38*(9), pp.1722-1726.

264. Martinez-Outschoorn, U.E., Prisco, M., Ertel, A., Tsirigos, A., Lin, Z., Pavlides, S., Wang, C., Flomenberg, N., Knudsen, E.S., Howell, A. and Pestell, R.G., 2011. Ketones and lactate increase cancer cell "stemness," driving recurrence, metastasis and poor clinical outcome in breast cancer: achieving personalized medicine via Metabolo-Genomics. *Cell cycle*, *10*(8), pp.1271-1286.

265. Kaplan, B. and Meier-Kriesche, H.U., 2002. Death after graft loss: an important late study endpoint in kidney transplantation. *American journal of transplantation*, *2*(10), pp.970-974.

266. Patschan, D., Witzke, O., Dührsen, U., Erbel, R., Philipp, T. and Herget-Rosenthal, S., 2006. Acute myocardial infarction in thrombotic microangiopathies—clinical characteristics, risk factors and outcome. *Nephrology Dialysis Transplantation*, *21*(6), pp.1549-1554.

267. Zhang, T., Chen, H., Liang, S., Chen, D., Zheng, C., Zeng, C., Zhang, H. and Liu, Z., 2014. A non-invasive laboratory panel as a diagnostic and prognostic biomarker for thrombotic microangiopathy: development and application in a Chinese cohort study. *PLoS One*, *9*(11), p.e111992.

268. Yan, Y., Yang, Y., Wang, F., Ren, H., Zhang, S., Shi, X., Yu, X. and Dong, K., 2020. Clinical characteristics and outcomes of patients with severe covid-19 with diabetes. BMJ open diabetes research and care, 8(1), p.e001343.

269. Wang, F., Yang, Y., Dong, K., Yan, Y., Zhang, S., Ren, H., Yu, X. and Shi, X., 2020. Clinical characteristics of 28 patients with diabetes and COVID-19 in Wuhan, China. *Endocrine Practice*, *26*(6), pp.668-674.

270. Mez, J., Daneshvar, D.H., Kiernan, P.T., Abdolmohammadi, B., Alvarez, V.E., Huber, B.R., Alosco, M.L., Solomon, T.M., Nowinski, C.J., McHale, L. and Cormier, K.A., 2017. Clinicopathological evaluation of chronic traumatic encephalopathy in players of American football. Jama, 318(4), pp.360-370.

271. Singh, A. K. & Singh, R. 2020. Hyperglycemia without diabetes and new-onset diabetes are both associated with poorer outcomes in COVID-19. Diabetes Research and Clinical Practice, 167, 108382.

272. Beigel, J.H., Tomashek, K.M., Dodd, L.E., Mehta, A.K., Zingman, B.S., Kalil, A.C., Hohmann, E., Chu, H.Y., Luetkemeyer, A., Kline, S. and Lopez de Castilla, D., 2020. Remdesivir for the treatment of Covid-19—preliminary report. New England Journal of Medicine, 383(19), pp.1813-1836.

273. Mundial, A.M., 2019. Declaración de Helsinki de la AMM-Principios éticos para las investigaciones médicas en seres humanos.

274. Beigel, J.H., Tomashek, K.M., Dodd, L.E., Mehta, A.K., Zingman, B.S., Kalil, A.C., Hohmann, E., Chu, H.Y., Luetkemeyer, A., Kline, S. and Lopez de Castilla, D., 2020. Remdesivir for the treatment of Covid-19. *New England Journal of Medicine*, *383*(19), pp.1813-1826.

ORIGINAL ARTICLE

A C G publications

J. Chem. Metrol. 16:1 (2022) 49-59

journal of chemical metrology

A highly selective and sensitive spectrofluorometric method for quantification of meropenem in its dosage form and fresh human plasma

Ali Fahim Mohammed [1*], An Alshirifi [1] and Kasim Hassan Kadhim [1]

Department of Chemistry, College of Science, Babylon University, Hilla-51002, Iraq

(Received February 23, 2022; Revised May 20, 2022; Accepted May 24, 2022)

Abstract: The present study aims to develop and validate a robust, fast, simple, and sensitive spectrofluorimetric approach for the estimation of meropenem (MRP) in its dosage form and fresh human plasma. The developed method is mainly depending on a nucleophilic substitution reaction of MRP with 4-Nitro-7-chlorobenzofurazan (NBD-Cl) in alkaline media (pH 9.0), which results in a strongly fluorescent yellow adduct measured at 536 nm when excited at 471 nm. The variables that influence the stability and development of reaction product were thoroughly investigated and optimized. Calibration curve is rectilinear within the concentration range of 25-650 ng/mL of MRP with a linear correlation coefficient (r =0.9981). Detection and quantification limits were estimated to be 9.55 ng/mL and 3.15 ng/mL respectively. The presented approach was successfully used to the analysis of commercial meropenem vials and meropenem-containing fresh human plasma with good results.

Keywords: NBD-Cl; meropenem; human plasma; spectrofluorimetry.

1. Introduction

Meropenem is an intravenous beta-lactam antibacterial with an ultra-broad spectrum of activity against both gram-positive and gram-negative bacteria Figure S1 [1-4]. Meropenem reveals good stability toward β-lactamases and is used as a last-resort antibiotic, particularly in intensive care units, to treat intra-abdominal infection, peritonitis, bacterial meningitis, febrile neutropenia, gynaecological, pneumonia, anthrax, and sepsis. Meropenem is a new antibiotic from the carbapenem family of antibacterial that has a truly extended spectrum when used alone [5-8]. Meropenem can be used to treat various infections that are caused by multiple drug-resistant organisms, as well as infections due to mixed aerobic and anaerobic organisms [9]. Meropenem, like other beta-lactam antibiotics, penetrates the cell wall of bacteria and inhibits the enzymes known as penicillin-binding proteins (PBPs), which catalyze the cross-linking of glycopeptides that form the bacterial cell wall. Consequently, preventing cell wall synthesis [10]. Despite having a similar structure to imipenem, meropenem has some advantages over it,

* Corresponding author E-Mail: alifahim490@gmail.com

The article was published by ACG Publications
http://www.acgpubs.org/journal/journal-of-chemical-metrology January-June 2022 EISSN:1307-6183
DOI:http://doi.org/10.25135/jcm.70.2202.2363
Available online: June 02, 2022

Printed in the Republic of Korea
ANALYTICAL SCIENCE & TECHNOLOGY
Vol. 35 No. 1, 24-31, 2022
https://doi.org/10.5806/AST.2022.35.1.24

Spectrofluorometric quantification of Clozapine in pharmaceutical formulations and human plasma

Ali Fahim Mohammed[1,2,★], AN Alshirifi[1], and Kasim Hassan Kadhim[1]

[1]*Chemistry Department, College of Science, Babylon University, Hilla 51002, Iraq*
[2]*Medical Physics Department, Al-mustaqbal University College, Hilla 51002, Iraq*

(Received October 20, 2021; Revised November 3, 2021; Accepted December 8, 2021)

Abstract: Herein, we present a simple, precise, accurate, and ultra-sensitive spectrofluorimetric method for estimation of clozapine (CLZ) in tablets and human plasma was developed and then validated. A highly fluorescent brown-yellowish fluorophore was formed (λ_{ex}=469 nm, λ_{emi}=540 nm) as a nucleophilic substitution reaction occurred between CLZ and 4-chloro-7-nitro-2,1,3-benzoxadiazole (NBD-Cl) in alkaline mcllavine buffer (pH 9.0). Optimum values of experimental parameters were carefully determined and optimized. The calibration curve was rectilinear over the concentration range of 80-900 ng mL^{-1} with a linear correlation coefficient (r =0.9984). The LOD and LOQ were determined to be 14 ng mL^{-1} and 42 ng mL^{-1}, respectively. The proposed approach has been used successfully to quantification of Clozapine in its commercial formulations and human plasma.

Key words: clozapine, NBD-Cl, spectrofluorimetric, human plasma

1. Introduction

Clozapine [3-chloro-6-(4-methylpiperazin-1-yl)-11H benzo[b][1,4]benzodiazepine], a member of the dibenzodiazepine derivatives *Fig.* 1, is considered a second-generation anti-psychotic commonly used in the treatment of both negative and positive symptoms of schizophrenic patients[1-3]. CLZ is regarded as an effective choice for patients who suffer from resistance or are unresponsive to conventional neuroleptic medications like haloperidol.[4,5] Clozapine is metabolized by liver through microsomal oxidative cytochrome to the relatively inactive metabolites clozapine-N-oxide and N-Desmethylclozapine.[6] Despite its excellent effectiveness, clozapine's usage is severely limited due to the incidence of drug-induced agranulocytosis in 1-2 % of patients.[7-10] This effect is attributed to the toxicity of one of the clozapine's metabolites, N-desmethylclozapine, that appears to be more harmful to the bone marrow than CLZ itself, leading to decreased white blood cells. Thus, Regular monitoring of the white blood cell count is recommended to reduce this risk.[11-14] It was reported that clozapine metabolism is inhibited by fluvoxamine medication, resulting in considerably higher clozapine levels in the blood.[15] The Physicochemical properties of clozapine were

★ Corresponding author
Phone : +964-780-7245731
E-mail : ali.fahim@mustaqbal-college.edu.iq

الخلاصه

في هذه الدراسه تم تطوير طرق جديدة تشبه تفاعلات النقر لتقدير بعض الأدوية في شكلها الصيدلاني والبلازما البشرية الطازجة. تتضمن الدراسة أربعة أجزاء ، يتضمن الجزء الأول تقدير دوائي الميروبينيم والكلوزابين في صيغتهما الصيدلانية والبلازما البشرية باستخدام المركب NBD-Cl ككاشف اشتقاق تفلوري. تعتمد الطريقة المطورة بشكل أساسي على تفاعل الاستبدال النيوكليوفيلي لـ MRP أو CLZ مع 4 (NBD-Cl) 4-Nitro-7-chlorobenzofurazan- في محلول منظم من البورات القلوي (pH 9.0) ، مما ينتج عنه فلوروفور أصفر متفلور يقاس عند λ_{em} = 536 نانومتر عند اثارته بطول موجي λ_{ex} = 471 نانومتر بالنسبه لـ MRP و اما فلوروفور ال CLZ فيقاس عند 540 نانومتر عند اثارته بطول موجي λ_{ex} = 469 نانومتر. تم فحص المتغيرات التي تؤثر على استقرار وتطوير ناتج التفاعل بدقة وتحسينها. يكون منحنى المعايرة مستقيمًا في نطاق تركيز 25-650 و 80-900 نانوغرام مل $^{-1}$ مع معامل ارتباط خطي (r^2 = 0.9981) و (r^2 = 0.9984) لـ MRP و CLZ على التوالي. تم العثور على حدود الكشف (LOD) لتكون 3.15 و 14 نانوغرام مل $^{-1}$ وبحد تقدير (LOQ) 9.55 و 42 نانوغرام مل $^{-1}$ بالنسبه للـ MRP و CLZ على التوالي.

الجزء الثاني يمثل تقدير دوائي الاملودبين والسيتاكلبتين في صيغتهما الصيدلانية والبلازما البشرية باستخدام O-phthalaldehyde ككاشف تحليلي مولد للفلوروفور في وجود 2-مركابتويثانول كماده يزيد من استقراريه الفلوروفور الناتج. استندت الطريقة المقترحة إلى تفاعل النقر لثلاثة مكونات تتمثل بالمركب الأمين الأولي (عقار AMB أو STA) مع O-phthalaldehyde و 2 mercaptoethanol- في محلول من بفر البورات القلوي pH = 10 و 10.5 لـ AMB و STA على التوالى. توفر مجموعة isoindole الاروماتيه الناتجة شدة تفلور مقاسة عند λ_{em} = 475 و 458 نانومتر بعد الإثارة بطول موجي λ_{ex} = 378و 335 نانومتر لـ AMB و STA على التوالي. تمت دراسة العوامل التجريبية التي تؤثر على شدة الفلوره للفلوروفور المتكون بعناية وتحسينها. تراوح تركيز الدواء الخطي من 125-1400 و 275-1650 نانوغرام مل -1 مع معامل الارتباط الخطي (r^2= 0.9986) و (r^2=0.9985) بالنسبه للـ AMB و STAعلى التوالي. تم العثور على حدود الكشف لتكون 31.29 و 58.94 نانوغرام مل$^{-1}$ مع حدود التقدير الكمي كانت 94.84 و 178.62 نانوغرام مل -1 لـ AMB و STA على التوالي.

الجزء الثالث يمثل تقدير دواء المتفورمين هيدروكلورايد في بلازما بشرية طازجه باستخدام 3,6- Dibromo-phenanthrenequinone ككاشف تحليلي مولد للفلوروفور. تعتمد الطريقة على التفاعل بين MET و PQ-2Br في الوسط القاعديه لإنتاج ناتج متفلور المقاس عند

λ_{em} = 420 بعد الإثارة λ_{ex} = 253 نانومتر. تمت دراسة وتحسين الظروف التي تؤثر على شدة التفلور للناتج المتكون. تراوح تركيز الدواء الخطي من 70-1300 نانوغرام مل$^{-1}$ مع معامل ارتباط خطي (r^2 = 0.9989). كان LOD=19.5 نانوغرام مل$^{-1}$ مع قيمةLOQ = 59.11 نانوغرام مل$^{-1}$.

تم التحقق من صحة الطريقه المطوره وفقًا لإرشادات ICH لإثبات أن نتائج الطرق المقدمة تتوافق مع متطلبات الأداء التحليلي المقترح.

يتضمن الجزء الرابع فحص مستوى المؤشرات الحيوية مثل(D-dimer و LDH و GPT و TG و plasma metformin) في مرضى السكري وغير المصابين بمرض السكري COVID-19 الذين يتناولون دواء.Remdesivir

واخيرا تم استنتاج بان طرق قياس التفلور الطيفي الموصوفة تعتبر طريقه بسيطة وسريعة ودقيقة لتقدير الأدوية في شكل جرعاتها الصيدلانية والبلازما البشرية الطازجة دون وجود متداخلات من منشأ البلازما أو السواغات الشائعة. علاوة على ذلك ، أظهرت الطرق المطورة انتقائية واعدة ، وحساسية ، ونطاق خطي جيد ، واسترداد كمي ممتاز ، وانحراف معياري نسبي(R.S.D) أقل من 2٪.

أخيرًا ، تم استخدام جميع الطرق المطورة بنجاح لتقدير الأدوية في شكل جرعاتها الصيدلانية والبلازما البشرية الطازجة. تمت مقارنة البيانات التي تم الحصول عليها إحصائيًا مع تلك التي تم الحصول عليها من الطرق البحثيه أو الرسمية وفقًا لاختبار t-student و -F اختبار بمستوى ثقة 95٪. ووجد النتائج المتعلقة بقيم اختبار f و t-test أقل من القيم الحرجة المقابلة (المجدولة) ، مما يشير إلى عدم وجود فرق كبير إحصائيًا بين الطريقة الرسمية وكذلك الطريقة البحثيه مع الطريقه المقترحة.

تظهر النتائج السريرية أن المرضى غير المصابين بمرض السكري COVID-19 أظهروا تعافيًا أسرع من مرضى السكري COVID-19 لأن دواء remdesivir يحسن مستوى D-dimer و LDH. تشير النتائج إلى أن المؤشرات الحيوية D-dimer و LDH يمكن أن تساعد في تشخيص عدوى -COVID 19.

وزارة التعليم العالي والبحث العلمي
جامعة بابل/ كلية العلوم – قسم الكيمياء

التقدير الكمي بتقنية الفلوره لبعض الادويه في اشكالها الصيدلانيه وفي البلازمه البشريه مع دراسه سريريه

أطروحة مقدمة

إلى مجلس كلية العلوم – جامعة بابل

وهي جزء من متطلبات نيل درجة الدكتوراه فلسفه في العلوم/ الكيمياء

تقدم بها

علي فاهم محمد عبد علي الخفاجي

بكالوريوس علوم كيمياء/ جامعة بابل 2013

ماجـــستير علوم كيمياء/ جامعة بابل 2016

بإشراف

أ.د. عباس نور محمد الشريفي

أ.د. قاسم حسن كاظم (رحمه الله)

1444 هـ

2022 م